

THESIS

ASSESSING CORN WATER STRESS USING SPECTRAL REFLECTANCE

Submitted by

Brenna S. Mefford

Department of Civil and Environmental Engineering

In partial fulfillment of the requirements

For the Degree of Master of Science

Colorado State University

Fort Collins, Colorado

Summer 2014

Master's Committee:

Advisor: José L. Chávez

Kendall DeJonge  
Bill Bauerle

Copyright by Brenna Sue Mefford 2014

All Rights Reserved

## ABSTRACT

### ASSESSING CORN WATER STRESS USING SPECTRAL REFLECTANCE

Multiple remote sensing techniques have been developed to identify crop water stress, but some methods may be difficult for farmers to apply. Unlike most techniques, shortwave vegetation indices can be calculated using satellite, aerial, or ground imagery from the green (525-600 nm), red (625-700 nm), and near infrared (750-900 nm) spectral bands. If vegetation indices can be used to monitor crop water stress, growers could use this information as a quick low-cost guideline for irrigation management, thus helping save water by preventing over irrigating. This study occurred in the 2013 growing season near Greeley, CO, where pressurized drip irrigation was used to irrigate twelve corn (*Zea mays L.*) treatments of varying water deficit. Multispectral data was collected and four different vegetation indices were evaluated: Normalized Difference Vegetation Index (NDVI), Optimized Soil-Adjusted Vegetation Index (OSAVI), Green Normalized Difference Vegetation Index (GNDVI), and the Wide Dynamic Range Vegetation Index (WDRVI). The four vegetation indices were compared to corn water stress as indicated by the stress coefficient ( $K_s$ ) and water deficit in the root zone, calculated by using a water balance that monitors crop evapotranspiration (ET), irrigation events, precipitation events, and deep percolation. ET for the water balance was calculated using two different methods for comparison purposes: (1) calculation of the stress coefficient ( $K_s$ ) using FAO-56 standard procedures; (2) use of canopy temperature ratio ( $T_{c \text{ ratio}}$ ) of a stressed crop to a non-stressed crop to calculate  $K_s$ . It was found that obtaining  $K_s$  from  $T_{c \text{ ratio}}$  is a viable option, and requires less data to obtain than  $K_s$  from FAO-56. In order to compare the indices to  $K_s$ , vegetation ratios were developed in the

process of normalization. Vegetation ratios are defined as the non-stressed vegetation index divided by the stressed vegetation index. Results showed that vegetation ratios were sensitive to water stress as indicated by good  $R^2$  values ( $N_{ratio} = 0.53$ ,  $G_{ratio}=0.46$ ,  $O_{ratio}=0.49$ ) and low RMSE values ( $N_{ratio} = 0.076$ ,  $G_{ratio}=0.062$ ,  $O_{ratio}=0.076$ ) when compared to  $K_s$ . Therefore it can be concluded that corn spectral reflectance is sensitive to water stress. In order to use spectral reflectance to manage crop water stress an irrigation trigger point of 0.93 for the vegetation ratios was determined. These results were validated using data collected by a MSR5 multispectral sensor in an adjacent field (SWIIM Field). The results from the second field proved better than in the main field giving higher  $R^2$  values ( $N_{ratio} = 0.66$ ,  $G_{ratio} = 0.63$ ,  $O_{ratio} = 0.66$ ), and lower RMSE values ( $N_{ratio} = 0.043$ ,  $G_{ratio} = 0.036$ ,  $O_{ratio} = 0.043$ ) between  $K_s$  and the vegetation indices. SWIIM field further validated the results that spectral reflectance can be used to monitor corn water stress.

## ACKNOWLEDGEMENTS

Thank you to my advisor, Dr. José Chávez, for all of your support and guidance. To the Agricultural Research Service Water Management Unit thank you for allowing me to use your data and supporting me through this process, I really appreciate it. Thank you to my committee members Kendall DeJonge and Bill Bauerle for your intelligent comments and advice. To the many professors who have influenced and guided me, thank you. A special thank you to Walter Bausch for getting me interested in remote sensing and teaching me so much along the way. Thank you to my parents who inspire me to go after my dreams and never stop supporting me. Finally thank you to Jason, for always being there for me and supporting me every step of the way.

## TABLE OF CONTENTS

ABSTRACT.....	ii
ACKNOWLEDGEMENTS.....	iv
TABLE OF CONTENTS.....	v
LIST OF TABLES.....	vii
LIST OF FIGURES.....	viii
LIST OF SYMBOLS AND ABBREVIATIONS.....	xi
CHAPTER 1: INTRODUCTION.....	1
1.1 Global Water and Food Supply.....	1
1.1.1 Climate Change.....	1
1.1.2 Population Growth.....	3
1.2 Limited/Deficit Irrigation.....	3
1.2.1 Field Studies of Regulated Deficit Irrigation.....	4
1.2.2 Evapotranspiration and Crop Water Stress.....	7
1.3 Spectral Reflectance of Vegetation.....	13
1.3.1 Spectral Reflectance of Water Stressed Crops.....	14
1.4 Vegetation Indices.....	14
1.4.1 Normalized Difference Vegetation Index (NDVI).....	15
1.4.2 Wide Dynamic Range Vegetation Index.....	17
1.4.4 Optimized Soil Adjusted Vegetation Index.....	17
1.4.5 Green Normalized Difference Vegetation Index (GNDVI).....	20
1.5 Fractional Vegetation Cover.....	20
1.6 Previous Studies on Vegetation Indices and Water Stress.....	22
1.7 Literature Summary.....	23
1.8 Research Objectives.....	24
1.9 Research Scope.....	24
CHAPTER 2: METHODOLOGY.....	26
2.1 General Overview.....	26
2.2 Data Collection.....	32
2.3 Data Processing Methods.....	35
2.3.1 Imagery Processing and Geo-referencing.....	35

2.3.2 Calculation of Vegetation Indices.....	37
2.4 Water Stress Crop Coefficient Calculation.....	39
2.4.1 FAO-56 Procedure.....	40
2.4.2 Calculation of $K_{cb}$ and $K_e$ .....	42
2.4.3. $K_s$ Calculation following FAO-56 .....	43
2.4.4 $K_s$ Calculation by $T_{c\ ratio}$ .....	43
2.4.5 Water Balance.....	44
2.5 SWIIM Field Data Processing .....	47
CHAPTER 3: RESULTS AND ANALYSIS .....	49
3.1 Fractional Vegetation Cover.....	49
3.2 Vegetation Indices .....	52
3.3 Comparison of Evapotranspiration .....	58
3.4 Soil Water Deficit Comparison.....	64
3.5 Stress Indicated from Vegetation Indices .....	71
3.5.1 Comparison of $K_s$ from FAO-56 to Vegetation Indices .....	72
3.5.2 Comparison of $K_s$ from $T_{c\ ratio}$ to Vegetation Indices.....	73
3.5.3 Development of Vegetation Ratios.....	75
3.6 Irrigation Trigger Determination .....	81
3.6.1 Irrigation Amount Determination .....	83
3.7 Calculation of Index Ratio with Minimal Data.....	83
3.8 Validation of Method to Obtain Vegetation Ratios .....	86
3.9 Use of the index ratio as $K_s$ .....	87
3.10 Validation Using SWIIM Field Data .....	88
CHAPTER 4: CONCLUSION .....	99
4.1 Recommendations for Future Study .....	102
REFERENCES .....	104
APPENDIX A: COMPARISON OF DAILY $K_s$ VALUES .....	109
APPENDIX B: DAILY $D_i$ AND RAW GRAPHS FOR $K_s$ FROM $T_{c\ ratio}$ .....	111
APPENDIX C: DAILY $D_i$ AND RAW GRAPHS FOR $K_s$ FROM FAO-56.....	114

## LIST OF TABLES

Table 2.1. Percent of maximum ET applied for each treatment during the vegetative and maturity growth phases, respectively. All treatments received 100% ET during the reproductive (tasseling and silking) phase .....	30
Table 3.1. Statistical values for comparing estimated $D_i$ to measured $D_i$ for the two different methods.....	66
Table 3.2. Cumulative $D_i$ (mm) with $K_s$ from FAO-56 during vegetative and maturation growth stages and final grain yields, averaged by treatment .....	71
Table 3.3. RMSE and MBE values for the error between $K_s$ and the vegetation ratios excluding Treatment 12. ....	80
Table 3. 4. VF, NDVI, GNDVI, and OSAVI values for fully irrigated corn corresponding to corn major growth stages using data collected in 2009 to 2011 by the ARS-WMU.....	86
Table 3.5. RMSE and MBE values for the vegetation ratios obtained from SWIIM field.....	96

## LIST OF FIGURES

Figure 2.1. LIRF Field Layout Schematic. Number in each plot (i.e. A11) is a plot identifier used in data collection and logistics. Text in middle of plot identifies ET treatment, defined in Table 2.1.....	28
Figure 2.2. LIRF and SWIIM Location .....	29
Figure 2.3. Layout of SWIIM field, Irrigation pipe was placed at north end of field, which is sloped downward going south. ....	31
Figure 2.4. High Boy Tractor with sensor platform being run through the corn field.....	32
Figure 2.5. Sensor platform layout and descriptions. GPS antenna is hidden from view. ....	33
Figure 2.6. Processing example for FLUX multispectral camera. All images are from plot C12 (Treatment 1), DOY 214. The corn just began reproduction (growth stage of R1). a.) Red bandwidth image b.) NIR bandwidth image c.) Green bandwidth image d.) CIR composite image e.) Final Processed Image from VF program (VF = 0.86).....	36
Figure 2.7. Processing example from Canon RGB camera. Both images are from C12 (Treatment 1) DOY 214 a) Red Green Blue image from Canon 50d. b.) Processed image output from VF program in R Project (VF = 0.82).....	37
Figure 2.8. $K_{cb}$ values over the corn growing season .....	41
Figure 3.1. Comparison of VF obtained for RGB and multispectral images for both Treatment 1 and Treatment 12.....	50
Figure 3.2. FLUX multispectral and output images for DOY 199 for a.) Treatment 1 (VF = 0.85) and b.) Treatment 2 (VF = 0.70).....	50
Figure 3.3. Canon image RGB and output images for DOY 199 a.) Treatment 1 (VF = 0.84) and b.) Treatment 12 (VF = 0.57).....	52
Figure 3.4. Time-series plots for all treatments of a.) NDVI b.) GNDVI c.) OSAVI and d.) WDRVI.....	53
Figure 3.5. NDVI versus VF.....	54
Figure 3.6. GNDVI versus VF.....	54
Figure 3.7. OSAVI versus VF.....	55
Figure 3.8. WDRVI versus VF .....	55

Figure 3.9. $K_{cb}$ values for Treatment 1 calculate using both Trout and Johnson (2007) and FAO-56 guidelines (Allen et al., 1998).....	59
Figure 3.10. $K_s$ Daily values from Treatment 2 for the two different methods .....	60
Figure 3.11. $K_s$ daily values for Treatment 6 for the two different methods .....	61
Figure 3.12. Daily actual ET for each method calculated for Treatment 1 .....	62
Figure 3.13. Daily ET for Treatment 6 calculated with $K_s$ from FAO-56 and from $T_{c\ ratio}$ .....	64
Figure 3.14. Daily $D_i$ and RAW for corn in Treatment 6 calculated from $K_s$ from FAO-56 .....	65
Figure 3.15. Daily $D_i$ and RAW for corn in Treatment 6 calculated from $K_s$ from $T_{c\ ratio}$ .....	65
Figure 3.16. $D_i$ for Treatments 1, 2, 3, 6, 8, and 12 calculated using $K_s$ from FAO-56 .....	68
Figure 3.17. $D_i$ for Treatments 1, 2, 3, 6, 8, and 12 calculated using $K_s$ from $T_{c\ ratio}$ .....	69
Figure 3.18. $K_s$ from FAO-56, NDVI, GNDVI, and OSAVI values for DOY 192.....	72
Figure 3.19. $K_s$ from $T_{c\ ratio}$ , NDVI, GNDVI, and OSAVI values for DOY 211 .....	74
Figure 3.20. $K_s$ from $T_{c\ ratio}$ , NDVI, GNDVI, and OSAVI values for DOY 206 .....	74
Figure 3. 21. $N_{ratio}$ , $G_{ratio}$ , $O_{ratio}$ , and $K_s$ from $T_{c\ ratio}$ values for DOY 206.....	76
Figure 3. 22. $K_s$ from $T_{c\ ratio}$ versus $N_{ratio}$ for all treatments and days with data .....	77
Figure 3. 23. $K_s$ from $T_{c\ ratio}$ versus $G_{ratio}$ for all treatments and days with data .....	77
Figure 3.24. $K_s$ from $T_{c\ ratio}$ versus $O_{ratio}$ for all treatments and days with data .....	78
Figure 3.25. $K_s$ from $T_{c\ ratio}$ versus $N_{ratio}$ for all Treatments except Treatment 12.....	79
Figure 3.26. $K_s$ from $T_{c\ ratio}$ versus $G_{ratio}$ for all Treatments except Treatment 12.....	79
Figure 3.27. $K_s$ from $T_{c\ ratio}$ versus $O_{ratio}$ for all Treatments except Treatment 12.....	80
Figure 3.28. $K_s$ from $T_{c\ ratio}$ calculated using the second method values for the second half of the growing season, the thick black line being the proposed irrigation trigger point. The $K_s$ values are used as a representation of the index ratios because of the lack of enough data for determining an irrigation trigger using just index ratio values. ....	82
Figure 3.29. Daily ET (mm/day) for Treatment1 (FI) in SWIIM field.....	89
Figure 3. 30. Daily ET (mm/day) for Treatment 2 (LFDI) in SWIIM field .....	89
Figure 3. 31. Daily ET (mm/day) for Treatment 3 (HFDI) in SWIIM field.....	90
Figure 3.32. Daily $K_{cb}$ values for FAO-56, and calculated from Trout and Johnson (2007) for Treatment 2 and 3. ....	91
Figure 3.33. Daily $K_s$ values for Treatment 2.....	92

Figure 3.34. Time-series of daily $D_i$ and RAW for Treatment 2, calculated using $K_s$ from FAO-56.....	93
Figure 3. 35. Time-series of daily $D_i$ and RAW for Treatment 2, calculated using $K_s$ from $T_{c \text{ ratio}}$ .....	93
Figure 3.36. $K_s$ from $T_{c \text{ ratio}}$ versus $N_{\text{ratio}}$ for Treatment 1, 2, and 3.....	94
Figure 3. 37. $K_s$ from $T_{c \text{ ratio}}$ versus $G_{\text{ratio}}$ for Treatment 1, 2, and 3.....	95
Figure 3.38. $K_s$ from $T_{c \text{ ratio}}$ versus $O_{\text{ratio}}$ for Treatment 1, 2, and 3.....	95
Figure 3.39. Time-series of $K_s$ from $T_{c \text{ ratio}}$ with irrigation trigger point highlighted by black line. Like with LIRF this line is an estimate for the irrigation trigger point for the vegetation ratios since not enough data was available to use the vegetation ratios to determine it.....	98
Figure A.1. $K_s$ Daily values from Treatment 1 for the two different methods.....	109
Figure A.2. $K_s$ Daily values from Treatment 3 for the two different methods .....	109
Figure A.3. $K_s$ Daily values from Treatment 8 for the two different methods .....	110
Figure A.4. $K_s$ Daily values from Treatment 12 for the two different methods .....	110
Figure B.1. $D_i$ and RAW for Treatment 1 calculated with $K_s$ from $T_{c \text{ ratio}}$ .....	111
Figure B.2. $D_i$ and RAW for Treatment 2 calculated with $K_s$ from $T_{c \text{ ratio}}$ .....	111
Figure B.3. $D_i$ and RAW for Treatment 3 calculated with $K_s$ from $T_{c \text{ ratio}}$ .....	112
Figure B. 4. $D_i$ and RAW for Treatment 8 calculated with $K_s$ from $T_{c \text{ ratio}}$ .....	112
Figure B.5. $D_i$ and RAW for Treatment 12 calculated with $K_s$ from $T_{c \text{ ratio}}$ .....	113
Figure C.1. $D_i$ and RAW for Treatment 1 with $K_s$ from FAO-56.....	114
Figure C.2. $D_i$ and RAW for Treatment 2 with $K_s$ from FAO-56 .....	114
Figure C.3. $D_i$ and RAW for Treatment 3 with $K_s$ from FAO-56 .....	115
Figure C.4. $D_i$ and RAW for Treatment 8 with $K_s$ from FAO-56 .....	115
Figure C.5. $D_i$ and RAW for Treatment 8 with $K_s$ from FAO-56 .....	116

## LIST OF SYMBOLS

$\alpha$	weighting coefficient in the calculation of WDRVI
CIR	color infrared
$D_i$	daily soil water deficit for that day (mm)
$D_{i-1}$	daily soil water deficit of previous day (mm)
$D_{i\_RAW}$	deficit when the deficit is greater than readily available water (mm)
$D_s$	soil water deficit attributed to stress in the root zone (mm)
DOY	day of year
DP	deep percolation (mm)
ET	evapotranspiration (mm/day, mm/hr)
$ET_a$	actual crop evapotranspiration
$ET_c$	crop evapotranspiration (mm/day)
$ET_o$	grass reference evapotranspiration (mm/day, mm/hr)
$ET_R$	alfalfa reference evapotranspiration (mm/day, mm/hr)
$ET_{ref}$	reference evapotranspiration (mm/day, mm/hr)
EVI	enhanced vegetation index
FC	field capacity (%)
$FC_{RZ}$	field capacity in the root zone (%)
$f_{ew}$	fraction of the soil that is both exposed to solar radiation and that is wetted
fPAR	fraction of photosynthetically active radiation
GNDVI	green normalized difference vegetation index
$Green_I$	incident green light
$Green_R$	reflected green light
I	total net irrigation amount applied (mm)
IRT	infrared thermometer ( $^{\circ}C$ )
$K_c$	crop coefficient
$K_{cmax}$	maximum value of $K_c$ following rain or irrigation
$K_{cb}$	basal crop coefficient
$K_e$	soil water evaporation coefficient
$K_s$	stress reduction coefficient
$K_r$	evaporation reduction coefficient
LAI	leaf area index
LIRF	Limited Irrigation Research Facility
MSAVI	modified soil adjusted vegetation index
NDVI	normalized difference vegetation index
NIR	near Infrared
$NIR_I$	incident near infrared light
$NIR_R$ :	reflected near infrared light
OSAVI	optimized soil adjusted vegetation index
P	amount of precipitation that infiltrates the soil (mm)
p	depletion fraction
$R^2$	coefficient of determination
RAW	readily available water (mm, %)

RH	relative humidity (%)
RH <sub>min</sub>	minimum daily relative humidity (%)
Red	light in the red wavelength
Red <sub>I</sub>	incident red light
Red <sub>R</sub>	reflected red light
REW	readily evaporable water (mm)
RGB	red green blue
RMSE	root mean square error
RZ	root zone (m, mm)
SAVI	Soil Adjusted Vegetation Index
SR	Simple Ratio
SWD <sub>15</sub>	soil water deficit at 15 cm (mm, %)
SWD <sub>30</sub>	soil water deficit at 30 cm (mm, %)
SWD <sub>45</sub>	soil water deficit at 45 cm (mm, %)
SWD <sub>60</sub>	soil water deficit at 60 cm (mm, %)
SWD <sub>75</sub>	soil water deficit at 75 cm (mm, %)
SWD <sub>90</sub>	soil water deficit at 90 cm (mm, %)
TAW	total available water (%)
TDR	time domain reflectometer
TEW	total evaporable water (mm, %)
TSAVI	transformed soil adjusted vegetation index
VF	vegetation fraction
VWC	volumetric water content (m <sup>3</sup> ,%)
VWC <sub>i</sub>	Volumetric water capacity for a specific day (m <sup>3</sup> , %)
VE	emergence of corn plants from soil
V7	vegetative growth stage – 7 collars visible on corn plants
V12	vegetative growth stage – 12 collars visible on corn plants
R1	reproductive growth stage – silk becomes visible
R3	reproductive growth stage – kernels fill with milky white fluid
R5	reproductive growth stage – dent forms on top on kernels
WDRVI	wide dynamic range vegetation index
WP	wilting point (%)
Z	ratio sensitivity value used in the calculation of the vegetation indices

## CHAPTER 1: INTRODUCTION

### 1.1 Global Water and Food Supply

As climate change progresses and populations continue to grow, fresh water is becoming scarce. Water is needed for irrigation, urban landscaping, recreation, and human consumption/use. Irrigation is the largest single consumer of fresh water, consuming about 80% of total freshwater in the world (Hoffman and Evans, 2007). As demand for freshwater from non-agriculture increases and populations increase (more demand for food) growers will continued to be pressured to use less water, but still produce enough food to feed a growing population. A changing climate will affect water sources that farmers rely on for irrigation. Thirsty cities will continue to buy water rights from farmers in order to bring the water to growing cities. Populations will continue to rise in developing countries and require more food that is sustainably irrigated to meet the needs of the people. Therefore it is important to address how climate change and increased food supply are going to affect irrigated agriculture.

#### 1.1.1 Climate Change

As the implications of climate change begin to emerge, more pressure will be put on water resources to sustain an ever growing population. Global warming due to enhanced greenhouse gases is very likely to have significant effects on the hydrological cycle (IPCC, 2013). Some areas could see increased precipitation while others could see longer droughts, depending on the degree of climate change. According to Arnell (1999) global average precipitation will increase with climate change, but much of the increase will occur over the oceans, with large areas of land surface experiencing reduction in precipitation. Dore (2005) also found this to be true and

stated that the wet areas will become wetter, with dry areas becoming drier. Therefore, the global climate change scenario will very likely put high stress on available water resources and irrigated agriculture, since 80% of the available fresh water is used for irrigation (Hoffman and Evans, 2007). Thus, due to this water stress scenario farmers will feel increased pressure to use less water from rising populations, and other competing sectors, but yet want to sustain high or economical yields.

To help farmers deal with increased competition for water resources, irrigation infrastructures will need to be updated and fixed. Some estimate that 50% of the water withdrawals for agricultural purposes actually reached the crops and the rest was lost in outdated and or broken irrigation infrastructures (Fisher et al., 2007). These authors also studied the implications of mitigating (i.e. reducing the severity of) climate change for irrigation water requirements and withdrawals, and in what situations mitigation matter the most. They found that effects of climate change mitigation on irrigation water requirements could result in large overall water savings, both on the global and regional scale. Overall the analysis concluded that mitigation is going to be an important part in helping agriculture adjust to changes in climate and water resources. If mitigation is not used farmers will not be able to adapt to changes by themselves, and with the increased economic pressure on irrigation and agriculture as a whole (regionally and globally) farmers will suffer along with the public who relies on affordable food. Irrigation infrastructure will need to be updated to help prevent water loss so farmers can maximize water use and food production. Modernized methods of irrigation management will need to be introduced to farmers and mitigation will be necessary to help farmers deal with climate change.

### 1.1.2 Population Growth

Along with the changes in climate that will ultimately affect the water supply differently in different areas, populations around the world continue to increase. World population numbers are supposed to hit 9.7 billion by 2050 (United Nations, 2012). While farmers are economically pressured into using less water, they must sustain or even increase food production to feed this growing population, despite increasing water scarcity. In the future farmers will be expected to use less water, but yet somehow still produce high yields that can fulfill the needs of the human population, livestock, and biofuels. In order for farmers to be able to attempt to feed the growing population and use less water new management methods of irrigation and technology are going to need to be used.

### 1.2 Limited/Deficit Irrigation

One of the most researched management approaches to saving farmers water is regulated deficit irrigation. Regulated deficit irrigation is an irrigation strategy in which the net irrigation water applied is less than the full crop-water requirements. Crop water requirements are normally determined using the evapotranspiration (ET) of the crop, which is defined as the combination of two separate processes where water is lost or evaporated from the soil and plant surface and/or transpired from within the plants tissue (Allen et al., 1998). For corn the most drought sensitive growth stages occur during reproduction (tasseling and silking). In deficit irrigation, agriculture growers try to apply less water at non drought sensitive growth stages, such as vegetative stages and the late ripening period (after reproduction, Zhang and Oweis, 1999). Growers can determine how much water to apply (or reduce) depending on how much decrease in crop yield they are willing to allow. Regulated deficit irrigation is often applied to maximize economic production

when the grower has high value and low value crops. The high value crop can be applied with full water to meet its ET demands, and deficit irrigation can be applied to the low value crops to be able to still obtain some sort of yield from the crops. Another potential use of saved water is to lease it to other farmers or non-agricultural sources (cities, companies, etc.). There has been much research on deficit irrigation including both field studies and crop models however, crop models will not be discussed in this manuscript as they are outside the scope of this project.

### 1.2.1 Field Studies of Regulated Deficit Irrigation

While regulated deficit irrigation has been shown to save water, inducing water stress can affect the biophysical properties of the plant. Aydinsakir (2013) studied the effects of deficit irrigation on two corn genotypes. It was reported that protein content of both corn genotypes decreased when irrigation levels decreased. Sugar content (glucose, fructose, and sucrose) contents increased with decreasing water. They also concluded that it was possible to grow corn with a moderate level of water deficiency without significant decreases in grain yield. While this study found that the protein of the corn decreased and sugar increased, the nutritional content of the corn is still beneficial for both humans and livestock. Ertek and Kara (2013) reported similar results for sweet corn in that sugar levels increased with deficit irrigation, but found that the 30% deficit treatment in their study had higher protein content than other irrigation treatments. This is including the fully irrigated treatment and the 15% deficit treatment that was tested. While corn has few quality standards it is still important when applying regulated deficit irrigation to consider the nutritional implications that could occur and how it could affect consumers.

Timing of deficit is an important consideration so that implications on yields are minimized. Doorenbos and Kassam (1979) concluded that corn appeared to be relatively tolerant of water deficits during the vegetative and ripening periods, although water deficits during tasseling and ear formation caused large decreases in grain yields. Results of Doorenbos and Kassam (1979) study have also been concluded by numerous other studies including Çakir (2004) who conducted a study to identify the effects of water stress at different growth stages on corn. When water stress was only applied during the vegetative growth stages, it had only a small effect on the yield, and if a single irrigation was missed during the sensitive growth stages (reproduction), it could cause up to a 40% decrease in grain yield during years without much precipitation. If water is very scarce it would be most beneficial to apply irrigation during tasselling and cob formation stages. Farré and Faci (2009) also reported that during water shortages it is possible to maintain relatively high yields if water deficit is not applied during “flowering stage” (tasseling, ear development). They concluded that it was possible to implement deficit irrigation by increasing intervals between irrigations during growth stages other than “flowering”. Applying deficit irrigation would allow for reduction in agricultural water use, thereby allowing for the water to be used somewhere else where it is more economically valuable.

While most of the studies on deficit irrigation conclude that applying water stress during the vegetative and maturity stages resulted in only slight reductions in grain yield, Kang et al. (2000) conducted a study in which deficit irrigation was applied to corn at both seedling and stem-elongation stages. They found that treatments that experience an early soil drying at the seedling stage plus a further mild water deficit could potentially maintain grain yield and substantially reduce water consumption. Plants that were stressed at the seedling stage that were then stressed again at the stem-elongation stage had less of an effect on photosynthesis. The most likely cause

for this phenomenon is deficit at the seedling stage promotes a large deep root system (Kang et al., 2000). Their results show that grain yield was not significantly reduced for their mild treatment and only marginally reduced for the severe mild treatment. Applying water deficit at the seedling stages makes the plants better adapted for further water deficit during later stages. This approach of applying deficit irrigation to seedlings allows for more water to be saved throughout the season as the crop can handle larger water deficits later on without much grain yield reduction.

Zhang and Oweis (1999) reported that for deficit irrigation probability of rainfall and available soil moisture in the root zone need to be considered when irrigating. If a farmer is in an area that receives most of its irrigation water during tasseling and ear formation, deficit irrigation can be applied by stressing the corn early and hopefully using any precipitation to get the crop through its critical stages. The water not used can then be used on other crops or leased out for other uses. In areas in which salinity is a problem Katerji et al. (2004) found that corn yield response to water stress did not change whether the cause was salinity or drought.

Regulated deficit irrigation is a viable option for when the cost of water is high and/or abundant water is not readily available. As discussed, deficit irrigated crops will have responses to water stress. It is important when applying deficit irrigation to understand how the crops biophysical features will change, including vegetation fraction (VF), leaf area index (LAI), spectral reflection, etc. It is fairly obvious that VF and LAI will decrease with increased crop water stress, but how canopy spectral reflectance changes due to crop water stress is important to determine. It is also important to be able to detect crop water stress using only the spectral response of the crop so that remote sensing can be used to make it easy to identify crop water stress.

## 1.2.2 Evapotranspiration and Crop Water Stress

When applying regulated deficit irrigation it is important to monitor water deficit that is being imposed to the crops. One of the more common ways of monitoring water stress is to track the crops ET throughout the growing season. Estimates of crop ET can be calculated using methods described in The Food and Agriculture Organization Irrigation and Drainage Paper No. 56 (FAO-56, Allen et al., 1998). Estimates of ET can be obtained from the standardized Penman-Monteith equation that calculates reference ET ( $ET_{ref}$ ). Grass reference ET ( $ET_o$ ) or alfalfa reference ET ( $ET_r$ ) can be calculated using the Penman-Monteith equation.  $ET_o$  is defined by Doorenbos and Pruitt (1977) in FAO-24 as the ET rate from an extensive surface of 8 to 15 cm tall green grass, that is actively growing, completely shading the ground, is healthy, and not short on water.  $ET_r$  as described by ASCE-EWRI (2005) as the rate of ET from actively growing alfalfa with 50 cm of canopy height and is well watered. Many different equations have been developed for calculating reference ET. Equation 1.1 shows how  $ET_{ref}$  is calculated in which T is air temperature ( $^{\circ}C$ ),  $R_n$  is net radiation ( $MJ\ m^{-2}\ d^{-1}$ , or  $MJ\ m^{-2}\ hr^{-1}$ ), G is soil heat flux ( $MJ\ m^{-2}\ d^{-1}$ , or  $MJ\ m^{-2}\ hr^{-1}$ ),  $u_2$  is wind speed at 2 m height (m/s),  $(e_s - e_a)$  is the vapor pressure deficit (kPa),  $\Delta$  is the slope of the saturation vapor pressure temperature curve ( $kPa\ ^{\circ}C^{-1}$ ), and  $C_n$  and  $C_d$  are constants defined by reference type and time step. This equation is recommended by both FAO-56 (Allen et al., 1998) and ASCE-EWRI (2005).

$$ET_{ref} = \frac{0.408\Delta(R_n - G) + \gamma \frac{C_n}{T + 273} u_2 (e_s - e_a)}{\Delta + \gamma(1 + C_d u_2)} \quad (1.1)$$

The two constants  $C_n$  and  $C_d$  used in the Standardized Penman-Monteith  $ET_{ref}$  equation can be obtained from ASCE-EWRI (2005). The slope of the saturation vapor pressure-temperature curve ( $\Delta$ ,  $kPa\ ^{\circ}C^{-1}$ ) was calculated using Equation 1.2.

$$\Delta = \frac{2503 \exp\left(\frac{17.27T}{T+237.3}\right)}{(T+237.3)^2} \quad (1.2)$$

Saturation vapor pressure function ( $e^0$ ) is calculated using Equation 1.3, in which T is air temperature ( $^{\circ}\text{C}$ ).

$$e^0 = 0.6108 \exp\left(\frac{17.27T}{T+237.3}\right) \quad (1.3)$$

Equation 1.4 shows how saturation vapor pressure ( $e_s$ ) is calculated for daily time steps, in which  $T_{\max}$  and  $T_{\min}$  are the maximum and minimum air temperature ( $^{\circ}\text{C}$ ) that occurred for that day, respectively.

$$e_s = \frac{e^0(T_{\max}) + e^0(T_{\min})}{2} \quad (1.4)$$

Psychrometric constant ( $\gamma$ ) is calculated using Equation 1.5, in which P is atmospheric pressure in kPa (Equation 1.6).

$$\gamma = 0.000665P \quad (1.5)$$

$$P = (2.406 - 0.0000534z)^{5.26} \quad (1.6)$$

In Equation 1.6 the variable z is the elevation of the field (m) above sea level. Daily net radiation is calculated using Equation 1.7, in which  $R_{ns}$  is net short wave radiation ( $\text{MJ m}^{-2} \text{d}^{-1}$ ) and  $R_{nl}$  is net outgoing long-wave radiation ( $\text{MJ m}^{-2} \text{d}^{-1}$ ). Equation 1.8 and 1.9 show how to calculate  $R_{ns}$  and  $R_{nl}$  respectively. For Equation 1.8  $R_s$  is measured solar radiation (obtained from a weather station), and  $\alpha$  is albedo assumed as a fixed value of 0.23.

$$Rn = R_{ns} - R_{nl} \quad (1.7)$$

$$R_{ns} = (1 - \alpha)R_s \quad (1.8)$$

$$R_{nl} = \sigma f_{cd} (0.34 - 0.14 \sqrt{e_a}) \left[ \frac{T_K^{4 \max} + T_K^{4 \min}}{2} \right] \quad (1.9)$$

In Equation 1.9  $f_{cd}$  is a cloudiness function,  $T_K$  is the maximum and minimum temperature in Kelvin and  $\sigma$  is the Stefan-Boltzmann constant,  $4.901 \times 10^{-9}$  MJ K<sup>-4</sup> d<sup>-1</sup>. Equation 1.10 shows how  $f_{cd}$  is calculated in which  $R_{so}$  is the calculated clear-sky radiation.  $f_{cd}$  has limits of 0.05 to 1.0.

$$f_{cd} = 1.35 \frac{R_s}{R_{so}} - 0.35 \quad (1.10)$$

Clear sky solar radiation ( $R_{so}$ ) is computed by Equation 1.11, where  $R_a$  is exoatmospheric radiation (MJ m<sup>-2</sup> d<sup>-1</sup>).

$$R_{so} = (0.75 + 2 \times 10^{-5} z) R_a \quad (1.11)$$

Exoatmospheric radiation ( $R_a$ ) is defined by Equation 1.12, in which  $G_{sc}$  is the solar constant and equal to 4.92 MJ m<sup>-2</sup> d<sup>-1</sup>,  $d_r$  is the inverse relative distance factor (squared) for the earth-sun (Equation 1.13),  $\omega_s$  is the sunset hour angle (radians, Equation 1.14),  $\phi$  is the station latitude (radians),  $\delta$  is the solar declination in radians (Equation 1.15). In Equation 1.13 and 1.15 DOY is the Day of Year.

$$R_a = \frac{24}{\pi} G_{sc} d_r [\omega_s \sin(\phi) \sin(\delta) + \cos(\phi) \cos(\delta) \sin(\omega_s)] \quad (1.12)$$

$$d_r = 1 + 0.033 \cos\left(\frac{2\pi}{365} DOY\right) \quad (1.13)$$

$$\omega_s = \arccos[-\tan(\phi) \tan(\delta)] \quad (1.14)$$

$$\delta = 0.409 \sin\left(\frac{2\pi}{365} DOY - 1.39\right) \quad (1.15)$$

Soil heat flux ( $G$ ) is the last variable that needs to be calculated for Equation 1.1. If  $ET_{ref}$  is being calculated for daily timestamps soil heat flux is assumed to be equal to zero.

To simplify the calculation of  $ET$ , the crop coefficient ( $K_c$ ) was developed.  $K_c$  is used to adjust  $ET_{ref}$  for different crop types.  $K_c$  changes through the growing season and is affected by crop height, crop-soil resistance, surface albedo, and fraction of ground cover.  $K_c$  is calculated using equation 1.16, where  $K_{cb}$  is the basal crop coefficient,  $K_s$  is the water stress reduction coefficient, and  $K_e$  is the soil water evaporation coefficient

$$K_c = K_{cb} \cdot K_s + K_e \quad (1.16)$$

In order to calculate  $K_{cb}$  Equation 1.17 is used, in which  $K_{cb(Tab)}$  is the value for  $K_{cb\ mid}$  ( $K_{cb}$  value in the middle of the growing season) or  $K_{cb\ end}$  ( $K_{cb}$  value in the end of the growing season) taken from a table in FAO-56,  $u_2$  (m/s) is the mean value for daily wind speed at 2 m height over grass during the mid or late season growth stage,  $RH_{min}$  (%) is the mean value for daily minimum relative humidity during the mid- or late season growth stage, and  $h$  (m) is the mean plant height during mid or late season stage.

$$K_{cb} = K_{cb(Tab)} + [0.04(u_2 - 2) - 0.004(RH_{min} - 45)] \left(\frac{h}{3}\right)^{0.3} \quad (1.17)$$

Using Equation 1.17 requires weather data, and using tabulated values ( $K_{cb(Tab)}$ ) for certain crops that might not always be accurate for different climates. Therefore Trout and Johnson (2007) developed another method based on using  $VF$  to estimate  $K_{cb}$ . For this method  $K_{cb}$  is calculated using Equation 1.18, in which “a” and “b” are empirical coefficients calibrated to get the best relationship between  $K_{cb}$  and  $VF$ .

$$K_{cb} = a + b * VF \quad (1.18)$$

Trout and Johnson (2007) developed this equation by plotting “measured”  $K_{cb}$  (calculated using a weighing lysimeter) versus measured VF. They reported a strong linear correlation between  $K_{cb}$  and VF for three different types of crop (lettuce, pepper, garlic). Since many growers don’t have the equipment to monitor VF (this is done using crop canopy images and processing software), Trout and Johnson (2007) also developed an equation (Equation 1.19) to calculate VF based on the Normalized Difference Vegetation Index (NDVI, Eq. (1.28)).

$$VF = 1.22 * NDVI - 0.21 \quad (1.19)$$

For growers who are assuming no water stress,  $K_s$  is assumed to have a value of one in Equation 1.16. If water stress is being included then  $K_s$  needs to be calculated. According to FAO-56 (Allen et al., 1998)  $K_s$  can be computed as in Equation 1.20, where TAW is the total available soil water in the crop root zone (mm),  $D_r$  is root zone soil water depletion (mm), and  $p$  is the fraction of TAW that a crop can extract from the root zone without suffering water stress, typically assumed as 0.5.

$$K_s = \frac{TAW - D_r}{(1-p)*TAW} \quad (1.20)$$

In order to determine the parameters in Equation 1.20, accurate soil moisture measurements throughout the growing season are required. If soil moisture measurements are unavailable, Bausch et al. (2011) proposed that  $K_s$  could be estimated from a ratio of canopy temperatures ( $T_{c\ ratio}$ , Equation 1.21). To be able to apply this method of estimating  $K_s$ , infrared thermometers (IRTs) are required to monitor crop canopy temperature ( $^{\circ}C$ ) in both the stressed and non-stressed fields.

$$T_{c\ ratio} = \frac{T_{c\ no-stress}}{T_{c\ stress}} = \frac{T_{c\ ns}}{T_{c\ s}} \sim K_s \quad (1.21)$$

The last parameter needed to calculate  $K_e$  (Equation 1.16) is the soil water evaporation coefficient ( $K_e$ ).  $K_e$  is at a maximum value of 1.0 when the soil surface is wet and at a minimum value of zero when the soil surface is dry. According to Allen et al. (1998)  $K_e$  is calculated using Equation 1.22 in which  $K_r$  is an evaporation reduction coefficient (Equation 1.23),  $K_{c \max}$  is the maximum value of  $K_c$  (the actual crop coefficient) following rain or irrigation as defined by Equation 1.24, and  $f_{ew}$  is the fraction of soil that is both exposed to solar radiation and that is wetted (Equation 1.25). For Equation 1.23 REW (mm) is the readily evaporable water determined by the soil type, and  $D_{e, i-1}$ (mm) is the cumulative depth of evaporation from the soil surface layer at the end of the previous day. For Equation 1.24  $h$  is the average maximum plant height during the period of calculation (initial, development, mid, or late-season). In Equation 1.25  $f_c$  is the fraction of vegetation cover, and  $f_w$  is the average fraction of soil surface wetted by irrigation or precipitation.

$$K_e = K_r(K_{c \max} - K_{cb}) \leq f_{ew} K_{c \max} \quad (1.22)$$

$$K_r = \frac{TEW - D_{e, i-1}}{TEW - REW} \text{ for } D_{e, i-1} > REW \quad (1.23)$$

$$K_{c \max} = \max \left( \left\{ 1.2 + [0.04(u_2 - 2) - 0.004(RH_{\min} - 45)] \left( \frac{h}{3} \right)^{0.3} \right\} \{K_{cb} + 0.05\} \right) \quad (1.24)$$

$$f_{ew} = f_w \left( 1 - \left( \frac{2}{3} \right) f_c \right) \quad (1.25)$$

Actual crop ET is then calculated using  $ET_{ref}$  and  $K_c$  shown in Equation 1.26.

$$ET_c = K_c \cdot ET_{ref} \quad (1.26)$$

Once crop ET ( $ET_c$ ) has been estimated soil water deficit can be determined by water balance.

Water deficit is calculated using net irrigation (Irr, mm), effective precipitation (P, mm),  $ET_c$

(mm), deep percolation (DP, mm), and ground water inputs (GW, mm). Unless the field is in an area with a high water table, GW inputs are mainly assumed to not occur. Hoffman et al. (2007) uses Equation 1.27 to describe how the water deficit for a certain day ( $D_i$ ) is calculated, with  $D_{i-1}$  being the deficit from the previous day.

$$D_i = D_{i-1} + ET_a - P - Irr + DP - GW \quad (1.27)$$

### 1.3 Spectral Reflectance of Vegetation

Current research of regulated deficit irrigation often uses remote sensing to monitor the crops water stress status. Information using remote sensing is obtained using satellites, aerial flights, or ground based sensors. Using remote sensing allows for an entire field to be easily monitored, instead of just certain locations. This can be helpful for finding disease, locating water stress, nutrient stress, etc. Remote sensing can save water by helping pinpoint leaks or other problems with irrigation systems, or by indicating where water needs to be applied too. One application of remote sensing in agriculture is monitoring spectral reflectance of crop canopies. Spectral radiometers are used to obtain values of spectral reflectance of crop canopies along with incident light upon the crop canopy. Using canopy reflectance data obtained from spectral radiometers vegetation indices can be estimated, which can indicate the status of the vegetation in concern. The spectral characteristics of healthy vegetative surfaces have low reflectance in blue, high in green, low in red, and very high in the near infrared (NIR) spectrums (Genc et. al., 2013). Vegetation has a characteristic spectral reflectance signature in comparison to soil and water. Water has a relatively low reflectance in the visible light region (400-700 nm) and is almost zero in the NIR region. Bare soil has a relatively low reflectance in the NIR and Red and has a

slightly higher reflectance in the visible light region. Since vegetation has such a distinct spectral signature, remote sensing can be used to monitor vegetation density and water status. This is extremely useful in agriculture when the health of the crop can change dramatically depending on the location in a field.

### 1.3.1 Spectral Reflectance of Water Stressed Crops

Spectral reflectance of crops can be used to monitor crop health. If applying deficit irrigation, it is helpful to understand how the crop's spectral reflectance is going to be affected by the water stress. While healthy (non-stressed) crops absorb almost all of the incident red and reflect incident NIR light, stressed crops have shown to reflect more red light when water stressed (Jackson and Ezra, 1985) because water stress affects the light absorption of leaf chloroplasts. Köksal et al. (2011) studied the spectral reflectance of sugar beets under different levels of irrigation and showed that well watered sugar beets reflectance values increased as the crop grew and covered the bare soil. While the drought stressed sugar beets showed similar reflectance values as the bare soil at the end of the growing season. Köksal et al. (2011) reported strong relationships between vegetation indices, LAI, biomass, and sugar beet yield. The spectral reflectance of the sugar beets changed with water stress, which shows that water stress can be monitored using remote sensing of spectral reflectance.

## 1.4 Vegetation Indices

Spectral vegetation indices are mathematical combinations of different spectral bands mainly in the visible and NIR wavelengths (Viña et al., 2011). Vegetation indices have been developed to

relate canopy/leaf reflectance with canopy characteristics such as VF, LAI, chlorophyll content, and intercepted photosynthetically active radiation (PAR, Hatfield et al., 2008). Mainly vegetation indices are seen as a simple way to obtain/quantify biophysical characteristics of vegetation from remotely sensed data (Gitelson, 2013).

#### 1.4.1 Normalized Difference Vegetation Index (NDVI)

NDVI is the most commonly used vegetation index; it has been shown to be correlated with some biophysical properties of the vegetation canopy including LAI, VF, and biomass (Jiang et al., 2006). NDVI is a function of NIR and Red reflectance, with NIR being the reflectance in the near infrared spectrum (~800 nm), and Red being the reflectance in the red spectrum (~675 nm). NDVI is calculated by Equation 1.28, and ranges from a minimum value of -1 to a maximum value of 1.

$$NDVI = \frac{NIR-Red}{NIR+Red} \quad (1.28)$$

NDVI was developed by Deering in 1978, and is a benchmark for the newer indices being developed (Hatfield et al., 2008). Theoretically NDVI should have a linear relationship with many of the biophysical properties such as LAI, VF, and biomass (Jiang et al. 2006). While NDVI theoretically has a linear relationship with VF it has been seen that NDVI tends to become saturated after VF cover gets to a certain density depending on the crop type being monitored. This occurs when the crop obtains full cover yet there is relatively no change in the reflectance of the canopy until the crop starts drying out or senescing. Saturation causes the NDVI values to plateau off, stay constant, and not continue increasing on a 1 to 1 scale with VF. Since NDVI mainly responds to the red spectrum, values of the overall index will saturate when the red

spectrum begins to saturate. It was found that this saturation is not crop dependent and many different experiments with different varieties of crop show that NDVI will reach its maximum value and saturate at many different VF values. Huete et al. (1985) showed NDVI approached its maximum value around VF values of 80% to 90%. Meza Díaz and Blackburn (2003) showed NDVI saturation occurring at VF values of only 60%. Huete et al. (1985) reported that NDVI responded primarily to red reflectance and is relatively insensitive to NIR variation when vegetation becomes very dense (as VF reaches full cover). In order to address the saturation issue with NDVI many other vegetation indices have been developed. Since the NDVI equation has an “open loop” (no correction for soil or atmospheric effects) structure it is susceptible to large sources of error and uncertainty caused by atmospheric and canopy background conditions (Liu and Huete, 1995).

While there have been reported uncertainties with using NDVI, it remains extremely popular. NDVI is used not only in agricultural settings, but also in forests, deserts, etc. For example Mancino et al. (2014) used Landsat imagery and NDVI to detect vegetation change in a forest in southern Italy. NDVI is also often used as a parameter in forecasting models for predicting vegetation growth, abundance, and ET models. Therefore it is important to calculate NDVI using accurate sensors and verify the results. Advances in technology are happening quickly, and it is important to test new sensors and see how they perform compared to older technology. Ground based remote sensing, often referred to as “ground-truth” based sensing, combined with newer sensors can help to calculate accurate estimates of NDVI.

#### 1.4.2 Wide Dynamic Range Vegetation Index

The Wide Dynamic Range Vegetation Index (WDRVI) was developed by Gitelson (2004), who reported that NDVI was only sensitive to changes in VF when VF values were between 40 to 50%. This saturation level was seen for wheat, maize, and soybean. Gitelson (2004) then developed WDRVI (Equation 1.29) to help avoid the saturation problem. As shown in Equation 1.29 an alpha weighting coefficient ( $\alpha < 1$ ) is applied to the NIR band. Typical values of  $\alpha$  range from 0.1 to 0.3. It was found in Gitelson (2004) that WDRVI had a stronger near-linear relationship with VF than NDVI did.

$$WDRVI = \frac{\alpha NIR - Red}{\alpha NIR + Red} \quad (1.29)$$

Peng et al. (2013) found that WDRVI was one of the most accurate indices for estimating gross primary productivity of crops (GPP). WDRVI is one of the better indices that is able to distinguish agricultural land and intermediate forests in tropical rain forests, but this was based solely on remote sensed data therefore ground based measurements would be needed to validate this conclusion (Viña, 2012). Although WDRVI was developed to help avoid the saturation problem that occurs with NDVI and the other NDVI based indices, strong saturation has been seen to occur in WDRVI after full VF has occurred (Vescovo et al., 2012).

#### 1.4.4 Optimized Soil Adjusted Vegetation Index

Huete (1988) proposed a Soil-Adjusted Vegetation Index (SAVI). The purpose of SAVI was to eliminate soil background effects in NDVI and prevent saturation as was common with NDVI. SAVI is defined in Equation 1.30 as:

$$SAVI = \frac{NIR-Red}{NIR+Red+L} \times (1 + L) \quad (1.30)$$

In Equation 1.30 L is a constant that can be adjusted for soil background affects. The factor of (1 + L) was applied to keep SAVI in the same boundaries as NDVI (-1 to 1). Huete (1988) varied L from 0 to 1, and 1 to 100 in order to determine the effect and the sensitivity to see if SAVI performed better than NDVI. It was reported that as the vegetation density increased throughout the growing season L could be adjusted from 0 to 1. At very low vegetation densities L=1, at intermediate densities L=0.5, higher densities L= 0.25 (Huete, 1988). SAVI was originally thought to be an improvement on NDVI, and Huete (1988) reported improved linearity between LAI and SAVI in comparison to NDVI.

While SAVI seemed to be an improvement over NDVI, many found that it still had some faults such as saturation. Therefore, Baret et al. (1989) proposed the Transformed Soil Adjusted Vegetation Index (TSAVI). Unlike SAVI, TSAVI is a distance based vegetation index. Distance based vegetation indices main objective is to minimize the effect of soil brightness. Distance based vegetation indices are obtained through linear regression of the near-infrared band against the red band for samples of bare soil pixels. Baret and Guyot (1991) reported that TSAVI was the best vegetation index for low LAI, but it reached saturation level before SAVI, but after NDVI. TSAVI is calculated using Equation 1.31, where a and b are the parameters of the soil line and X is assumed to be equal to 0.08. TSAVI equals zero for bare soil, and is about 0.70 for very dense canopies (Baret and Guyot, 1991).

$$TSAVI = \frac{a*(NIR-a*Red-b)}{(a*NIR+r-ab+X(1+a^2))} \quad (1.31)$$

After TSAVI was developed a second version of the SAVI was proposed by Major et al. (1990) called SAVI<sub>2</sub>. Vegetation isoline behavior was used to develop SAVI<sub>2</sub> (Equation 1.32), where b is

the intercept and  $a$  is the slope of each isoline. The downfall of  $SAVI_2$  is that it requires LAI in the modeling to obtain values for  $a$  and  $b$ . Most users of vegetation indices use them to estimate LAI, but  $SAVI_2$  requires that it already be known.

$$SAVI_2 = \frac{NIR}{Red+b/a} \quad (1.32)$$

Modified Soil Adjusted Vegetation Index (MSAVI) was proposed by Qi et al. (1994). MSAVI was based off of the original SAVI using the L factor. Instead of using L as a single value, Qi et al. (1994) proposed an empirical L function to help further reduce soil background effects. Therefore the constant L becomes self-adjusting. The L factor does not appear in the MSAVI equation (Equation 1.33) instead the L function was taken into account using coefficients in the equation. Qi et al. (1994) reported that MSAVI minimized soil background effects. MSAVI behaved like NDVI at high vegetation densities, and like SAVI for intermediate densities.

$$MSAVI = \frac{2*NIR+1-\sqrt{(2*NIR+1)^2-8(NIR-Red)}}{2} \quad (1.33)$$

After MSAVI was proposed, Rondeaux et al. (1996) suggested the Optimized Soil Adjusted Vegetation Index (OSAVI, Equation 1.34), which was used in this project.

$$OSAVI = \frac{(NIR-Red)}{(NIR+Red+0.16)} \times (1.16) \quad (1.34)$$

OSAVI is a simplification of TSAVI with the parameters  $a=1$  and  $b=0$  (Rondeaux et al., 1996).

An optimum adjusting factor was calculated as 0.16 to use in the calculation of OSAVI.

Rondeaux et al. (1996) suggest that OSAVI be used for agricultural applications, whereas MSAVI can be used for more general applications.

#### 1.4.5 Green Normalized Difference Vegetation Index (GNDVI)

The Green Normalized Difference Vegetation Index (GNDVI) is based off of NDVI, but instead of using the red band, it uses the green band (Equation 1.35).

$$GNDVI = \frac{NIR - Green}{NIR + Green} \quad (1.35)$$

GNDVI, one of the more popular vegetation indices, was developed by Gitelson et al. (1996). This vegetation index was first used because of its sensitivity to chlorophyll concentration in leaves. GNDVI was found to be more sensitive to a wide range of chlorophyll concentrations than the original NDVI (Gitelson et al., 1996). While GNDVI was first developed for estimation of chlorophyll content, Pradhan et al. (2012) reported that GNDVI was better than Simple Ratio (SR) and NDVI for prediction of grain yield and biomass yield for wheat. SR is defined as NIR divided by Red. GNDVI has also been used for estimating nitrogen status, LAI, fPAR, and VF. GNDVI has been shown to be a better estimator of fraction of absorbed photosynthetically active radiation (fPAR) than NDVI (Cristiano et al., 2010), because GNDVI does not saturate as much at high vegetation cover as NDVI (Gitelson et al., 1996).

#### 1.5 Fractional Vegetation Cover

Monitoring of crop biophysical properties is very important in making sure the crop is healthy, and helps track crop progress throughout the season. VF can tell a grower a lot about how their crop is growing throughout the growing season. VF is important for describing surface vegetation, and ecosystem health. In agriculture VF is associated with the stage of the crop, and can help determine irrigation scheduling. Most growers do not have the technology and/or the time to directly quantify VF for their crop; therefore VF is typically only directly calculated in

research. VF can be obtained using a digital camera and image processing software packages which calculate the ratio of vegetation pixels to the total number of pixels. Most software packages find VF for green vegetation by calculating the number of green pixels (wavelength range 462 to 638nm) to the total number of pixels in the image (Equation 1.36).

$$VF = \frac{\# \text{ of vegetation pixels}}{\# \text{ of total pixels}} = \frac{\# \text{ of green pixels}}{\# \text{ of total pixels}} \quad (1.36)$$

Vegetation indices indirectly calculate VF since they are correlated with crop biophysical properties, including VF. NDVI is the most widely used index for the calculation of VF, however NDVI can often over estimate VF when vegetation is sparse and there is high volume of substrate or senescent vegetation in the background (Xiao and Moody, 2005). This problem often occurs in the beginning of the crop season when VF is low, and no till or strip till practices are used. Xiao and Moody (2005) reported that estimating VF from NDVI is suitable for some landscapes in arid and semi-arid regions. Theoretically NDVI should have a linear relationship with VF, because as VF changes NDVI will also change at the same rate and both are on a scale of 0 to 1. However, there has been much discussion over whether VFs relationship with NDVI in reality is linear or nonlinear. Gitelson et al. (2002) reported that both NDVI and GNDVI did not have a linear relationship with VF. A linear correlation of VF and NDVI has been found only 72% of the time in semi-arid regions with sparse vegetation cover (Barati et al., 2011). Other indices like WDRVI along with NDVI and GNDVI were shown to have nonlinear relationships with the biophysical property of LAI (Viña et al., 2011), while theoretically they should have a linear relationship. Multiple other studies have showed these same results, but most of the data were collected using satellite or airborne data. Today's sensors have better accuracy and more capabilities than those used in the former studies. Therefore there is a research need to re-assess

the relationships between VF and spectral vegetation indices using ground based data collected with modern ground-based sensors.

### 1.6 Previous Studies on Vegetation Indices and Water Stress

Throughout the past thirty-five years there has been research conducted using vegetation indices to detect crop water stress. Jackson et al. (1983) took spectral reflectance measurements throughout a winter wheat crop with a handheld radiometer. They reported that NDVI did not work well for discriminating stress when stress occurred at high levels of VF. Increased atmospheric path radiance decreased NDVI, therefore showing that NDVI calculated using satellite data most likely needs atmospheric corrections. Strachan et al. (2002) reported that no one single index was able to detect stress (both nitrogen and water stress were applied in this study), but that several reflectance signatures and indices were needed to monitor the health of the corn. Other indicators like plant temperatures can indicate the onset and degree of stress at a particular time, while reflected solar radiation measurements detect the effects of stress over time (Jackson et al., 1986). But if plant temperatures are not available, and reflected solar radiation measurements are, then it is important to know what indices can be used to detect stress, not just monitor it over time. Wang et al. (2012) identified that the SR had the best correlation with water use efficiency (WUE), which is defined as how much biomass is produced over a growing season relative to the net amount of water used. They reported that the simple ratio index showed the highest correlation with WUE out of all of the indices tested, and can be used to assess WUE in desert shrubs. Genc et al. (2013) used spectral reflection to determine water stress in sweet corn. Deficit irrigation was used on the sweet corn (planted in pots), and a classification tree analysis was used to determine what indices determined water stress in the sweet corn. It was

reported by Genc et al. (2013) that GNDVI was the main index to determine water stress in the study.

## 1.7 Literature Summary

Main conclusions of this literature review presented in this chapter are as follows.

- 1) Population growth and climate change will require farmers to maintain or increase worldwide production, while likely using less water.
- 2) By applying regulated deficit irrigation at the correct time, grain yields along with nutrient content can be maintained. Wide adoption of deficit irrigation will require better knowledge of management and monitoring of crop water stress, with simple methods that do not require research-grade equipment or intensive calculations from the user.
- 3) Remote sensing of spectral reflectance of water stressed crops can serve as a good way to monitor vegetation biophysical characteristics.
- 4) Vegetation indices have been widely used for monitoring crop biophysical properties, but researchers have gotten mixed results on how exactly vegetation indices are related to crop biophysical properties. There is not any strong consensus on which vegetation index is better to use for predicting different biophysical properties.
- 5) VF is an important crop biophysical property that can help determine the health of the plant, and can be accurately predicted using vegetation indices.

## 1.8 Research Objectives

This study aims to use short wave spectral bands-based vegetation indices to indicate crop water stress using remotely sensed data taken throughout the growing season for corn in 2013. Actual water stress based on ET will be calculated to verify water stress indicated by the vegetation indices. The main objective of this study is to determine if these vegetation indices can be used to determine and quantify corn water stress. From this main objective the sub-objectives of this project are:

- 1.) For days that multispectral data are available use the data to obtain indices: NDVI, OSAVI, GNDVI, and WDRVI. Verify accuracy of multispectral data by quantifying relationship between indices and fractional vegetation cover.
- 2.) Calculate daily soil water deficit for each treatment using the method of water balance, and calculating daily corn ET using two different methods for the calculation of the stress coefficient  $K_s$ : FAO-56 (Allen et. al., 1998) and  $T_{c \text{ ratio}}$  (canopy temperature ratio, Bausch et al., 2011).
- 3.) Identify water stress using the stress coefficient from the two ET methods, and compare the stress coefficient to the vegetation indices. From this comparison determine an irrigation trigger value based on the vegetation indices.
- 4.) Verify results by repeating objectives 1 to 3 for an adjacent corn field during the same growing season.

## 1.9 Research Scope

This study focuses on the spectral response of deficit irrigated corn. Twelve different levels of regulated deficit irrigation were applied to corn throughout the 2013 growing season. During the

growing season readings from multispectral sensors and imagery from two different cameras were taken from a mobile platform above the field. One camera was a multispectral “FLUX” camera used to obtain red, green, and near infrared imagery of the plots, the other camera was a Canon digital camera used to obtain standard red, green, blue (RGB) imagery of the plots. Imagery from both cameras were run through software to obtain fractional vegetation cover for all of the twelve treatments. The data from the multispectral sensors were used to calculate four different vegetation indices: NDVI, OSAVI, GNDVI, and WDRVI for all of the twelve treatments. The four vegetation indices were plotted as a time series over the course of the summer to assess how they responded to induced water stress. Water stress observed using the vegetation indices can be seen by comparing the fully irrigated treatment to the other stressed treatments. Observed water stress for certain days throughout the season can then be compared to actual water stress (on that same monitored day) throughout the season using a water balance and the stress coefficient. More specific descriptions of how the indices and fractional vegetation cover were calculated along with the calculation of actual water stress are discussed in Chapter 2.

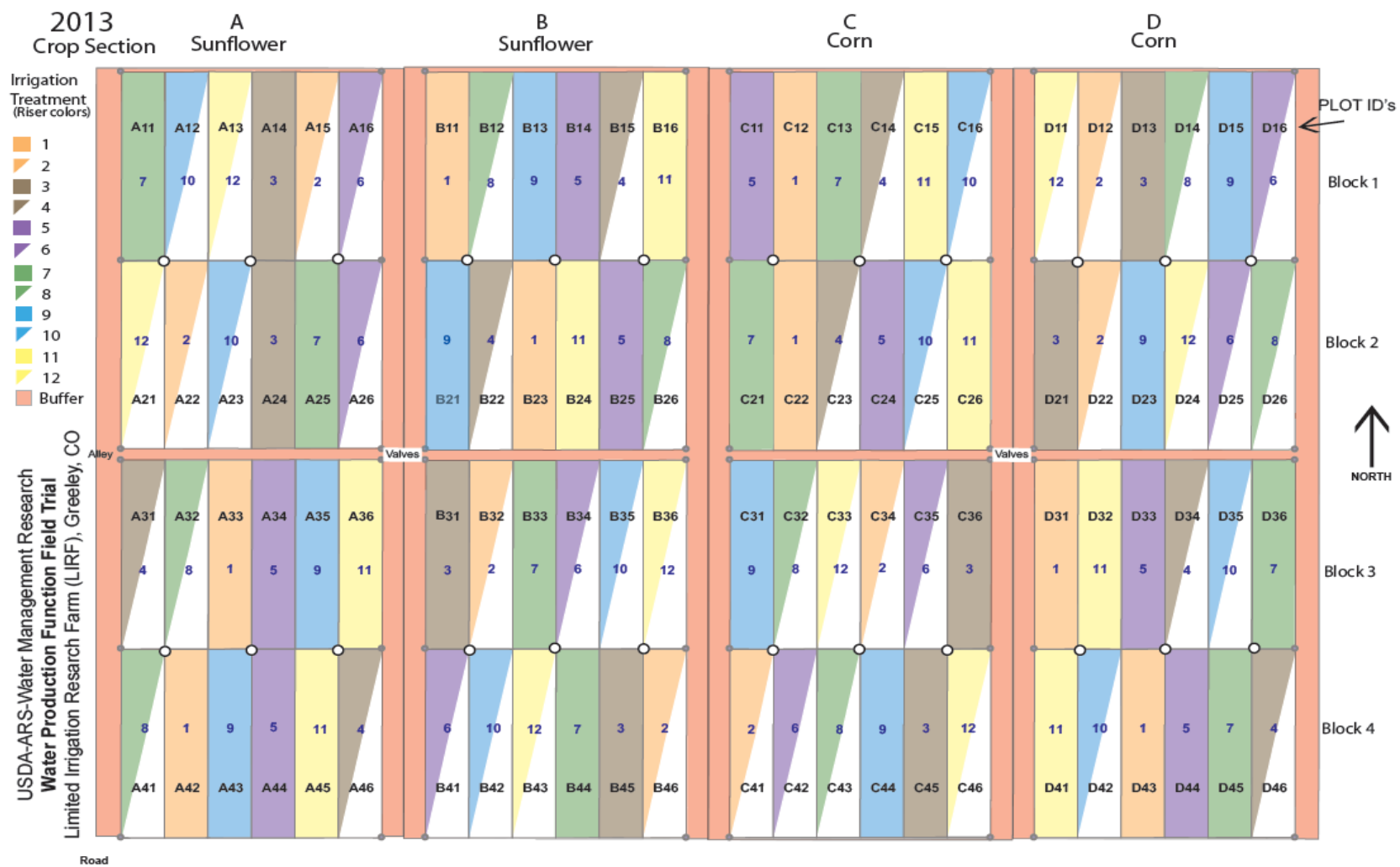
## CHAPTER 2: METHODOLOGY

### 2.1 General Overview

For this study data were collected during the 2013 growing season at the Limited Irrigation Research Facility [LIRF, (40° 26' N, 104° 38' W, and 1428 m elevation)] located near Greeley, Colo., USA. This 16 ha field research facility is run by the United States Department of Agriculture (USDA) Agricultural Research Service Water Management Unit (ARS-WMU). LIRF is made up of four main fields that are irrigated using pressurized drip irrigation with polyethylene header pipes connected to drip irrigation tubing (16 mm diameter, thick walled tubing with 1.1 L/h conventional inline emitters spaced 30 cm apart). The soil type is mainly sandy loam. In the 2013 field season two of the fields (A and B) were planted with sunflowers (*Helianthus annuus L.*) while the other two fields (C and D) were planted with corn (*Zea mays L.*), both fields are on an annual corn-sunflower rotation which started in 2012 (Figure 3.1). For this study only the data from the corn fields were used, due to poor emergence in the sunflower plots in 2013. Only one year of data was available for use as the sensors used in this project were purchased after the 2012 growing season. There were four replicates for each irrigation treatment, twelve total irrigation treatments, thus 48 total plots of each crop. Each plot was 40 m long (north to south orientation) and twelve rows wide with 0.76 m row spacing, and six border rows on each side of the field between fields (Figure 3.1). Each treatment received a varying amount of irrigation water depending on major growth stage and a percentage of full actual  $ET_c$ . Actual  $ET_c$  from the water balance was determined from neutron moisture meter volumetric soil water content samples that occurred two to three times per week, as well as estimates of  $ET_c$  based on reference ET and basal crop coefficients ( $K_{cb}$ ). For full crop ET Treatment 1 (100/100)

received an amount of water (net) equal to 100% of ET applied during vegetative growth stages and 100% during maturation growth stages, while Treatment 2 (100/50) received 100% ET applied during vegetative growth stages and 50% of its full ET applied during maturation growth stages. All of the treatments received full ET during the reproductive growth stage (tasseling and silking), to prevent yield loss during this critical growth stage. All twelve of the treatments target ET amounts are shown in Table 2.1. Target ET is not always achieved depending on precipitation, soil variability, leaks or breaks in the irrigation system.

Just south of the main plots in LIRF was the field used to verify the results found in this study (Figure 2.2). This adjacent site, referred to as the Sustainable Water and Innovative Irrigation Management (SWIIM) field, is the site of a collaborative project between USDA-ARS-WMU, Regensis Management Inc., Colorado Northern Water Conservancy District, and Colorado State University. This field was also planted in corn, but furrow irrigation with gated pipe was used instead of drip. SWIIM field was divided into three different plots, one fully irrigated (FI), one high frequency deficit irrigated (HFDI), and one low frequency deficit irrigated (LFDI, Figure 2.3). Each plot was composed of 63 rows, with 0.76 m row spacing and 396 m long. The dominant soil type where measurements were taken in SWIIM field is clay. However, the field is highly variable with other types of soils including sandy and alluvial soils. For further detail on field layout, soil type, sensors, etc. see Taghvaeian et al. (2013).



Total area 11.5 ac (5ha). 2 Crop rotation: Corn, Sunflower. Plot size: Width (12 row at 30" centers) 9m (30 ft), Length 44m (144 ft). 6 row or 4.5m (15 ft) buffers between crops.  
 12 Irrigation treatments (percent ET applied during vegetative growth stages / percent ET applied during maturation growth stages). All treatments receive full ET during reproductive stage.  
 1 = 100/100, 2 = 100/50, 3 = 80/80, 4 = 80/65, 5 = 80/50, 6 = 80/40, 7 = 65/80, 8 = 65/65, 9 = 65/50, 10 = 65/40, 11 = 50/50, 12 = 40/40.

Figure 2.1. LIRF Field Layout Schematic. Number in each plot (i.e. A11) is a plot identifier used in data collection and logistics. Text in middle of plot identifies ET treatment, defined in Table 2.1.



Figure 2.2. LIRF and SWIM Location

Table 2.1. Percent of maximum ET applied for each treatment during the vegetative and maturity growth phases, respectively. All treatments received 100% ET during the reproductive (tasseling and silking) phase

Treatment	Percent ET Applied	
	Vegetative Growth Stage	Maturity Growth Stage
1	100	100
2	100	50
3	80	80
4	80	65
5	80	50
6	80	40
7	65	80
8	65	65
9	65	50
10	65	40
11	50	50
12	40	40

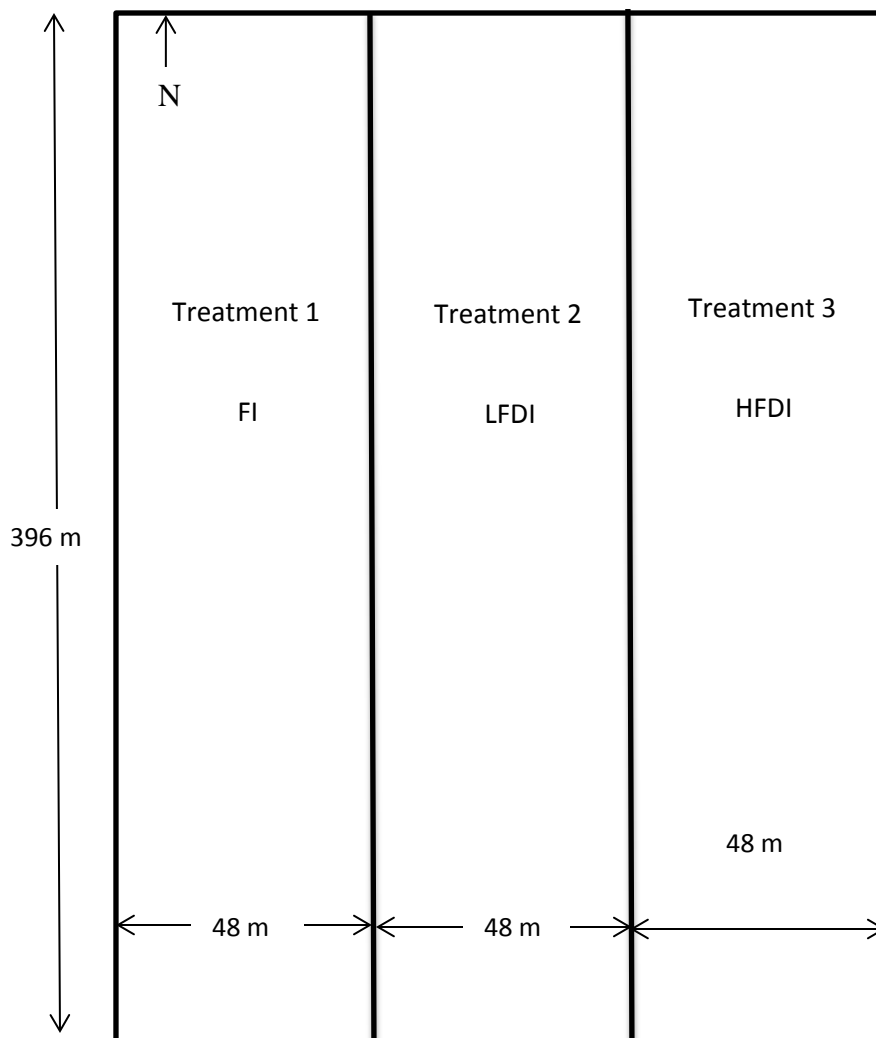


Figure 2.3. Layout of SWIIM field, Irrigation pipe was placed at north end of field, which is sloped downward going south.

## 2.2 Data Collection

Typically twice a week throughout the growing season a “high boy” tractor was run through the fields collecting remote sensing measurements (Figure 2.4). Measurements were typically taken around local solar noon (11a.m. to 1 p.m. MST). The frame of the “high boy” tractor is roughly 2 meters off the ground, and has a boom three meters in length on it. At the end of the boom is a sensor platform, that when the boom is extended is roughly 7.6 meters directly above the middle of the plot (Figure 2.5).



Figure 2.4. High Boy Tractor with sensor platform being run through the corn field

On the sensor platform there is a multispectral “FLUX” camera (FluxData, 3 CCD 3 Channel configuration: green (550nm), red (645nm), and NIR (825nm), Type ICZ285, 6.45 micron pixel, 1.4MP CCD sensor chip, 17fps). There are also two SKYE light sensors to measure reflected (model SKR1850ND) as well as incident (model SKR1850D) light at four different wavelengths (450nm-520nm (blue), 520nm-600nm (green), 630nm-690nm (red), and 760nm-900nm (NIR)). The last two items on the platform are a standard Canon 50d RGB digital camera and an antenna for GPS data collection (Trimble, AgGPS542, Zephyr Model 2 Antenna). The other

instrumentation on the sensor platform includes an infrared thermometer (IRT) and a forward-looking infrared (FLIR) thermal imaging camera; however data from this equipment were not used in this study and therefore will not be discussed further.

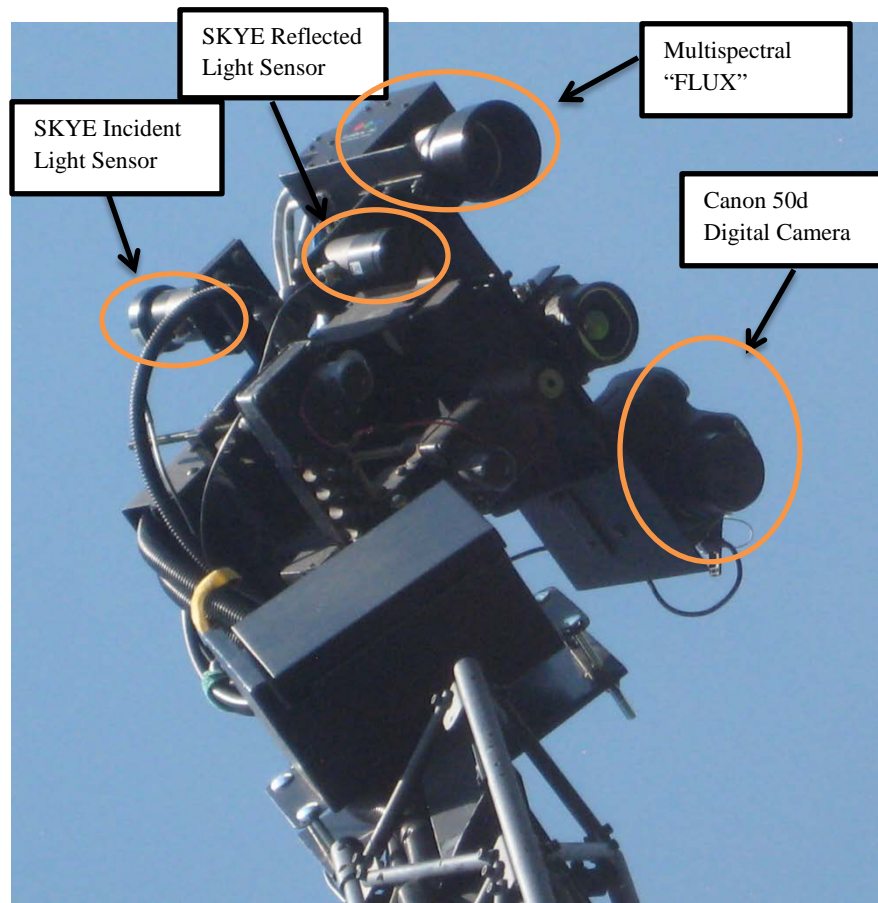


Figure 2.5. Sensor platform layout and descriptions. GPS antenna is hidden from view.

In order to obtain images, the tractor stopped at a pre-selected position in each plot. At the preselected spot in each plot a picture was taken with the Canon digital camera and the FLUX multispectral camera was triggered to take three simultaneous images (one for each band). A CR3000 (Campbell Scientific Inc., Logan, UT) data logger collected data every second from the SKYE light sensors. A laptop computer collected the GPS data, triggered the FLUX camera, and

monitored in real time the incoming light sensor data. A handheld push button was used to take pictures with the Canon 50d digital camera.

Besides data collected from the highboy tractor, other ground-based measurements were made. Growth stage data were taken twice a week in every plot, in order to keep track of how the corn was progressing. Canopy temperature data ( $^{\circ}\text{C}$ ) were collected continuously with IRTs (Apogee, SI-121-L29) placed for the growing season in priority plots: treatments 1, 2, 3, 6, 8, and 12. To obtain data from the center of the plot the IRTs were placed in the fourth row of each plot, facing  $45^{\circ}$  east of north, and pointed  $22^{\circ}$  below the horizon. IRTs were adjusted three times a week up until tasseling to maintain a height of 0.76 meters above canopy height. These IRTs were connected to CR1000 Campbell Scientific data loggers that sampled data every 5 seconds, and recorded 30 minute averages. Soil moisture measurements were made with a neutron probe (CPNInstroteck, 503DR AM-241) for depths of 30 cm to 200 cm typically before and after every irrigation event in every plot thus typically 2 or 3 times per week. A handheld time domain reflectometer (TDR) (miniTrase, 6050X3K1) was used to get soil moisture measurements at the 15 cm depth on the same days as the neutron probe measurements were made.

In SWIIM field IRTs were placed in each plot in order to obtain canopy temperature measurements. Neutron probe (CPNInstroteck, 503DR AM-241) readings were taken typically twice a week in order to obtain volumetric water content in each of the three treatments. A couple of multispectral radiometers with 5 channels (MSR5, CropScan, Inc. S/Ns: 570 and 586) were used about twice a week to obtain measurements of reflected light, in the five different wavelengths, from the canopy. Measurements were done using a telescoping pole to keep the sensor above the height of the corn, in order to take accurate readings. A Canon 50d camera was

used to obtain RGB images at different locations in the field using a telescoping pole to keep the camera over top the canopy.

## 2.3 Data Processing Methods

### 2.3.1 Imagery Processing and Geo-referencing

After a single day of ground-based remote sensing, the data that have been collected, from all of the plots, were taken to the office for post-processing. The first step was to process the images from the Canon and FLUX multispectral cameras. In order to obtain just one image from the FLUX camera, the three different band images (Figure 2.6a, b, and c) were combined to make one composite image using the ArcGIS “Composite Bands” tool (ESRI 2011. ArcGIS Desktop: Release 10.1). After the images were combined, the software created one composite color infrared image (CIR). In the composite image the NIR band is seen as the color red, and therefore vegetation is depicted in the CIR images by various shades of red (Figure 2.6d). Next the CIR images were processed through a VF program created by the ARS-WMU in R Project (R Package version 2.15.3) that turns the red (vegetation) pixels from the CIR image into white and all other (non-vegetation) pixels into black, information from which VF can then be calculated (Equation 1.36).

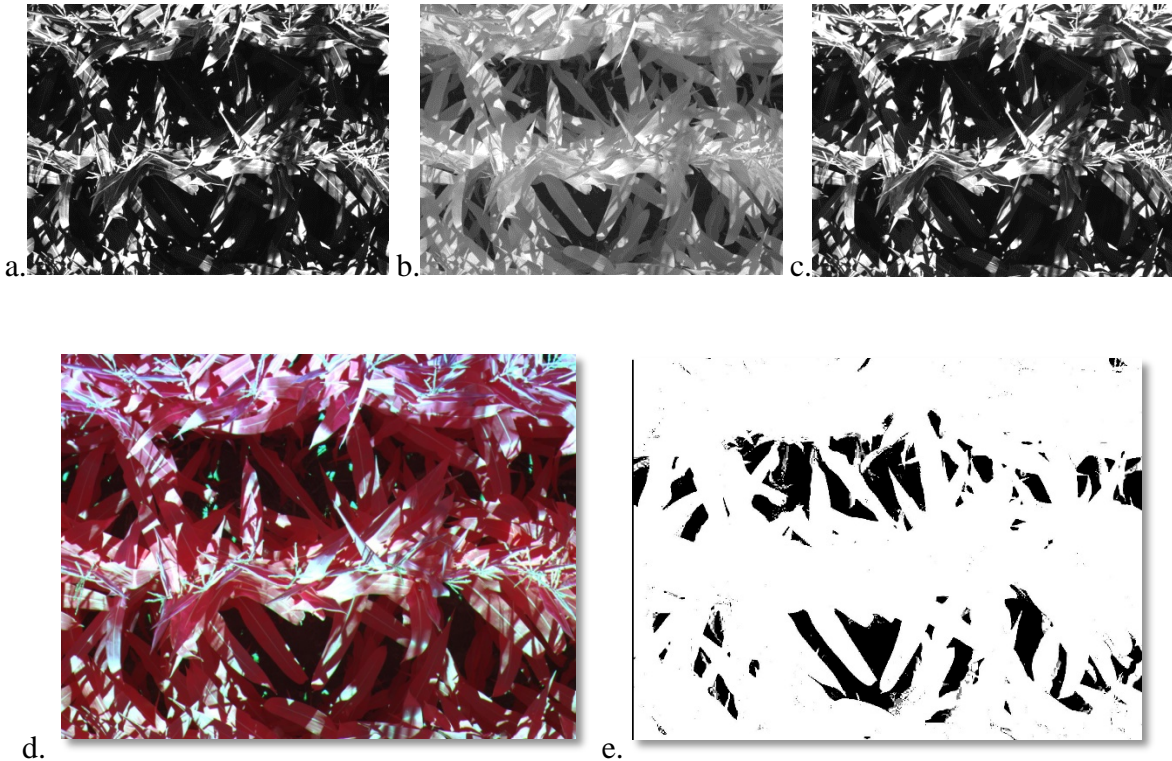


Figure 2.6. Processing example for FLUX multispectral camera. All images are from plot C12 (Treatment 1), DOY 214. The corn just began reproduction (growth stage of R1). a.) Red bandwidth image b.) NIR bandwidth image c.) Green bandwidth image d.) CIR composite image e.) Final Processed Image from VF program (VF = 0.86).

The Canon RGB images were also processed through the VF program in R Project, to calculate VF. For RGB images the program calculates the ratio of green pixels to total pixels in the image. Example images for the Canon original RGB image, and the processed image output by the VF program are shown in Figure 2.7. The image timestamp for both the FLUX images and the Canon images were geo-referenced in ArcGIS in order to identify what plot each image was from. Data collected by the data logger were also time-stamped, which can also be linked to the GPS data using ArcGIS. All of the data collected allowed for each plot in the field to have a CIR image, a RGB image, incident and reflected light wavelength data that were geo-referenced for every dataset taken with the highboy tractor.

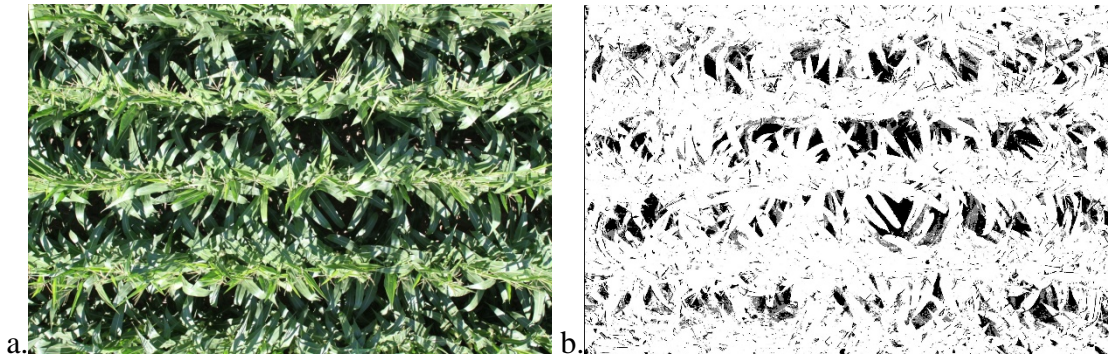


Figure 2.7. Processing example from Canon RGB camera. Both images are from C12 (Treatment 1) DOY 214 a) Red Green Blue image from Canon 50d. b.) Processed image output from VF program in R Project (VF = 0.82)

### 2.3.2 Calculation of Vegetation Indices

When all of the data were geographically linked, the vegetation indices were calculated for every plot. The SKYE light sensors were used to obtain light wavelength readings in every plot, these readings were used to calculate vegetation indices instead of the FLUX multispectral images. SKYE sensors were used instead because four different wavelengths could be measured (Red, Green, Blue, NIR) unlike with the FLUX multispectral images where only three wavelengths were measured (Red, Green, NIR). In order to be able to calculate vegetation indices from the SKYE sensors, both the incident and reflected light data needs to be used. The incident SKYE sensor has a cosine corrector that only allows light to be measured from the 180° hemisphere above the sensor, helping to eliminate measurement errors when the sun is not directly above the sensor. Without the cosine correcting head the sensor measures a 25° cone. SKYE corporation only provides an exact calibration for the sensor that has the cosine correcting head (only on the incident SKYE sensors), therefore a ratio sensitivity value ( $Z$ ) needs to be applied to the reflected values. This  $Z$  value is provided by SKYE with the sensor calibration certificate. For instances the NIR reflected values would be multiplied by the  $Z$  value in order to be able to compare to the

Red reflected values. Equation 2.1 shows how NDVI is calculated using the SKYE light sensor data, for which  $NIR_R$  is the NIR reflected light,  $NIR_I$  is the NIR incident light,  $Red_R$  is the red reflected light, and  $Red_I$  is the red incident light.

$$NDVI = \frac{\left(\frac{Z * NIR_R}{NIR_I}\right) - \left(\frac{Red_R}{Red_I}\right)}{\left(\frac{Z * NIR_R}{NIR_I}\right) + \left(\frac{Red_R}{Red_I}\right)} \quad (2.1)$$

GNDVI is calculated using Equation 2.2, in which  $Green_R$  is the Green reflected light, and  $Green_I$  is the green incident light.

$$GNDVI = \frac{\left(\frac{Z * NIR_R}{NIR_I}\right) - \left(\frac{Green_R}{Green_I}\right)}{\left(\frac{Z * NIR_R}{NIR_I}\right) + \left(\frac{Green_R}{Green_I}\right)} \quad (2.2)$$

OSAVI is calculated using Equation 2.3, and WDRVI is calculated using Equation 2.4.

$$OSAVI = \frac{\left(\frac{Z * NIR_R}{NIR_I}\right) - \left(\frac{Red_R}{Red_I}\right) * 1.16}{\left(\frac{Z * NIR_R}{NIR_I}\right) + \left(\frac{Red_R}{Red_I}\right) + 0.16} \quad (2.3)$$

$$WDRVI = \frac{\left(\alpha * Z * \frac{NIR_R}{NIR_I}\right) - \left(\frac{Red_R}{Red_I}\right)}{\left(\alpha * Z * \frac{NIR_R}{NIR_I}\right) + \left(\frac{Red_R}{Red_I}\right)} \quad (2.4)$$

As discussed in Chapter 2,  $\alpha$  (Equation 2.4) is defined as a factor that is less than one and recommended to be between 0.05 and 0.2 (Gitelson, 2004) recommended a value of 0.05 to 0.2 be used. Therefore to find what value of  $\alpha$  should be used, five different values (0.1, 0.2, 0.3, 0.4, 0.5) were tested to determine the best fit when WDRVI was plotted against VF. Out of the three values tested 0.3 gave the highest coefficient of determination ( $R^2$ ) and best visual fit.  $R^2$  is calculated as

$$R^2 = 1 - \frac{\sum_{j=1}^n (y'_j - \bar{y})^2}{\sum_{j=1}^n (y_j - \bar{y})^2} \quad (2.5)$$

where  $y'$  is the estimated value,  $\bar{y}$  is the averaged value, and  $y$  is the independent reference measurement.

Once the vegetation indices were calculated, all of the vegetation indices were plotted versus measured VF in order to verify the accuracy of the indices. As stated in Chapter 2, theoretically indices should have a strong relationship with VF because as VF fluctuates, indices will also fluctuate. For instance as corn leaves get bigger (VF increases), the leaves will reflect more NIR and absorb more Red and therefore the indices values will also increase.  $R^2$  was calculated for each index in order to determine strength of relationship with VF. The equation that was obtained for each index when a trend-line was fit to each index was also used to estimate VF. Estimated VF was then compared to the observed VF by using root mean square error (RMSE, Equation 2.6).

$$RMSE = \sqrt{\frac{\sum_{j=1}^n (y'_j - y_j)^2}{n}} \quad (2.6)$$

Along with RMSE, mean bias error (MBE, Equation 2.7) and mean absolute error (MAE, Equation 2.8) were also calculated to compare the estimated VF and the observed VF from imagery.

$$MBE = \frac{\sum_{j=1}^n y'_j - y_j}{n} \quad (2.7)$$

$$MAE = \frac{\sum_{j=1}^n |y'_j - y_j|}{n} \quad (2.8)$$

#### 2.4 Water Stress Crop Coefficient Calculation

Water stress coefficient ( $K_s$ ) is then calculated daily using two different methods for estimating daily crop ET. A water balance for each method was used to track/monitor daily stress induced

on the crop. In both methods the procedure outlined in Trout and Johnson (2007) was used to calculate  $K_{cb}$  and the method in the FAO-56 publication was followed for calculating  $K_e$ . The two methods differ in how  $K_s$  is estimated, which are determined by either (1) FAO-56 or (2) Bausch et al. (2011). The second method was only done for Treatments 1, 2, 3, 6, 8, and 12 as continuous IRT data were only available for those treatments.

#### 2.4.1 FAO-56 Procedure

Potential crop ET was calculated following FAO-56 guidelines by not incorporating the stress coefficient in order to set an upper limit of ET (e.g. assuming  $K_s = 1$  in Equation 1.16).

Calculating potential ET using this procedure was used as an envelope for determining the upper limit of daily ET in the field. In order to calculate ET following FAO-56 using the dual crop coefficient approach, the first step is to calculate  $K_c$ . Equation 2.9 defines  $K_c$  for FAO-56 procedures without including stress.

$$K_c = K_{cb} + K_e \quad (2.9)$$

The basal crop coefficient  $K_{cb}$  is obtained from tabular values in FAO-56 (Allen et al. 1998).

Three different  $K_{cb}$  values are chosen: one for initial, mid, and end of season, then  $K_{cb\ mid}$  and  $K_{cb\ end}$  are adjusted for local climatic conditions. Then a different table in FAO-56 is used to determine the length of time each  $K_{cb}$  value applies for and linear interpolation is used to get from one value to the next. A  $K_{cb}$  curve is then constructed in order to get daily  $K_{cb}$  values. This method is normally applied when using grass-based reference ET, but for this project alfalfa based (tall) reference ET is being used and a different method has to be applied. In the ASABE Monograph (Chapter 8, Allen et al., 2007) the alfalfa-based  $K_{cbr}$  crop coefficients can be

obtained. The table containing the  $K_{cb}$  values in the ASABE Monograph is divided into two sections, percent time from planting to effective full cover date, and days after effective full cover date. It was assumed to be able to use this table that corn in all regions progresses at the same rate, which in many climates is not a valid assumption. From this table a  $K_{cb}$  curve for  $ET_r$  was made, which is applied to all treatments (Figure 2.8).

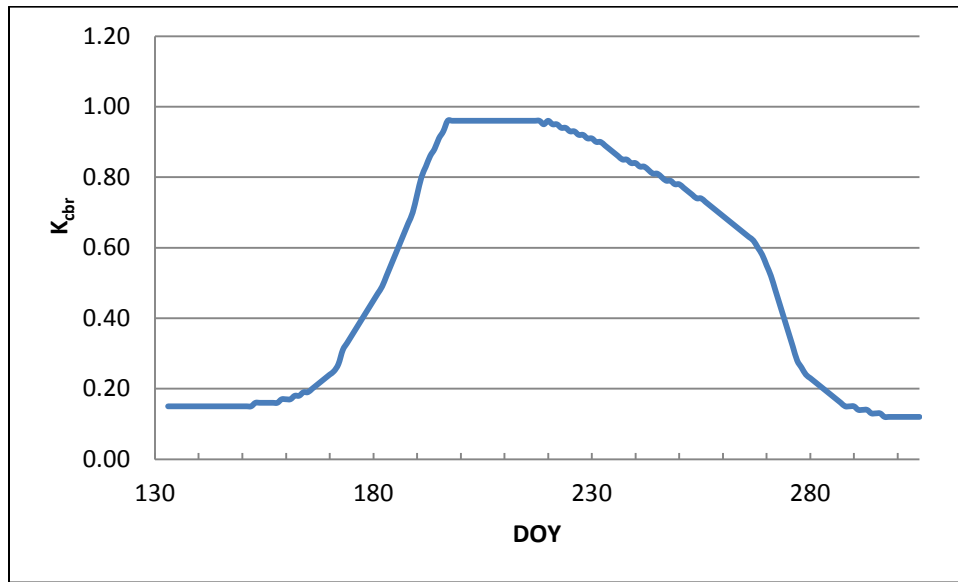


Figure 2.8.  $K_{cb}$  values over the corn growing season

For the calculation of  $K_e$ , instead of using Equation 1.24 to calculate  $K_{c\ max}$ , Equation 2.10 was used because, as stated before, for this project the alfalfa reference ET ( $ET_r$ ) was used and Equation 1.24 is for the grass reference ET ( $ET_o$ ).

$$K_{c\ max\ r} = \max(1.0, \{K_{cbr} + 0.05\}) \quad (2.10)$$

To calculate  $K_r$  (Equation 1.23), Readily Evaporable Water (REW) and Total Evaporable Water (TEW) values are needed, which can be obtained from FAO-56 (Allen et al., 1998). Because LIRF has a mainly sandy loam soil, a REW value of 8 mm was chosen and a TEW value of 28

mm was chosen. In the calculation of fraction of ground surface wetted  $f_{ew}$  (Equation 1.25) a value of 0.35 was chosen from FAO-56 (Allen et al., 1998).  $K_e$  can then be calculated (Equation 1.22), and therefore  $K_c$  (Equation 2.9) can also be calculated. After  $K_c$  is calculated, crop ET was then calculated using Equation 1.26. In Equation 1.26  $ET_r$  is calculated using the ASCE-EWRI (2005) Standardized Penman-Monteith Method (Equation 1.1). Wind speed, solar radiation, actual vapor pressure and temperature data were obtained from the weather station located at LIRF (CoAgMet Weather Station Network, Station GLY04, [www.coagmet.com](http://www.coagmet.com)), just west of the sunflower fields (Figure 2.2).

#### 2.4.2 Calculation of $K_{cb}$ and $K_e$

For both methods of calculating actual crop ET,  $K_{cb}$  and  $K_e$  are calculated the same way.  $K_{cb}$  is calculated using the Trout and Johnson (2007) method of calculating  $K_{cb}$  based on canopy cover throughout the growing season (Equation 1.18). Trout and Johnson (2007) originally calibrated the “a” and “b” values by plotting  $K_{cb}$  values obtained from a weighing lysimeter versus observed canopy cover values for bell peppers. Since there is no weighing lysimeter at LIRF, the values were calibrated using  $K_{cb}$  values obtained from actual crop ET calculated using air temperature and vapor pressure values collected with a Bowen Ratio Energy Balance system, located at LIRF, and using the coefficients originally calibrated from the weighing lysimeter. The ARS-WMU computations resulted with coefficient values of  $a = 0.15$  and  $b = 1.01$ , which were used for this project; therefore Equation 1.18 with the constants included becomes Equation 2.11. VF calculated using Equation 1.36 was only used if VF was less than full cover (assumed to be 0.80). If VF was greater than full cover, a maximum  $K_{cb}$  value of 0.96 was used.

$$\text{If } VF \leq K_{cb} \text{ Then } K_{cb} = 1.01 VF + 0.15 \text{ else } K_{cb} = 0.96 \quad (2.11)$$

$K_e$  was calculated using FAO-56 procedures which were described in section 2.4.1.

#### 2.4.3. $K_s$ Calculation following FAO-56

$K_s$  was calculated following FAO-56 procedures. In order to calculate  $K_s$  Equation 1.20 was used. According to FAO-56 (Allen et al. 1998) TAW is defined by Equation 2.12, and RAW is defined by Equation 2.13. In Equation 2.13  $p$  (fraction of depletion) is assumed to be 0.5.

$$TAW = (FC - WP)RZ \quad (2.12)$$

$$RAW = pTAW \quad (2.13)$$

For Equation 2.12 FC is the field capacity (mm/mm, %), WP is the wilting point (mm/mm, %), and RZ is the root zone depth (mm). In Equation 2.13  $p$  is the fraction of TAW that a crop can extract from the root zone without suffering from water stress. After  $K_s$  was calculated for every day Equation 1.20 was used to calculate ET in which  $ET_{ref}$  was calculated as explained in section 2.2.2.

#### 2.4.4 $K_s$ Calculation by $T_c$ ratio

For the second method of calculating actual crop ET,  $K_s$  was calculated using Bausch et al. (2011) method using canopy temperatures. To obtain canopy temperature values for both the non-stressed and stressed corn plots, semi-permanent IRTs were installed in plots for Treatments 1, 2, 3, 6, 8, and 12. Because of equipment restrictions IRTs could not be placed in every plot. While IRTs take a reading every five seconds, the data logger compiles these into half an hour

averages. Since there are four plots for every treatment, the four IRT values were averaged together to obtain one averaged canopy temperature value for each treatment that had IRTs. According to Bausch et al. (2011), IRT data collected from 13:00 to 15:00 should be used because this is the time of day when most stress occurs. Therefore for each day the IRT data from 13:00 to 15:00 were averaged to get a single daily IRT value for each treatment. Although IRTs were installed on DOY 183, Bausch et al. (2011) states that full cover needs to be achieved to use the  $T_{c \text{ ratio}}$  method, so this method was applied beginning on DOY 205, when 0.80 VF cover was achieved, and ending right before harvest (DOY 290). While all of the plots developed at different rates DOY 205 was assumed to be date of full cover for all of the treatments.  $T_{c \text{ ratio}}$  could then be calculated by calculating the ratio of canopy temperature of the non-stressed corn to the stressed corn (Equation 1.21). Since Treatment 1 is fully irrigated, it is assumed to have no stress and therefore  $K_s$  for Treatment 1 was equal to one for the entire season. For all of the other treatments Equation 1.21 is used with Treatment 1 average canopy temperatures being used as the non-stressed temperature ( $T_{c \text{ ns}}$ ).

#### 2.4.5 Water Balance

As daily ET is calculated (for each method) a water balance was created that tracked the irrigation events (I), effective precipitation events (P), deep percolation (DP) and calculates soil moisture deficit ( $D_i$ ) (Equation 1.27). When the  $D_i$  becomes greater than the readily available water (RAW) in the root zone (Equation 2.13), stress is assumed to occur in the corn. RAW is calculated daily; therefore it changes with root zone depth which is estimated throughout the growing season. Effective root zone depth ranges from a minimum value of 50 mm to a maximum value of 1050 mm. In order to calculate the TAW for use in Equation 2.13, the field

capacity in the root zone ( $FC_{RZ}$ ) was calculated. Field capacity of the root zone was determined as a weighted average of the field capacity of each layer the root zone covered. Field capacity values are specific to each plot, and separated into layers from 0-150 mm, 150-450 mm, 450-750 mm, and 750-1050 mm. After  $FC_{RZ}$  has been calculated, TAW in the root zone can be calculated using Equation 2.14, in which  $p$  is the depletion fraction of TAW in the root zone and was assumed to have a value of 0.5.

$$TAW = p \cdot FC_{RZ} \quad (2.14)$$

Deep percolation was calculated by first assuming that no deep percolation occurred and calculating the deficit, and then if the deficit was found to be negative then deep percolation was set equal to the negative deficit (an over replenishment of water in the root zone), and the deficit was re-calculated with the new value for deep percolation:

$$\text{If } D_i < 0 \rightarrow DP = -D_i \text{ otherwise } DP = 0$$

On days that soil moisture observations were taken the deficit used by the water balance was set equal to the soil water deficit calculated from volumetric soil water content readings. TDR readings taken at 150 mm and neutron probe readings taken at 300, 600, and 900 mm were used in the calculation of the soil water deficit. A calibration curve was used to obtain percent volumetric water content (VWC, %) from each of the readings. To obtain the soil water deficit (SWD), VWC (%) was subtracted from FC (%). FC for each treatment and for each depth (0 to 150, 150 to 450, and 750 to 1050 mm) was obtained from estimates from the ARS-WMU (Table 2.2).

Table 2.2. Average FC values for every treatment for four different depths

Treatment #	Depth (mm)			
	150	150-450	450-750	750-1050
1	28.0%	27.3%	20.8%	22.6%
2	27.3%	25.9%	24.8%	16.5%
3	26.5%	26.0%	24.5%	20.3%
4	27.5%	27.8%	24.4%	17.4%
5	26.5%	26.3%	22.3%	21.3%
6	27.3%	24.3%	19.8%	16.1%
7	26.5%	26.5%	23.3%	19.5%
8	26.0%	25.3%	19.2%	15.0%
9	25.8%	23.5%	22.2%	16.0%
10	29.0%	26.5%	22.2%	16.8%
11	27.8%	27.0%	26.8%	21.9%
12	27.8%	24.5%	22.9%	17.6%

In order to get the data from percent deficit into mm of deficit all of the soil moisture deficits

Equations 2.15 to 2.18 were used.

$$SWD_{150}(mm) = \frac{SWD_{0-150}}{100} \cdot 150 \quad (2.15)$$

$$SWD_{300}(mm) = \frac{SWD_{150-450}}{100} \cdot 300 \quad (2.16)$$

$$SWD_{600}(mm) = \frac{SWD_{450-750}}{100} \cdot 300 \quad (2.17)$$

$$SWD_{900}(mm) = \frac{SWD_{750-1050}}{100} \cdot 300 \quad (2.18)$$

To get soil water deficit in the root zone, the root zone was divided into three sections 450, 750, and 1050 mm. This was done to match the depth that VWC observations were obtained. The equations to calculate soil water deficit at these three sections in the root zone can be seen in

Equations 2.19, 2.20, and 2.21 respectively. If the conditions in Equations 2.19, 2.20, and 2.21 are not true then the deficit is set equal to zero for that root zone section.

$$\text{If } RZ < 450 \rightarrow SWD_{450} = SWD_{150} + \frac{RZ-150}{300} \times SWD_{300} \text{ else } SWD_{450} = 0 \quad (2.19)$$

$$\begin{aligned} \text{If } RZ > 450 \text{ and } RZ < 750 \rightarrow SWD_{750} = SWD_{150} + SWD_{600} \times \frac{RZ-450}{300} + SWD_{300} \\ \text{else } SWD_{750} = 0 \end{aligned} \quad (2.20)$$

$$\begin{aligned} \text{If } RZ > 750 \rightarrow SWD_{1050} = SWD_{150} + SWD_{900} \times \frac{RZ-750}{300} + SWD_{300} + SWD_{600} \\ \text{else } SWD_{750} = 0 \end{aligned} \quad (2.21)$$

Equations 2.19 to 2.21 are then summed to obtain a final soil water deficit in the root zone ( $SWD_{RZ}$ , mm). This value is then  $D_i$  for that day in the water balance instead of using Equation 1.27. Cumulative  $D_i$  was then determined for growth stages to see the amount of  $D_i$  that occurred during each major section of growth stages: vegetative, reproduction, and maturation. This was done to determine during what growth stage did large  $D_i$  effect yield the most.

## 2.5 SWIIM Field Data Processing

In order to verify the results found from the LIRF fields, data were obtained from SWIIM field by the ARS-WMU and the same methodology was used to process the data. Since the “high boy” tractor was not driven through SWIIM field (due to furrow spacing not allowing safe travel), the spectral reflectance data obtained from an MSR5 multispectral sensor were used to obtain vegetation index values throughout the growing season. Unlike the data from the SKYE sensors, the MSR5 does not require vegetation indices to be calculated with a correction factor.

Therefore, for the MSR5 data NDVI was calculated using Equation 1.28, GNDVI using Equation

1.35, OSAVI using Equation 1.34, and WDRVI using Equation 1.29. Images taken throughout the growing season using the Canon 50d RGB camera on a telescoping pole were run through the same canopy cover program as the images at LIRF to obtain VF values throughout the growing season. Two different water balance sheets were created using the two different methods for obtaining ET described in sections 2.4.2, 2.4.3, and 2.4.4. The water balances were made using the same method as described in the previous section (2.4.5). Even though surface irrigation can be highly variable the measurements were taken 1/3 down the field from the north, where the amount of irrigation infiltrating was going to be very similar to what originally left the gated pipe.

## CHAPTER 3: RESULTS AND ANALYSIS

### 3.1 Fractional Vegetation Cover

As described in the methods section, VF was obtained from two different sets of imagery: the FLUX multispectral camera and the Canon RGB camera. Both cameras performed fairly similarly throughout the year, except that the FLUX camera had issues with becoming over saturated with light. This was mainly seen on days and in treatments where water stress was occurring and VF decreased due to leaf curling. Figure 3.1 shows VF for Treatment 1 and Treatment 12 over the growing season. The VF measured from both the RGB and the multispectral imagery follow each other fairly well for Treatment 1, Treatment 12 on the other hand showed the multispectral being fairly smooth and the RGB with more scatter. After analyzing the imagery from both cameras where the RGB and multispectral VF values were in disagreement, it was observed that on days where the crop was visually stressed (corn leaves curled) the multispectral imagery did not correctly identify the leaves well when they were not visually stressed. For instance, Figure 3.2 shows the CIR and output image from a Treatment 1 plot and a Treatment 12 plot. Figure 3.2 b shows how over saturated the FLUX camera became with the stress treatment, as the multispectral image turned blue making it very hard to process and obtain an accurate VF. The output image in Figure 3.2 b showed many of the curled leaves weren't recognized by the camera, and other leaf areas were overestimated by the camera. While the RGB images were not perfect every time they were processed, the images were much more accurate and consistent to what was observed as vegetation and what wasn't.

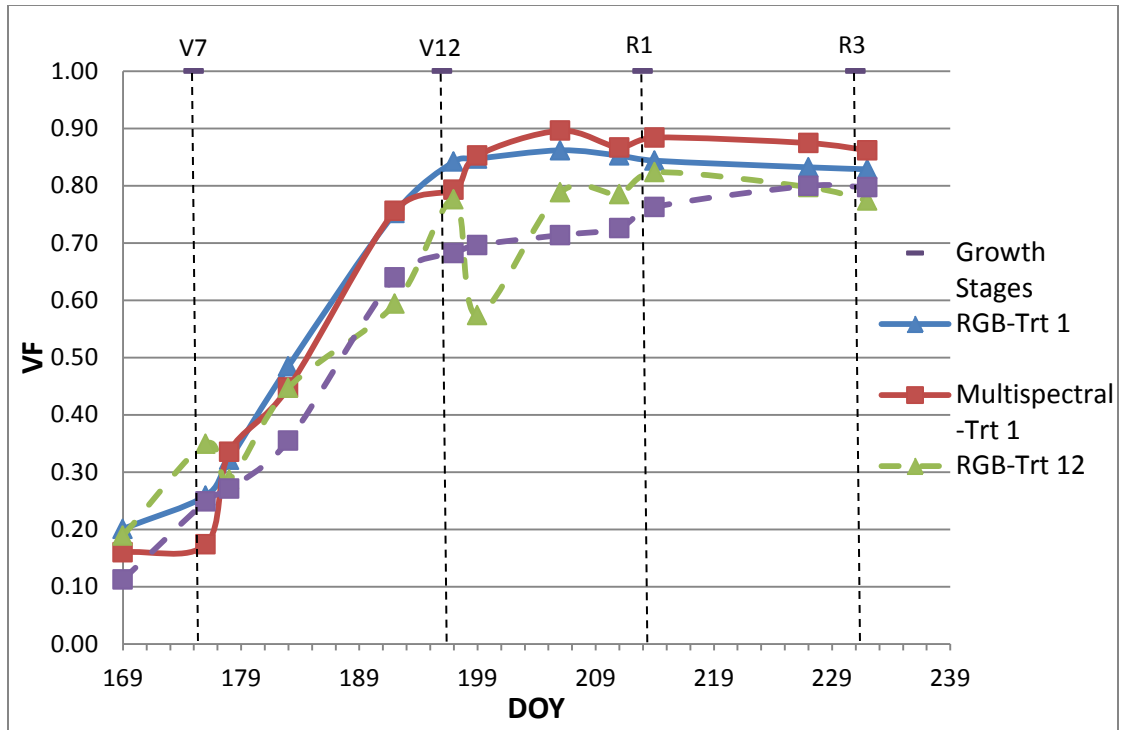


Figure 3.1. Comparison of VF obtained for RGB and multispectral images for both Treatment 1 and Treatment 12

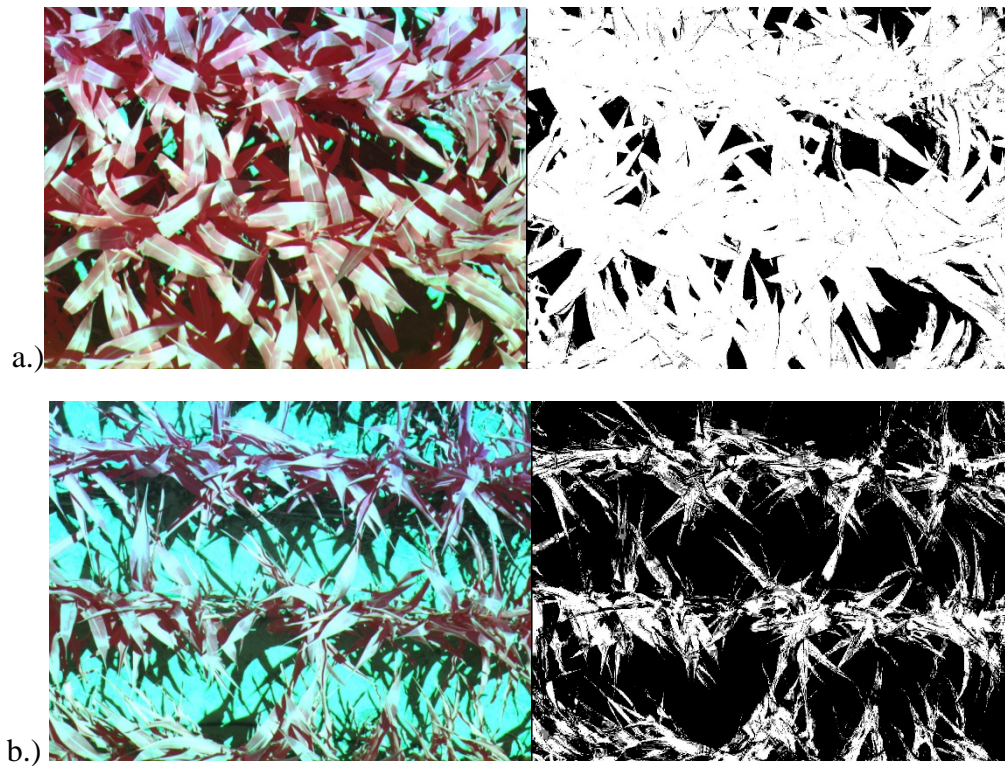


Figure 3.2. FLUX multispectral and output images for DOY 199 for a.) Treatment 1 (VF = 0.85) and b.) Treatment 2 (VF = 0.70)

Figure 3.3 shows the Canon images and output images for DOY 199 both Treatment 1 and 12 for comparison to Figure 3.2. In Figure 3.3 a and b, it can be seen that there is a shadow in the image from the boom on the highboy. This shadow had little effect on the VF as it was a small area and the leaves under the shadow were still a shade of green which the VF software was able to identify. To eliminate any error that occurred from the shadow of the boom it would be best to always take images from the west side of the plot so no shadow occurs, however data were not collected that way in 2013. Since VF needs to be used in the calculation of  $K_{cb}$  and for use with the vegetation indices, it is important to have accurate data. While the multispectral imagery worked very well with the non-stressed corn, since many days the corn was stressed the data from the RGB imagery were chosen as the better measured VF data for use in this project. This is consistent with what Alganzi et al. (2014) found that ground based digital RGB cameras did the best at estimating VF for corn and cotton. Although in that study multispectral Landsat images were used instead of a ground based multispectral camera. Smith et al. (1990) stated that one of the main limitations of using multispectral imagery is soil background effects. This was also seen with the multispectral imagery in this study since the camera had trouble mainly with days in which the crop was stressed because the camera became over saturated with soil background reflected light.

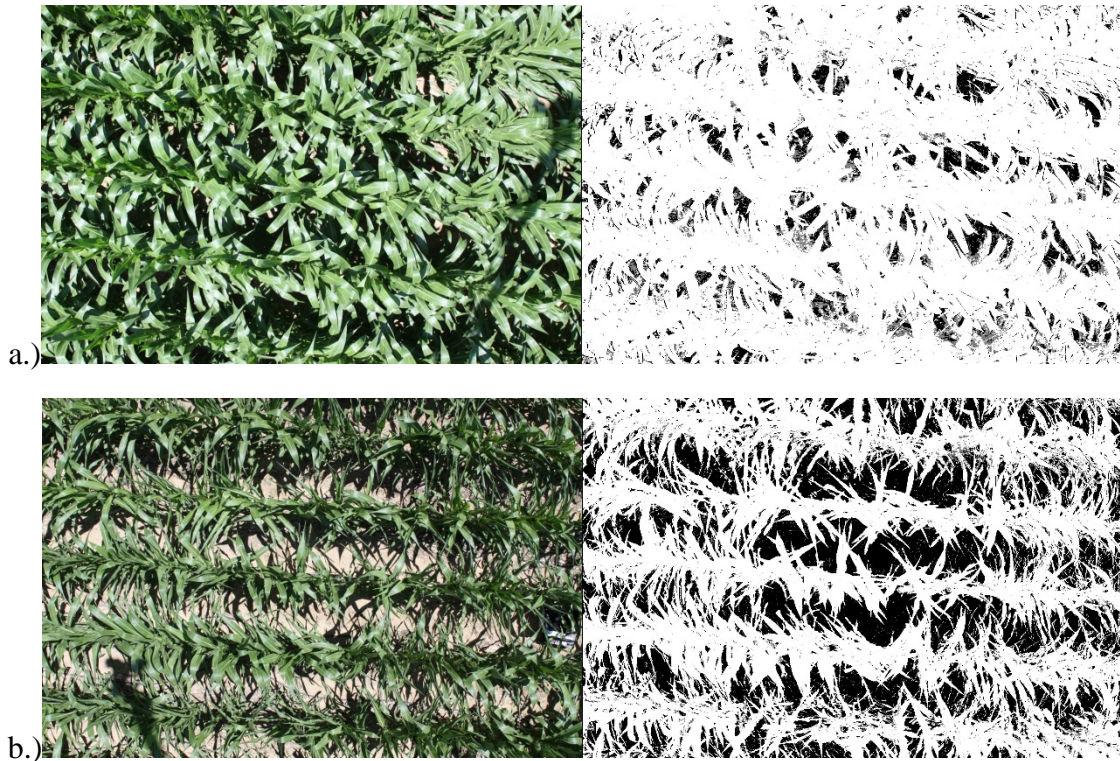


Figure 3.3. Canon image RGB and output images for DOY 199 a.) Treatment 1 (VF = 0.84) and b.) Treatment 12 (VF = 0.57)

### 3.2 Vegetation Indices

After the four vegetation indices were calculated for every day of data available, they were plotted as a time series (Figure 3.4). All of the time series did indicate days with stress, and on DOY 199 stress was the most apparent with Treatment 12 having a very low index value in all four graphs. By visual inspection WDRVI seems to have the most variations and be less of a smooth curve. To check the accuracy of the indices obtained from the SKYE sensors the indices were plotted versus VF to check that they had a strong relationship with VF. As described in the Introduction (Chapter 1), past research has shown indices should have a strong correlation (most often a linear correlation) to VF, since as VF increases the absorption and reflectance abilities of the plant increase. Figures 3.5 to 3.8 show the vegetation indices plotted versus VF.

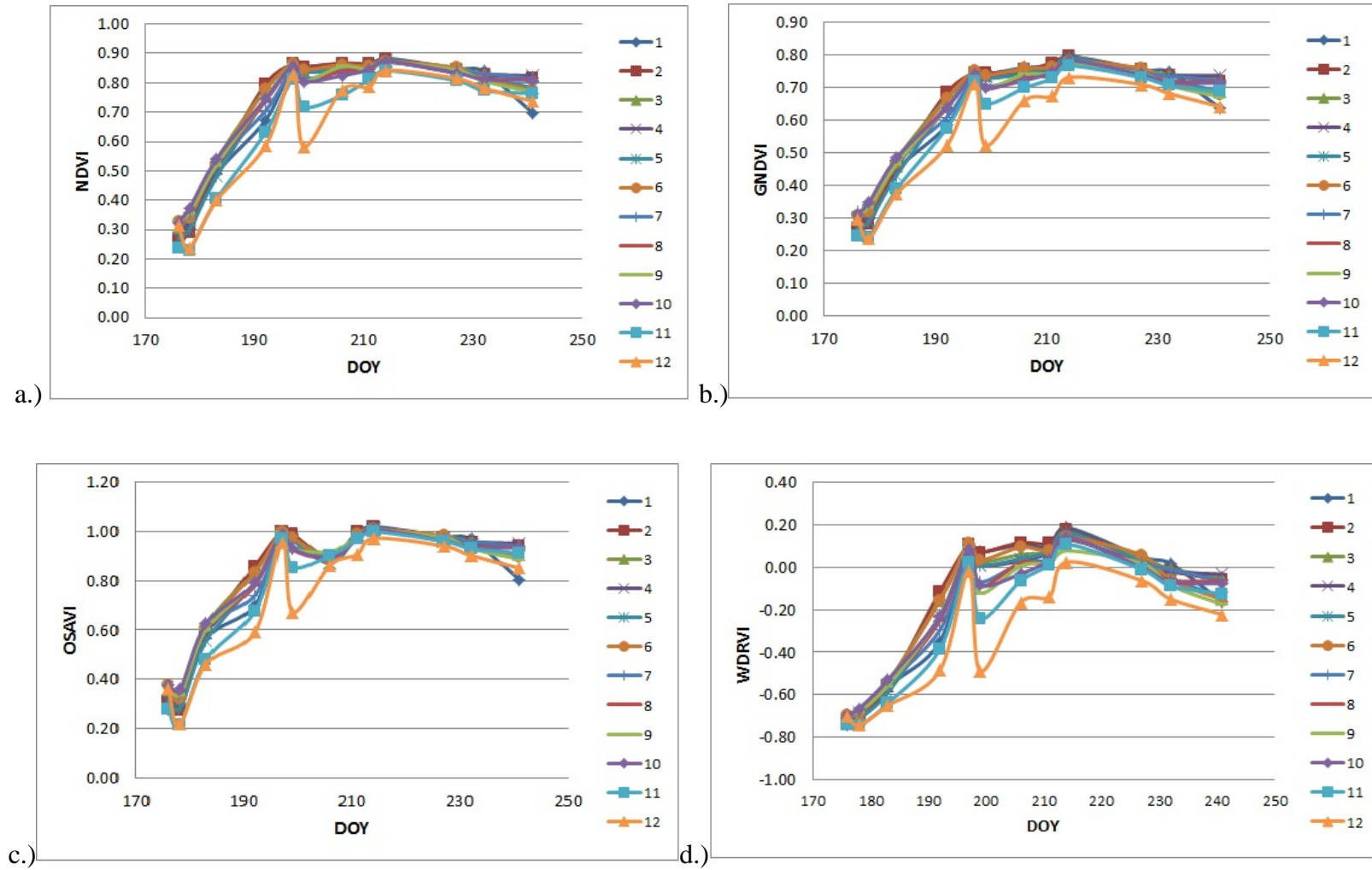


Figure 3.4. Time-series plots for all treatments of a.) NDVI b.) GNDVI c.) OSAVI and d.) WDRVI

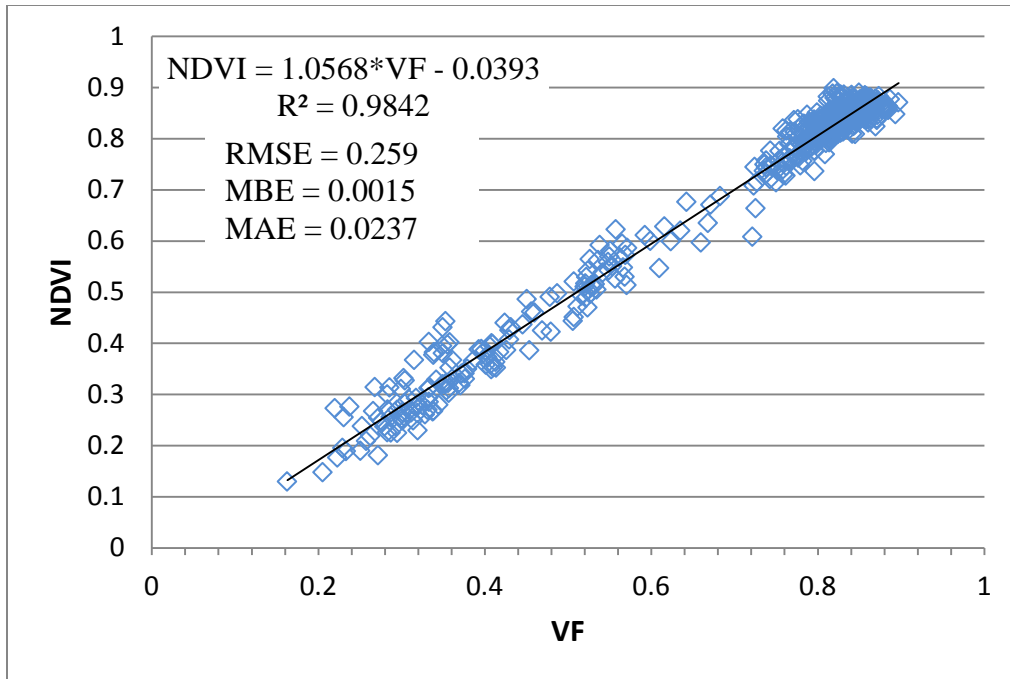


Figure 3.5. NDVI versus VF

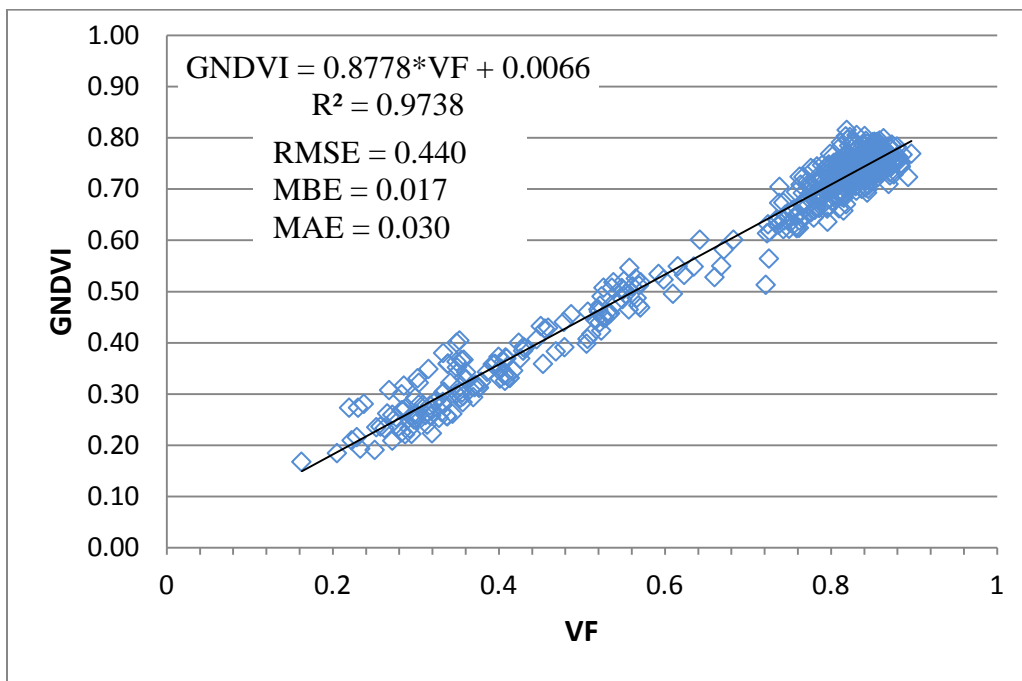


Figure 3.6. GNDVI versus VF

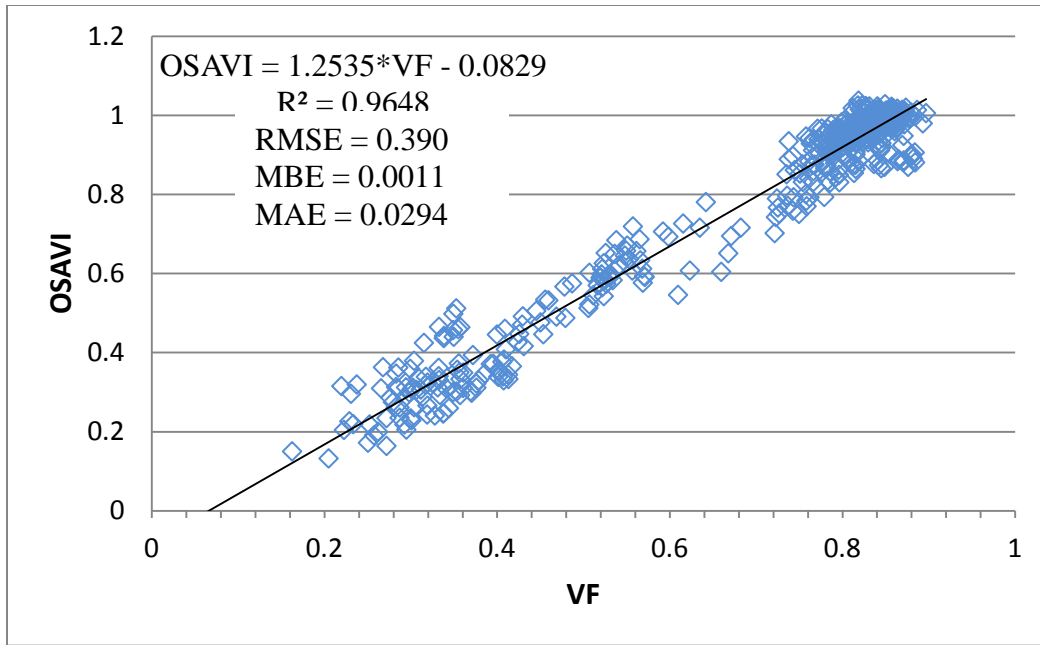


Figure 3.7. OSAVI versus VF

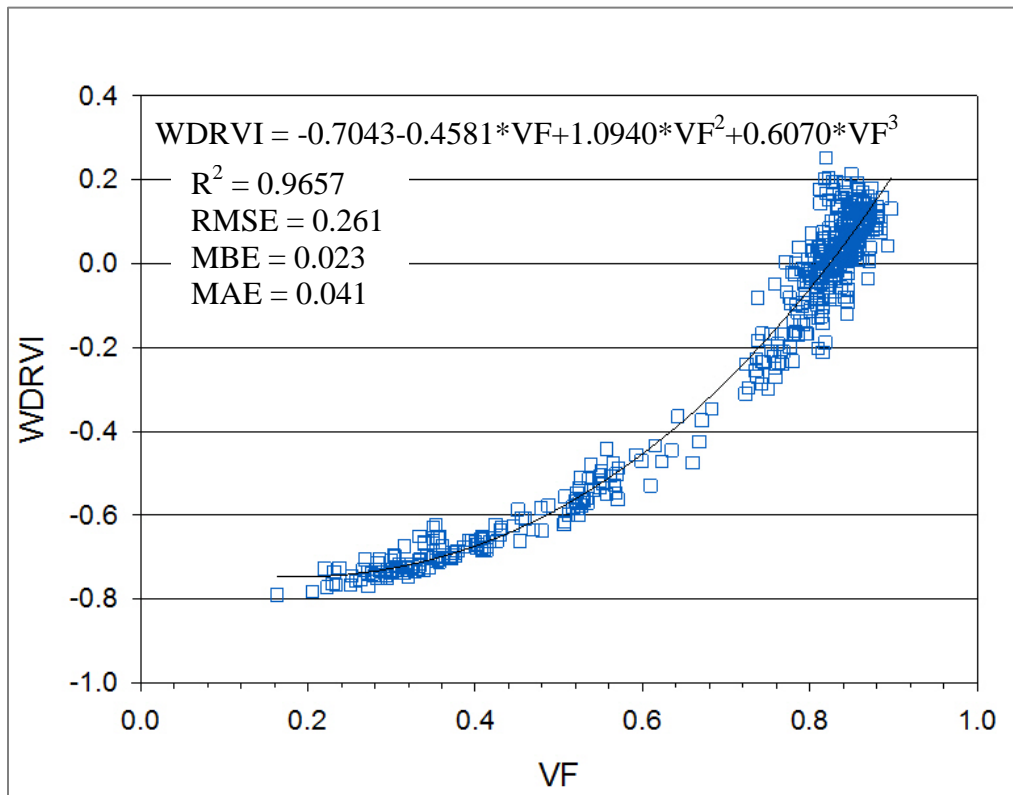


Figure 3.8. WDRVI versus VF

From Figures 3.5 to 3.8 it can be seen that all of the indices have a very strong correlation with VF. NDVI, GNDVI, and OSAVI all have linear relationships, while WDRVI has a 2<sup>nd</sup>-degree polynomial relationship with VF. NDVI had the highest R<sup>2</sup> value of 0.98 while OSAVI had the lowest at 0.96, which is still a very good R<sup>2</sup> value. The trend-line equations that can be seen in each of the Figures 3.5 to 3.8 were used to estimate VF. The trend-lines for NDVI (Figure 3.5) and GNDVI (Figure 3.6) have intercepts of almost zero which shows a well-defined relationship between the indices and VF. WDRVI in Figure 3.8 should range from -1 to 1 as was stated in Gitelson (2004). As can be seen in Figure 3.8 WDRVI maximum value at full cover is about 0.20 which is very low, it should be around 0.8 or 0.9. After this was noticed it was figured out that the format and units of the data output by the SKYE light sensors does not allow for the calculation of WDRVI correctly. The SKYE sensors cannot calculate indices like WDRVI where the NIR value is multiplied by  $\alpha$ . SKYE sensors were made more for the calculation of NDVI, not other indices. Therefore for these reasoning's WDRVI will not be used the rest of the project, since it cannot be calculated correctly. This does not mean it is not sensitive to water stress, but it will not be able to be tested in this project.

RMSE was then used to find the error between the estimated VF and the VF observed from the Canon images. The RMSE values located under the R<sup>2</sup> values on each figure indicated that each vegetation index performed well, with NDVI having the lowest RMSE value. MBE and MAE were also calculated and can be found on each of the figures as well. OSAVI had the lowest MBE value of 0.0011, and NDVI had the lowest MAE value of 0.0237. Overall all of the MBE and MAE values were very low and close to zero, which shows that there was little error between estimated VF value and the VF values measured from the Canon imagery. As indicated by RMSE and R<sup>2</sup> values, the indices have a strong correlation with VF. VF decreases with stress

in response to curling of the corn leaves. Therefore this is a good indication that the indices will also respond well to the water stress induced on the corn.

As was stated earlier in Chapter 1 not always does NDVI perform the best as seen in this study. Jiménez-Muñoz et al. (2009) showed that both NDVI and GNDVI had linear relationships with VF, but GNDVI performed better than NDVI in that GNDVI had a higher  $R^2$  and lower standard error than NDVI. Both GNDVI and NDVI still had  $R^2$  above 0.9 and low standard error like was seen in this project. Jiménez-Muñoz et al. (2009) also found that data collected that did not require atmospheric correction like in the case of the data from this project performed better. Carlson and Ripley (1997) determined that NDVI has a linear relationship with VF as was found in this project, but the relationship got better when a scaled value of NDVI between 0% and 100% cover was used. Barati et al. (2011) found that NDVI had a better relationship with VF than OSAVI, and that GNDVI only had a good relationship with VF in well vegetated areas. VF for this study was determined using ground measurement, while multispectral image was obtained from a satellite. Overall most of the literature agrees with the results found that NDVI tends to overall perform best, with some studies (Carlson and Ripley, 1997) not agreeing with this result. VF tended to be better linearly correlated with NDVI, GNDVI, and OSAVI when ground based RGB imagery was used to calculate VF. This results corresponds to the results found in this project that NDVI, GNDVI, and OSAVI have strong linear relationships with VF when VF is measured using ground based RGB imagery.

### 3.3 Comparison of Evapotranspiration

As described in Chapter 2  $K_{cb}$  was calculated following Trout and Johnson (2007), which use VF to calculate  $K_{cb}$  throughout the season. FAO-56 procedures instead rely on tabulated values that assume all corn is growing about at the same rate. The climate in which corn was growing in for this study, can make a significant difference on how corn development progresses through the growing season. Figure 3.9 shows  $K_{cb}$  daily values from Trout and Johnson (2007) and using the tabulated values in FAO-56. As shown in Figure 3.9  $K_{cb}$  for both of the two methods were very similar until effective cover was reached ( $VF = 0.80$ ) and when  $K_{cb}$  reached its peak value at 0.96. For the rest of the season  $K_{cb}$  values from Trout and Johnson (2007) procedure were larger than FAO-56  $K_{cb}$  resulting values. Note that the fluctuations around DOY 180 for  $K_{cb}$  from Trout and Johnson (2007) are caused by functions in VF. The main advantage of using FAO-56 is that it allows for calculation of  $K_{cb}$  without any data collection. For many agricultural growers this can be very advantageous, as they may not have access to VF data to calculate a more accurate method like  $K_{cb}$  from Trout and Johnson (2007).

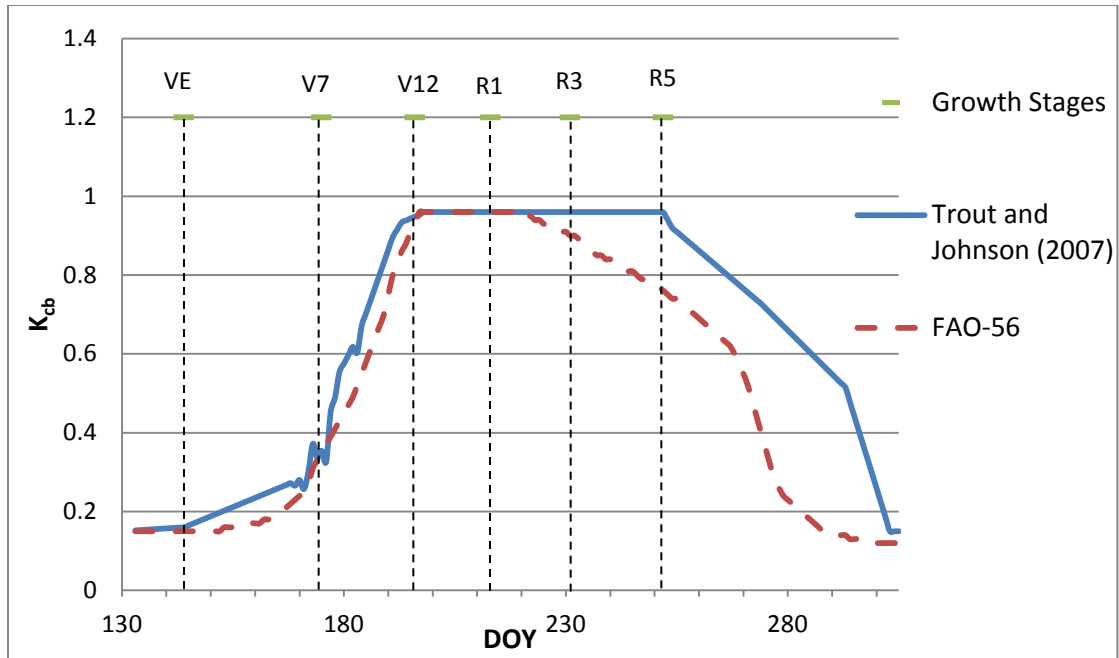


Figure 3.9.  $K_{cb}$  values for Treatment 1 calculate using both Trout and Johnson (2007) and FAO-56 guidelines (Allen et al., 1998)

ET was calculated in two different ways, each way using a different method of calculating  $K_s$ .  $K_s$  was calculated using FAO-56 (Allen et al., 1998), and calculated using Bausch et al. (2011). Since Bausch et al. (2011) cannot be used until full cover occurs,  $K_s$  from the two different methods can only be compared for the later part of the growing season. Figure 3.10 contains the time series of  $K_s$  from the two different methods, note that  $K_s$  calculated from  $T_{c\ ratio}$  does not start till DOY 205.

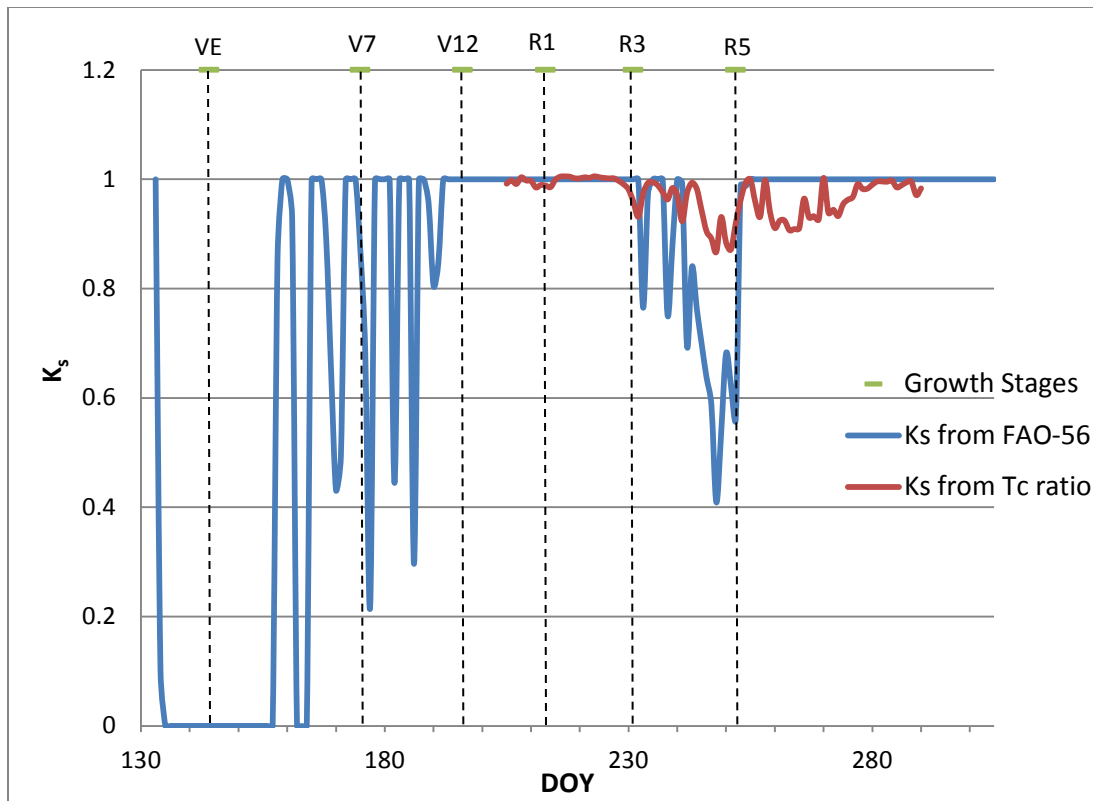


Figure 3.10.  $K_s$  Daily values from Treatment 2 for the two different methods

As shown in Figure 3.10  $K_s$  calculated following FAO-56 procedures showed a much larger degree of stress occurring than  $K_s$  calculated from  $T_c$  ratio. Since Figure 3.10 is for Treatment 2 which received only 50% of predicted full ET from R3 to R5 water stress should be occurring. During the vegetative growth stages VE to V7  $K_s$  dropped down to zero due to large stresses occurring which were caused by delays in getting the pressurized drip irrigation system set up so that the crop could be irrigated. Figure 3.11 shows  $K_s$  values for Treatment 6 which only received 40% of predicted required water from R3 to R5 and therefore the degree of stress was larger. Comparing Figure 3.10 and Figure 3.11 shows that both  $K_s$  from FAO-56 and  $K_s$  from  $T_c$  ratio show greater stress occurring in Treatment 6 (Figure 3.11). For both treatments,  $K_s$  from  $T_c$  ratio is more sensitive to small stress events, while  $K_s$  from FAO-56 seems to only identify large

stress events like the one that occurred around DOY 248. Time-series plots comparing  $K_s$  daily values for the other treatments are available in Appendix A. Figure 3.11 shows that  $K_s$  from  $T_{c\text{ ratio}}$  occasionally will rise above the value of 1, which is its theoretical limit. This is caused by when the other treatments have a canopy temperature that is actually cooler than Treatment 1. As stated earlier Treatment 1 was checked for stress using both  $K_s$  from FAO-56 and the water balance was used to make sure  $D_i$  never was greater than RAW. Thus, even though theoretically  $K_s$  from  $T_{c\text{ ratio}}$  should not go above 1, it is not a big deal if it does as this shows that the crop is far from stressing, and actually healthier than Treatment 1.

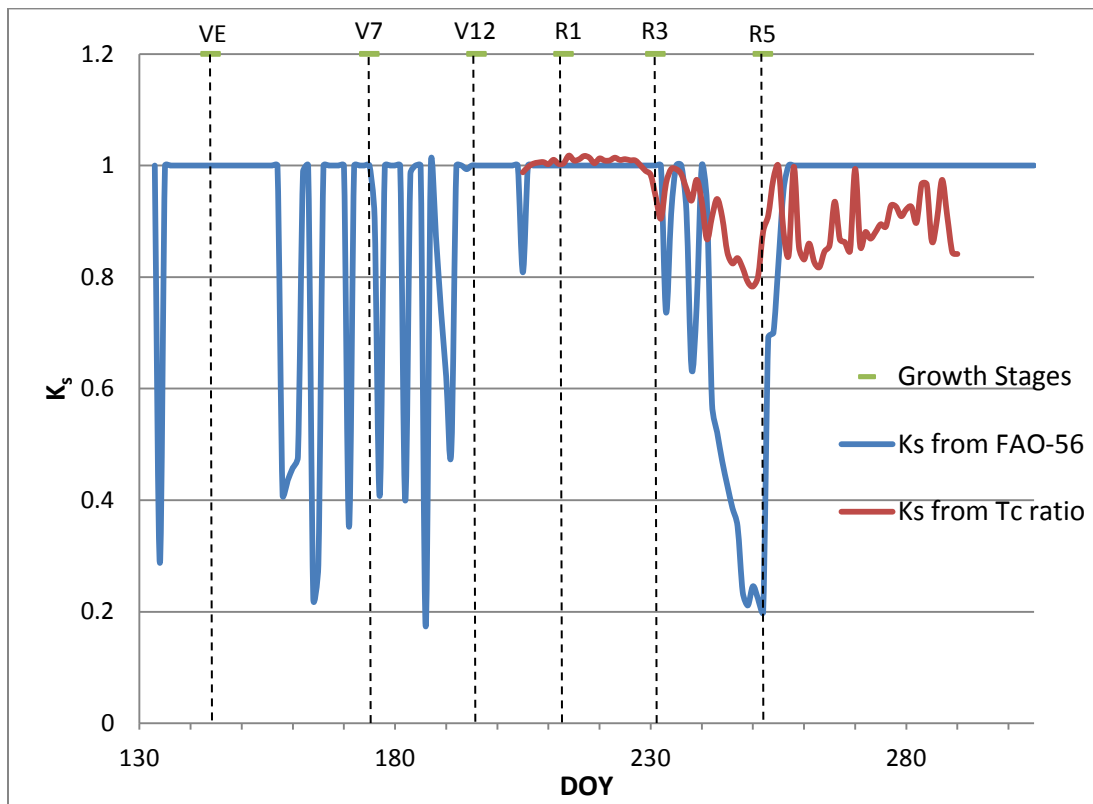


Figure 3.11.  $K_s$  daily values for Treatment 6 for the two different methods

Using the FAO-56 guidelines, the calculation of a theoretical upper (non-stress) corn ET limit was made. Therefore the two methods for calculating ET can be compared to the potential ET

calculated following the FAO-56 guidelines. While the ET from the FAO-56 guidelines was supposed to act as an upper limit, this result was not seen. Figure 3.12 shows the daily ET values from each of the three methods for calculating ET for Treatment 1. ET calculated using  $K_s$  from Bausch et al. (2011) is only shown for the second half of the season because it could not be used until full cover (0.80 VF for corn) was achieved, which occurred on DOY 205.

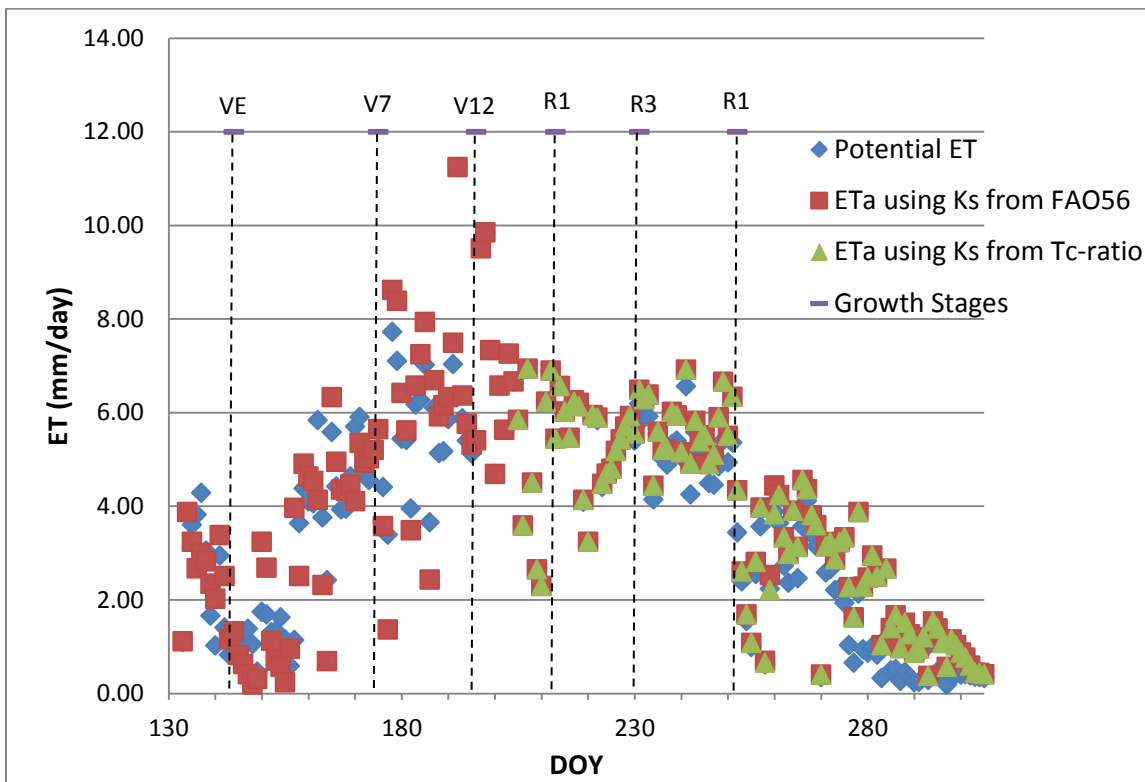


Figure 3.12. Daily actual ET for each method calculated for Treatment 1

$K_s$  from FAO-56 and  $K_s$  from  $T_{c\_ratio}$  daily actual ET values in the end of the season were consistently larger than potential ET calculated from FAO-56 with  $K_s = 1$  for the end of the season. Even though theoretically  $ET_a$  from both methods should not be larger than potential ET, because  $K_{cb}$  values from FAO-56 were underestimated for the reproduction and maturity stage, it makes sense that  $ET_a$  is larger than potential ET. Both methods of calculating actual ET gave

very similar results, even with different  $K_s$  values.  $K_e$  was calculated the same way for all three of the different ET values, while ET from FAO -56 was the only method in which  $K_{cb}$  was calculated using tabular values. From the beginning of the season to about DOY 230 (after effective cover was reached) potential ET and actual ET calculated with  $K_s$  from FAO-56 were fairly similar. Therefore the  $K_{cb}$  tabular values after effective cover are deemed too low for Greeley's semi-arid climate as was seen in Figure 3.9. Even with  $K_s$  calculated differently for the different daily actual ET values, the actual ET for both methods was still very similar. Only from DOY 242-252 large differences between the two methods were evident. These days correspond with the days that large stresses were seen (low  $K_s$  values) in Figures 3.10 and 3.11. Other than those days (DOY 242-252) visually from Figure 3.12 and 3.13 both methods give similar actual ET values. Therefore, even though the two different methods give different  $K_s$  values, daily ET is not affected too much and either of the two methods can be used to calculate  $K_s$ . If using  $K_s$  to monitor crop stress  $K_s$  calculated from  $T_{c\ ratio}$  seems to work best as it captures smaller and larger stress events ( $K_s$  greater than 0.8), while  $K_s$  from FAO-56 tends to only capture the larger stress events ( $K_s$  less than 0.8). Using the  $T_{c\ ratio}$  developed by Bausch et al. (2011) allows the calculation of  $K_s$  using limited data and still gives similar results for ET from FAO-56 procedures; therefore it seems to be a viable option for the calculation of  $K_s$  even with its limitations of only being able to be used after full cover has been achieved.

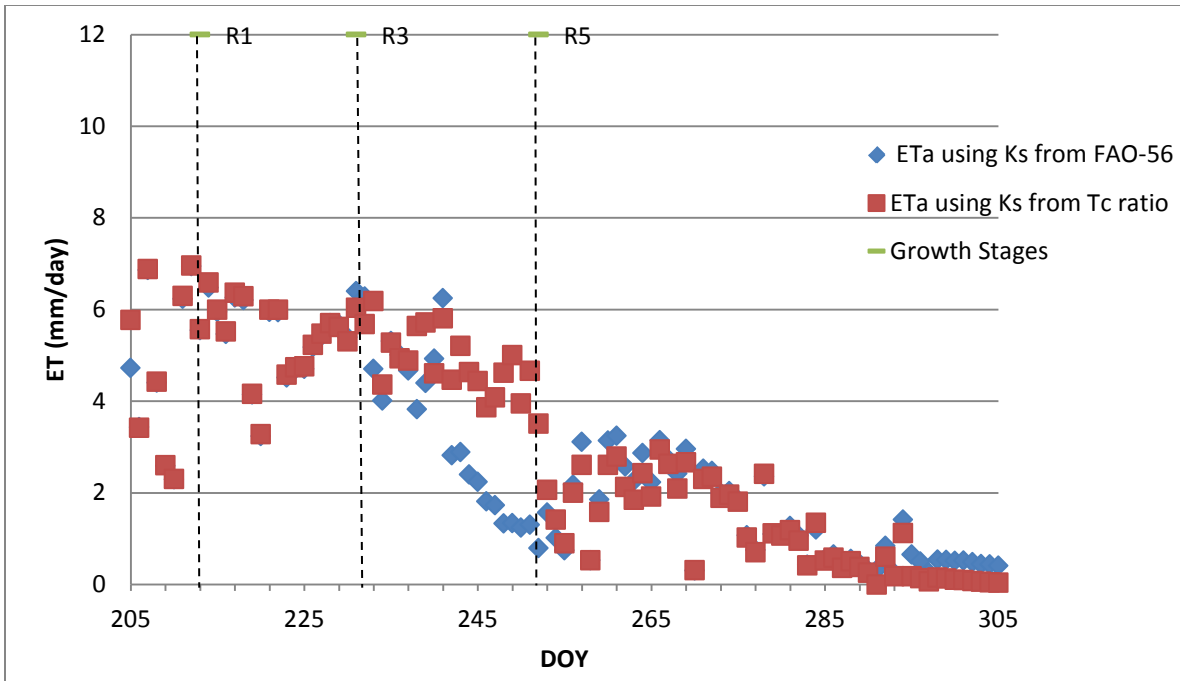


Figure 3.13. Daily ET for Treatment 6 calculated with  $K_s$  from FAO-56 and from  $T_{c \text{ ratio}}$

### 3.4 Soil Water Deficit Comparison

For every day in the growing season  $D_i$  (Equation 1.27) was calculated two different ways using the two water balances created for LIRF. The water balances only varied because ET was calculated differently for each one. Figure 3.14 shows the amount of daily  $D_i$  and RAW experienced by the corn in Treatment 6 using  $K_s$  calculated from FAO-56. Figure 3.15 shows the amount of daily  $D_i$  and RAW experienced in Treatment 6 using  $K_s$  calculated from  $T_{c \text{ ratio}}$ .

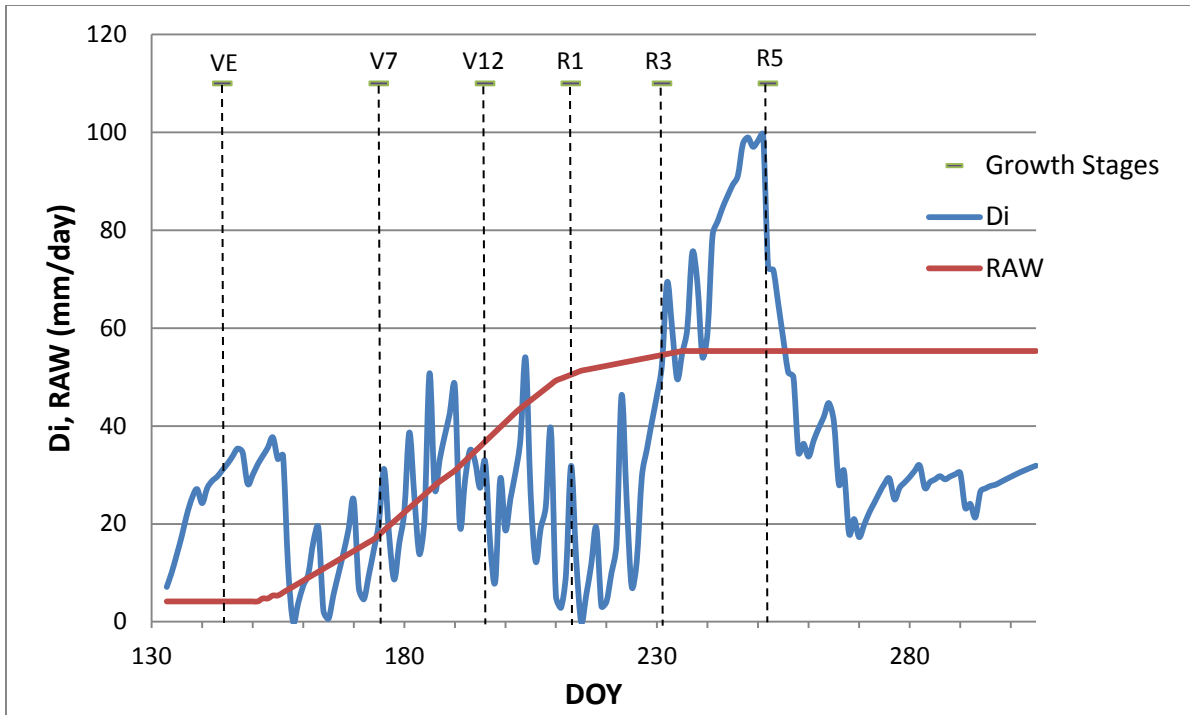


Figure 3.14. Daily D<sub>i</sub> and RAW for corn in Treatment 6 calculated from K<sub>s</sub> from FAO-56

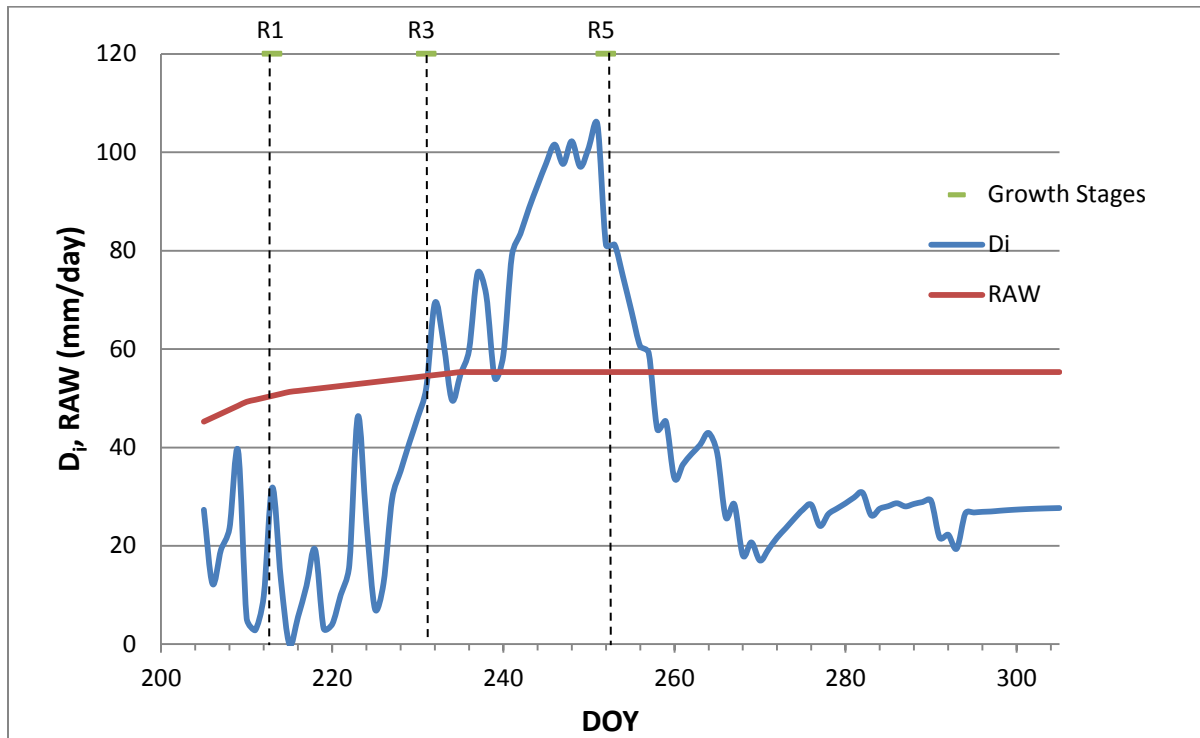


Figure 3.15. Daily D<sub>i</sub> and RAW for corn in Treatment 6 calculated from K<sub>s</sub> from T<sub>c</sub> ratio

Resulting  $D_i$  from both of two different methods was compared to measured  $D_i$  from the neutron probe and TDR. For every day after full cover was achieved for Treatment 6  $D_i$  was calculated for the two different methods using Equation 1.27. The  $D_i$  from Equation 1.27 was then compared to measured  $D_i$  for days that neutron probe and TDR data was available. This was done in order to determine which  $K_s$  estimated  $D_i$  better. RMSE, MBE, MAE, slope, intercept, and  $R^2$  were calculated for both methods and can be seen in Table 3.1. Estimated  $D_i$  from Equation 1.27 from both methods was not very accurate and had large errors compared to measured  $D_i$ .  $D_i$  calculated with  $K_s$  from  $T_{c \text{ ratio}}$  had better results with lower RMSE, MBE, and MAE values than  $D_i$  calculated from  $K_s$  from FAO-56.  $K_s$  from  $T_{c \text{ ratio}}$  also gave a slope closer to 1 and an intercept closer to zero.  $K_s$  from FAO-56 did give a higher  $R^2$  than  $K_s$  from  $T_{c \text{ ratio}}$ .

Table 3.1. Statistical values for comparing estimated  $D_i$  to measured  $D_i$  for the two different methods.

	Method of Calculating $D_i$	
	$K_s$ from FAO-56	$K_s$ from $T_{c \text{ ratio}}$
RMSE (mm/day)	19.69	15.45
MBE (mm/day)	-13.03	-3.59
MAE (mm/day)	16.86	12.41
Slope	1.33	1.06
Intercept	3.31	1.19
$R^2$	0.81	0.75

In Chapter 1, it was discussed when regulated deficit irrigation should be applied, and how this can have effects on the yield. It was determined from reviewing literature that induced water stress during reproduction can cause decreases in yield. From the two different water balances it was seen that all treatments (event Treatment 1) experienced some level of water stress during vegetative growth stages as is indicated when  $D_i$  is larger than RAW. Daily  $D_i$  and RAW time-

series for other treatments besides Treatment 6 can be seen in Appendix B for  $K_s$  from  $T_{c \text{ ratio}}$  and Appendix C for  $K_s$  from FAO-56. Only some of the treatments experienced stress during the maturation growth stages, with Treatment 6 and 12 having the greatest water stress ( $D_i > \text{RAW}$ ) during maturation. No stress occurred in the reproduction stages R1 to R3 for any treatment. Figure 3.16 shows the time-series of  $D_i$  that occurred in Treatments 1, 2, 3, 6, 8, and 12 calculated using  $K_s$  from FAO-56. Figure 3.17 shows the time-series of  $D_i$  calculated using  $K_s$  from  $T_{c \text{ ratio}}$ .

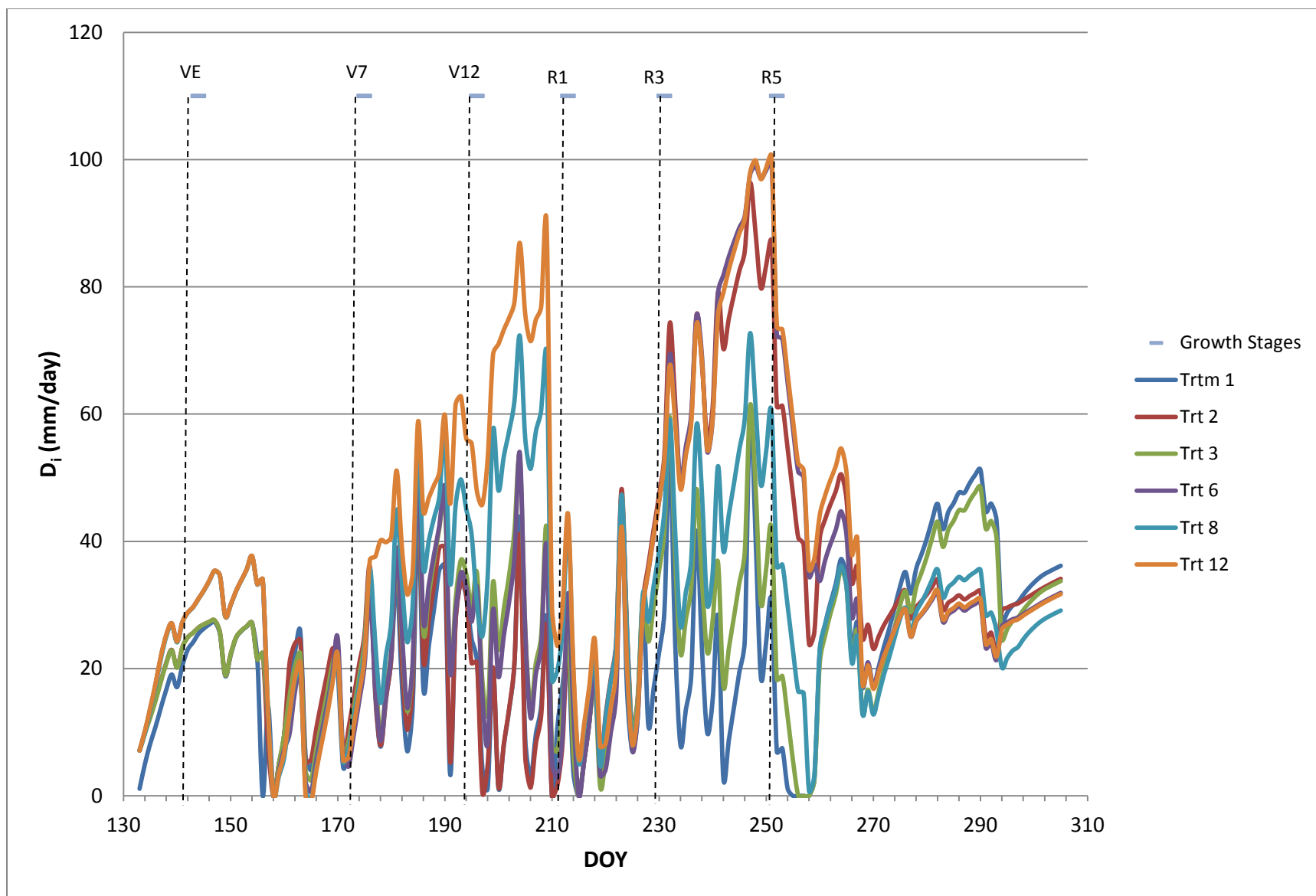


Figure 3.16.  $D_i$  for Treatments 1, 2, 3, 6, 8, and 12 calculated using  $K_s$  from FAO-56

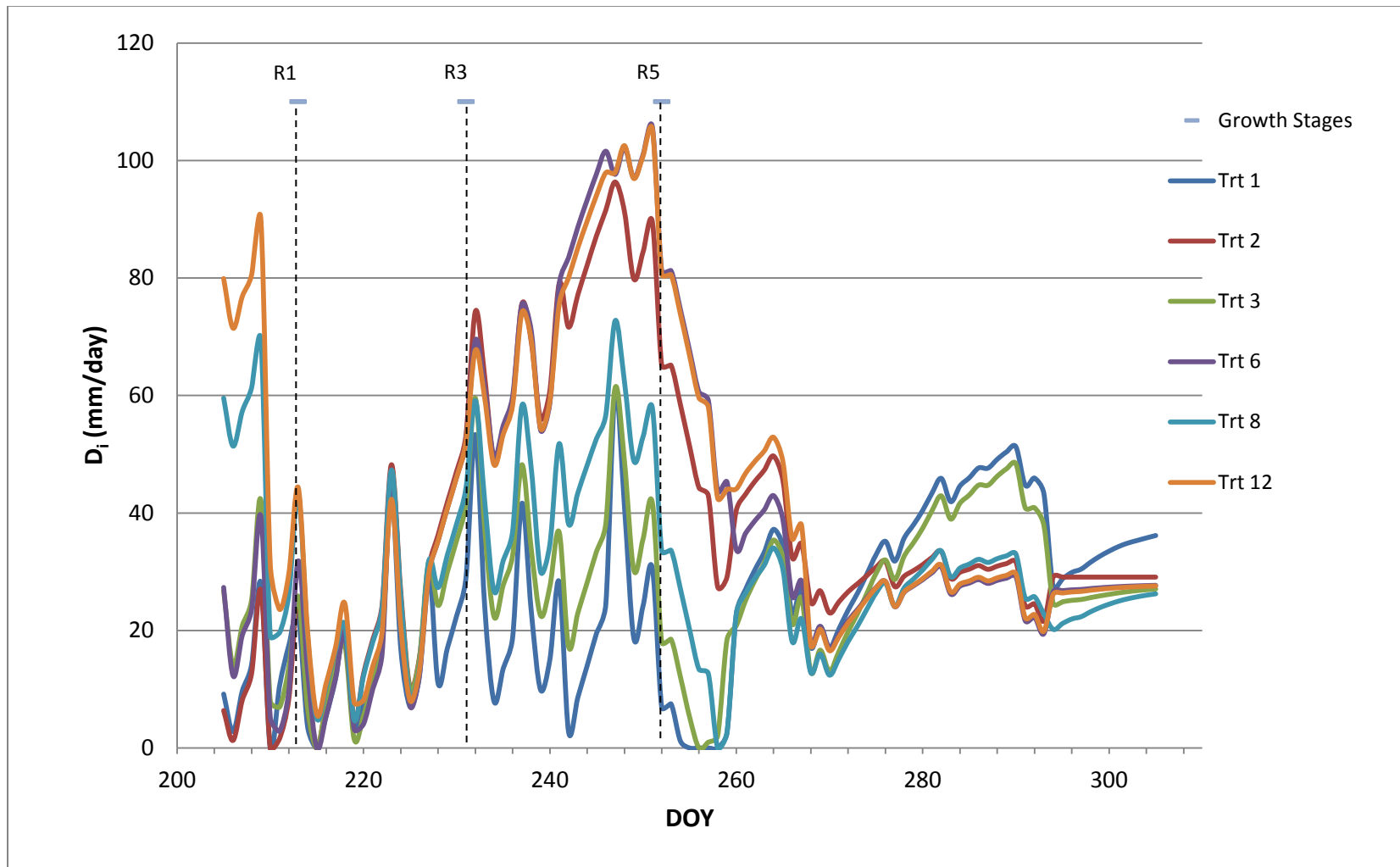


Figure 3.17.  $D_i$  for Treatments 1, 2, 3, 6, 8, and 12 calculated using  $K_s$  from  $T_c$  ratio

Any growth stage that starts with a “V” means it was in the vegetative growth stages. R1 to R3 is considered reproductive growth stages and 100% ET is received in irrigation for all treatments. About a week before R3 occurred deficit irrigation was implemented slowly again. After R5 occurred no more irrigation events occurred and the corn was allowed to dry until harvest which normally occurs in late October. From Figure 3.16 and 3.17 it can be seen that a large amount of  $D_i$  occurred between R3 and R5 (maturation stages) for Treatments 2, 6, and 12. Treatment 6 and 12 ended up having the lowest grain yield (Table 3.2). Both Treatment 2 and 6 had relatively normal  $D_i$  during vegetative growth stages, but still ended up with lower grain yields when compared to the other treatments. Treatment 2 had a cumulative  $D_i$  of 577 mm and Treatment 6 had a cumulative  $D_i$  of 707 mm during the vegetative growth stages calculated with  $K_s$  from FAO-56. Treatment 2 had a cumulative  $D_i$  of 281 mm, while Treatment 6 had a cumulative  $D_i$  of 504 mm during maturity growth stages calculated with  $K_s$  from FAO-56. Figure 3.16 and 3.17 shows that Treatment 8 had higher  $D_i$  (cumulative  $D_i = 945$  mm) occur in vegetative growth stages, and only one large stress event ( $D_i > RAW$ ) during maturity growth stages (cumulative  $D_i = 46$  mm). Even though it had higher cumulative  $D_i$  than Treatment 2 and 6 during vegetative growth stages it still had a higher grain yield than both Treatment 2 and 6. These results can also be seen in Table 3.2 which shows the cumulative  $D_i$  during vegetative and maturation growth stages and the resulting final grain yields. Table 3.2 shows that Treatment 1 and 3 had the highest grain yield of these treatments and the lowest  $D_i$  during maturation stages. From this analysis it can be concluded that large cumulative  $D_i$  during maturation has a greater effect on grain yield than large cumulative  $D_i$  events during vegetative growth stages as has been concluded by numerous other sources (Pandey et. al [2000], Geerts and Raes [2009], Geerts et. al [2008])

For this analysis cumulative  $D_i$  was calculated by first going through each day in the time period and determining if  $D_i$  is greater than RAW in order to calculate the daily soil water deficit that is larger than the RAW ( $D_{i\_raw}$ ). The calculation of  $D_{i\_raw}$  is shown in Equation 3.1.

$$\text{If } D_i > \text{RAW Then } D_{i\_raw} = D_i - \text{RAW else } D_{i\_raw} = 0 \quad (3.1)$$

Cumulative  $D_i$  was then calculated as the sum of the daily  $D_{i\_raw}$  values during the specified time period (vegetative and maturity growth stages).

Table 3.2. Cumulative  $D_i$  (mm) with  $K_s$  from FAO-56 during vegetative and maturation growth stages and final grain yields, averaged by treatment

Treatment #	$D_i$ (mm)		Yield (kg/ha)
	Vegetative	Maturity	
1	481	0	14988
2	577	281	13029
3	588	0	15221
6	707	504	10540
8	945	46	13830
12	1229	416	8925

### 3.5 Stress Indicated from Vegetation Indices

All of the vegetation indices seemed to indicate occasional stress, as shown by fluctuations in the vegetation index over the growing season. In order to determine if the vegetation index was actually fluctuating because of water stress, the indices were compared to the stress coefficients for the two different methods.

### 3.5.1 Comparison of $K_s$ from FAO-56 to Vegetation Indices

To efficiently compare the vegetation indices to  $K_s$  from FAO-56, the  $K_s$  value for each day (and treatment) was compared to the vegetation indices. This was done to see if the vegetation indices followed the fluctuations of  $K_s$ . During the vegetative growth stages before full canopy cover is reached, the vegetation index values are going to be much smaller than  $K_s$ . Therefore they are not going to compare well with  $K_s$  values; thus the only way to compare the index values to  $K_s$  is to monitor whether they are fluctuating with water stress as  $K_s$  is. Figure 3.18 shows the  $K_s$  values and the vegetation indices values for DOY 192 for all of the treatments.

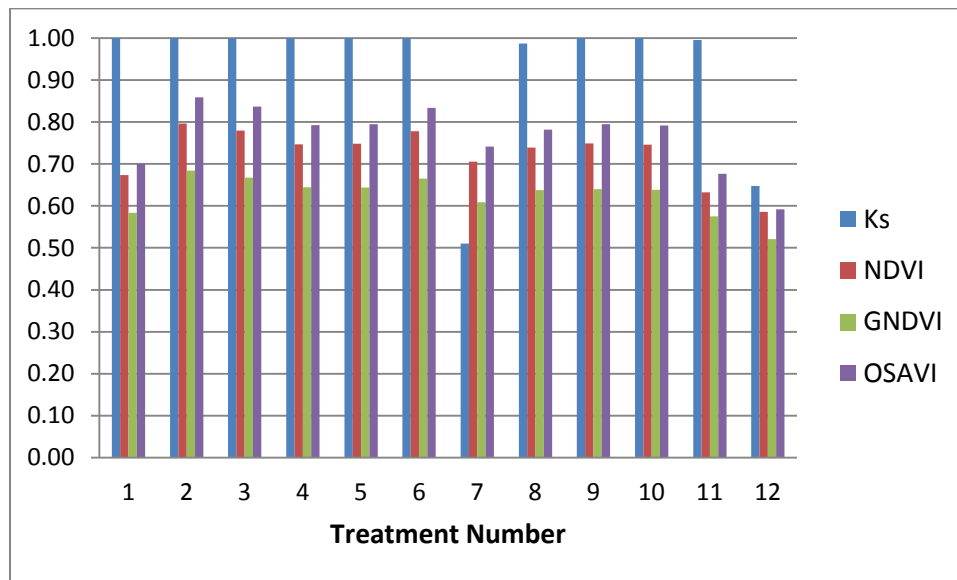


Figure 3.18.  $K_s$  from FAO-56, NDVI, GNDVI, and OSAVI values for DOY 192

From Figure 3.18 it can be seen that  $K_s$  for most of the treatments was a value of 1, indicating no corn stress. The indices show more fluctuations than  $K_s$ , but for Treatment 7 and 12 the  $K_s$  value dropped and so did the vegetation indices. Treatment 7 has a  $K_s$  value of 0.51, and an NDVI value of 0.70. Treatment 12 has a  $K_s$  value of 0.63 and an NDVI value of 0.58. This doesn't make sense that the NDVI value would be lower for Treatment 12 when the  $K_s$  value is greater

for Treatment 12. This is not the only day for which these sorts of results were seen. For DOY 214  $K_s$  from FAO-56 was calculated to be 1 for all of the treatments, but the vegetation indices slowly decreased with increase in treatment number. Hence even though Treatment 12 according to  $K_s$  is not experiencing any stress, all three vegetation indices show a decrease in value when compared to vegetation index values for Treatment 1. This could be caused by differences in VF and from Figure 3.18 it is impossible to tell if this is because of stress or VF. As was discussed early  $K_s$  from FAO-56 only captured larger stress events; then vegetation indices could be capturing a smaller stress event. When  $K_s$  was just slightly below 1, the indices tended to not respond as consistently. Because of differences in the stands of the corn, there are small fluctuations ( $\sim 0.01$ ) naturally in the vegetation indices. Therefore to be able to identify a fluctuation in the vegetation indices as stress, larger stress has to occur to compare to  $K_s$  from FAO-56. Unfortunately no good spectral reflectance data (i.e. no clouds, clear sky) was collected on days where large  $D_i$  occurred; thus no large changes in  $K_s$  were seen to compare to the vegetation indices.

### 3.5.2 Comparison of $K_s$ from $T_{c \text{ ratio}}$ to Vegetation Indices

As discussed earlier in the results the second method that calculated  $K_s$  using Bausch et al. (2011) was found to capture small and large stress events unlike  $K_s$  calculated from FAO-56. In the last section it was also discussed that the vegetation indices either were responding to differences in VF or small stress events. After comparing the indices to the  $K_s$  value for that day it was noticed that the indices followed the fluctuations of  $K_s$  from  $T_{c \text{ ratio}}$ . Figure 3.19 shows  $K_s$ , NDVI, GNDVI, and OSAVI values for the treatments 1, 2, 3, 6, 8, and 12 for DOY 211.

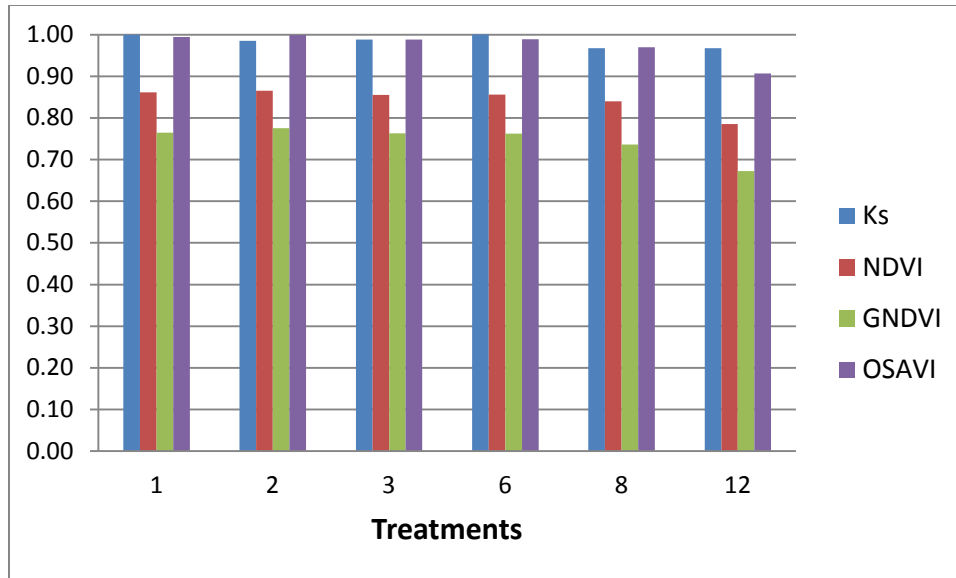


Figure 3.19.  $K_s$  from  $T_c$  ratio, NDVI, GNDVI, and OSAVI values for DOY 211

As shown in Figure 3.19 as the  $K_s$  value decreased as the treatment number increased, the vegetation indices also do this. This result was not only seen with DOY 211 it was seen on the other days that vegetation index data were available (days the reflectance tractor had collected data). Figure 3.20 shows another example of this for DOY 206.

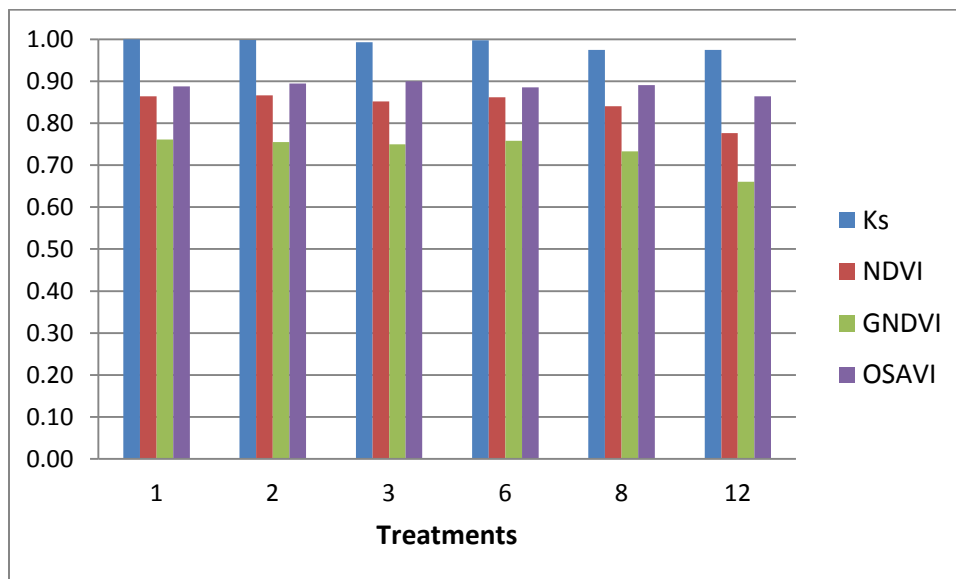


Figure 3.20.  $K_s$  from  $T_c$  ratio, NDVI, GNDVI, and OSAVI values for DOY 206

### 3.5.3 Development of Vegetation Ratios

While fluctuations can be seen in Figure 3.19 and 3.20, it is hard to compare to the vegetation indices since the indices values are lower than  $K_s$  values even when full cover and maximum vegetation index values occur. To be able to overcome this issue normalization was done and a new vegetation ratio was developed. This ratio was developed by aiming to make the indices on the same scale of  $K_s$ , and also decrease its value as  $K_s$  does when stress is apparent. Therefore it was decided to divide the index values for Treatments 2, 3, 6, 8, and 12 by the index values for Treatment 1 for every day that there were vegetation index data and  $K_s$  data from  $T_{c\ ratio}$ . To be able to use these ratios it is assumed that Treatment 1 did not experience any water stress. Treatment 1 was used to be consistent and because  $K_s$  from both FAO-56 and  $T_{c\ ratio}$  showed no stress ( $K_s = 1$ ) occurring in Treatment 1 from DOY 205 to harvest. The water balance was also used to check that Treatment 1 did not have water deficit past RAW on days that vegetation index data was available. Although this does not mean that some wilting did not occur especially in the sandier sections of soil in LIRF that do not hold water as well, or that bad stand in one of the Treatment 1 plots could lower the average, none of the stress was long lasting and to stay consistent with Bausch et. al (2011) procedures Treatment 1 was used as the non-stressed value. It was decided since  $K_s$  from FAO-56 only identified large stress events and the vegetation indices fluctuated like  $K_s$  from  $T_{c\ ratio}$  to only compare the developed vegetation ratios to  $K_s$  from  $T_{c\ ratio}$ . The vegetation ratio equation for NDVI can be seen in Equation 3.2, GNDVI in Equation 3.3, and OSAVI in Equation 3.4.

$$N_{ratio} = \frac{NDVI_{stressed}}{NDVI_{no\ stress}} \quad (3.2)$$

$$G_{ratio} = \frac{GNDVI_{stressed}}{GNDVI_{no\ stress}} \quad (3.3)$$

$$O_{ratio} = \frac{OSAVI_{stressed}}{OSAVI_{no\ stress}} \quad (3.4)$$

The ARS-WMU only had a total of six days in which good (i.e. no cloud cover) vegetation index data and  $K_s$  values from the second method were available. These ratios did very well at matching  $K_s$  from  $T_c$  ratio and were normally within 5% of it. Figure 3.22 shows the vegetation ratio values and  $K_s$  values for each treatment for DOY 206. Treatment 12 in Figure 3.21 is the only one where N and G ratios weren't within 5% of  $K_s$ . This could be caused by soil background effects since Treatment 12 had the lowest VF value on DOY 206, and OSAVI used in the calculation of O ratio could have corrected for some of these effects.

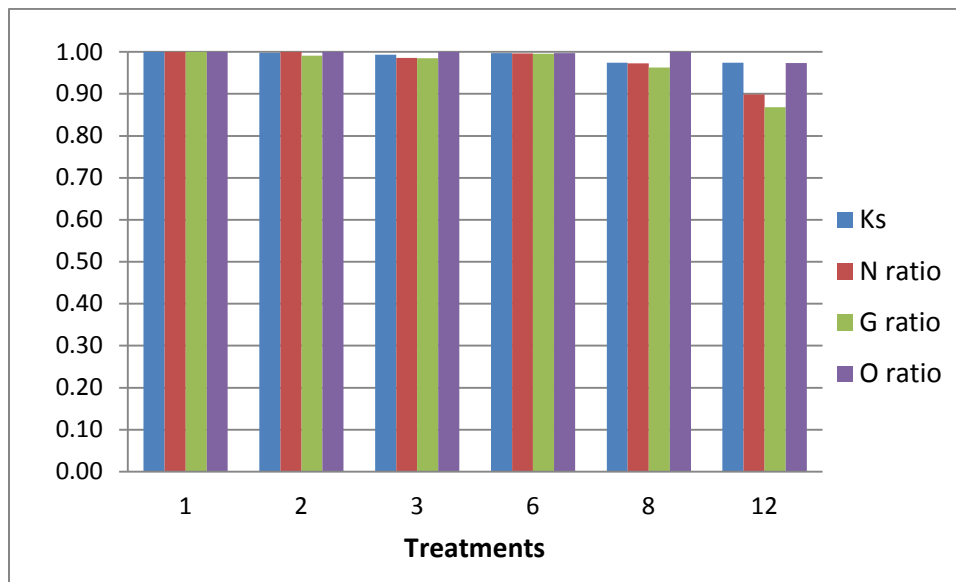


Figure 3. 21.  $N_{ratio}$ ,  $G_{ratio}$ ,  $O_{ratio}$ , and  $K_s$  from  $T_c$  ratio values for DOY 206

Now that  $K_s$  and the index ratios are normalized (on the same scale) they can be more directly compared than just visually using the bar charts seen in previous comparisons. Therefore Figure 3.22 shows  $K_s$  plotted versus  $N_{ratio}$  for all of the treatments and days with data. Figure 3.23 shows  $K_s$  plotted versus  $G_{ratio}$ , and Figure 3.24 shows  $K_s$  plotted versus  $O_{ratio}$ .

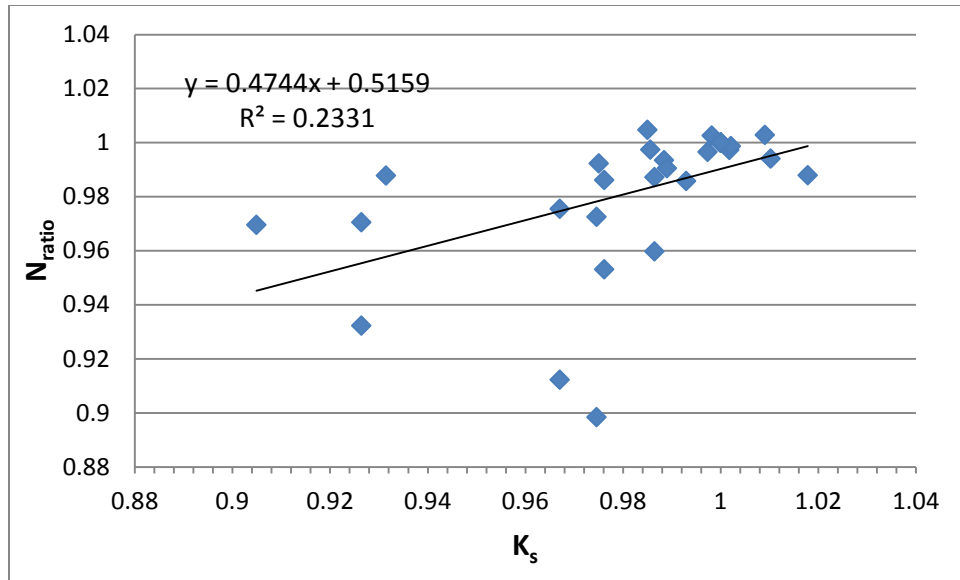


Figure 3. 22.  $K_s$  from  $T_{c\ ratio}$  versus  $N_{ratio}$  for all treatments and days with data

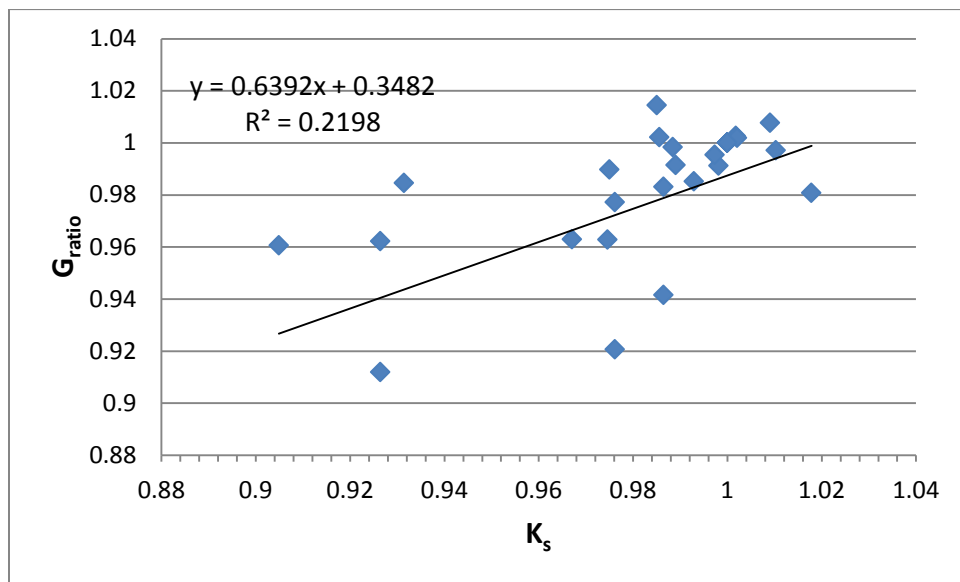


Figure 3. 23.  $K_s$  from  $T_{c\ ratio}$  versus  $G_{ratio}$  for all treatments and days with data

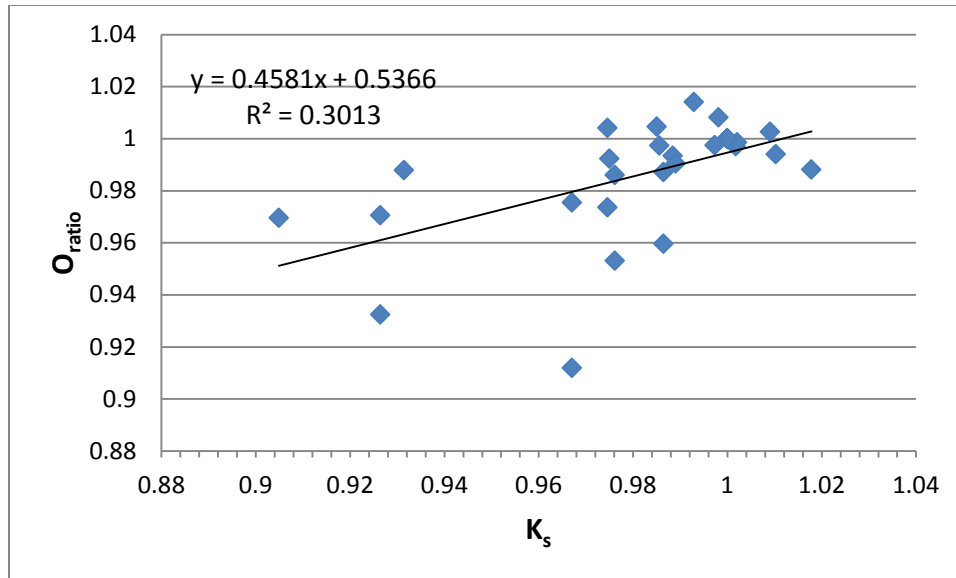


Figure 3.24.  $K_s$  from  $T_c$  ratio versus  $O_{ratio}$  for all treatments and days with data

Figure 3.22, 3.23, and 3.24 all have rather low  $R^2$  values, with  $O_{ratio}$  and  $K_s$  (Figure 3.24) having the highest  $R^2$  value of 0.30. While the  $R^2$  value is low, indicating the  $K_s$  does not have a strong correlation with the index ratios; it still does have a correlation with them. For Figure 3.22 to 3.24 there are a few outliers causing the low  $R^2$  value of 0.23. Treatment 12 had a low VF (less than full cover) the entire season which makes the temperature of the canopy even greater. When the VF is lower than full cover ( $\sim 0.80$ ) the data is often considered unusable. Calculating  $K_s$  from Treatment 12 IRTs could have affected obtaining accurate  $K_s$  values, therefore causing the low  $R^2$  values. Taking out Treatment 12 values from Figures 3.22 to 3.24 gave higher  $R^2$  values as can be seen in Figures 3.25, 3.26, and 3.27. Table 3.3 shows the RMSE and MBE values for the error between  $K_s$  and the vegetation ratios excluding Treatment 12. All of the vegetation ratios had small RMSE and MBE values close to zero. As shown in Figure 3.25 removing Treatment 12 data improved the  $R^2$  of the  $N_{ratio}$  about 56%.

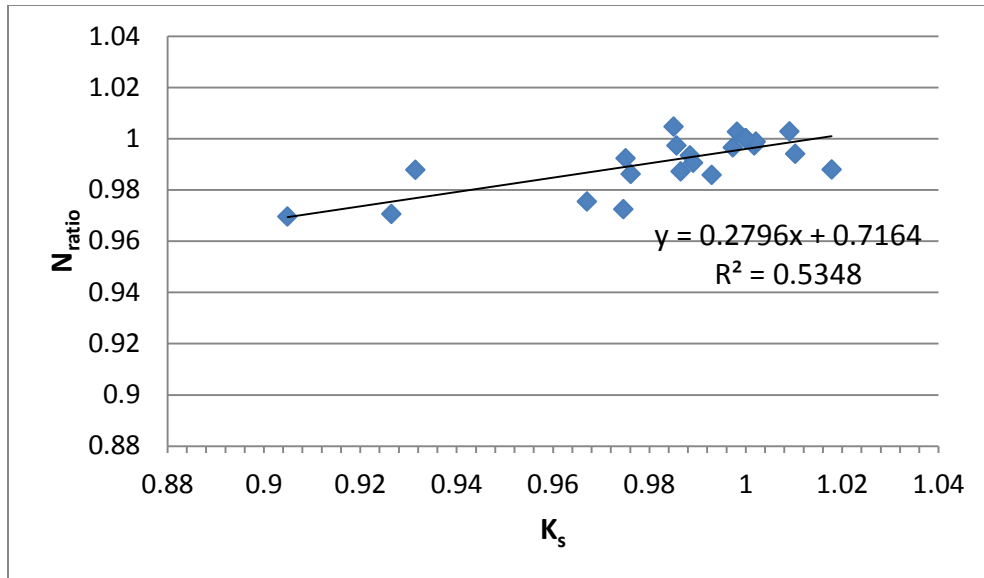


Figure 3.25.  $K_s$  from  $T_{c\ ratio}$  versus  $N_{ratio}$  for all Treatments except Treatment 12

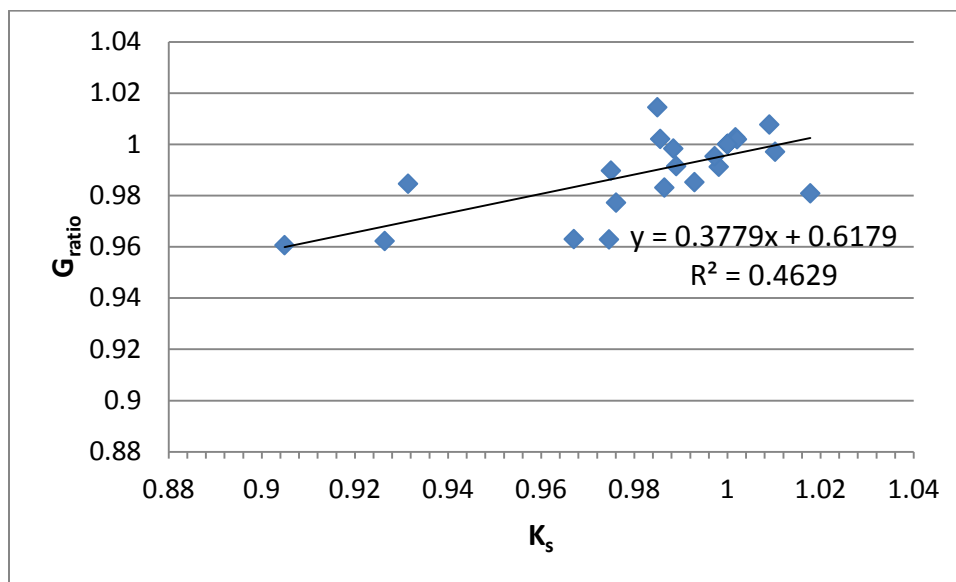


Figure 3.26.  $K_s$  from  $T_{c\ ratio}$  versus  $G_{ratio}$  for all Treatments except Treatment 12

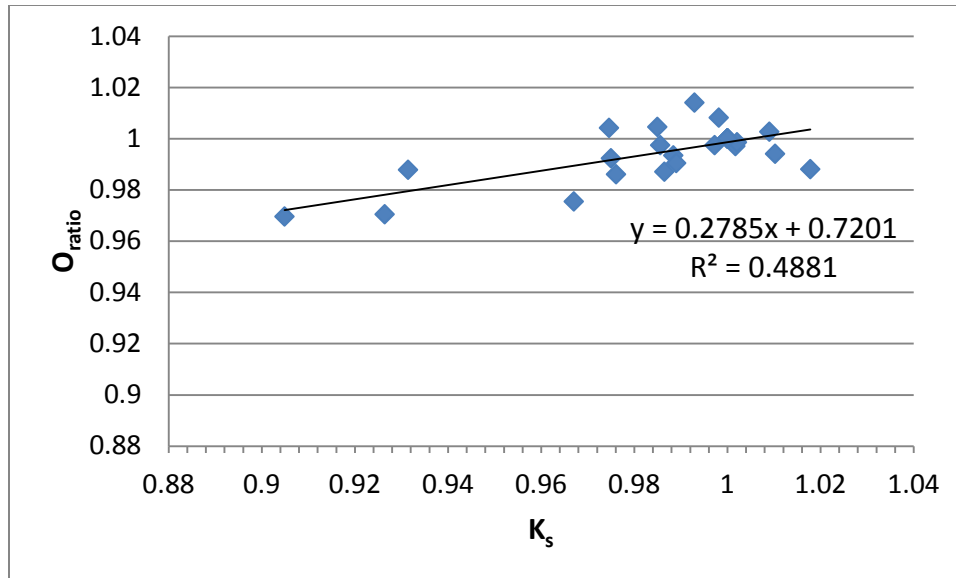


Figure 3.27.  $K_s$  from  $T_c$  ratio versus  $O_{ratio}$  for all Treatments except Treatment 12

Table 3.3. RMSE and MBE values for the error between  $K_s$  and the vegetation ratios excluding Treatment 12.

	RMSE	MBE
$N_{ratio}$	0.076	0.029
$G_{ratio}$	0.062	0.024
$O_{ratio}$	0.076	0.031

For Figures 3.25 to 3.27 there was a linear correlation and while there was some scatter, the scatter can be contributed to variations in treatment canopy structure and days with some cloud cover like DOY 241. Even though the  $R^2$  is still a little low with a value of 0.53, visually the results look better, and all three vegetation ratios had low RMSE and MBE values as shown in Table 3.3.  $G_{ratio}$  actually had the lowest RMSE (0.062) and MBE (0.024) values. With more data taken on cloudless days and less extreme deficit treatments the correlation could improve. This is also the first growing season the SKYE sensors have been used by the ARS-WMU, thus a lot of user error occurred. While the vegetation ratios did not always compare perfectly with  $K_s$ , they did respond to some level to corn water stress in the corn. Therefore it can be observed that water

stress in corn can be monitored using spectral reflectance measurements of the corn. Vegetation ratios are calculated with spectral reflectance measurement and give a method to monitor corn water stress.

### 3.6 Irrigation Trigger Determination

The final objective of this project was if the indices could be used to monitor corn water stress, then an irrigation trigger would be determined. Being able to trigger irrigation events just based on stress quantified by vegetation ratios, could be beneficial for farmers who do not want to take the time to create a water balance to schedule irrigation events. To obtain an irrigation trigger the values of the index ratios were compared to  $D_i$  from the water balance. For values of 1.0 to 0.93 small stress does occur, but no large stresses ( $D_i > 60$  mm, distinct change in VF) occurred. Here small stress is defined as stress that does not cause noticeable change in VF, and does not cause large water deficit in the root zone. After 0.93 large stresses (large decreases in VF and large water deficit in the root zone) occurred that could affect the grain yield as indicated by the fact that treatments that experienced decreases in grain yield experienced stresses during the season smaller than 0.93. Since there are only six days of data for the index ratios after full cover occurred,  $K_s$  from  $T_{c \text{ ratio}}$  values were used to obtain this value. The vegetation ratios have a linear correlation with  $K_s$  from  $T_{c \text{ ratio}}$  and follow the same trend as  $K_s$  from  $T_{c \text{ ratio}}$ . Therefore to have enough data to obtain an accurate irrigation trigger  $K_s$  from  $T_{c \text{ ratio}}$  was used to determine it for the index ratios. Figure 3.29 shows the  $K_s$  from  $T_{c \text{ ratio}}$  values for the second part of the growing season. The thick black line represents the trigger irrigation point (vegetation ratios = 0.93). As shown in Figure 3.28 this black line keeps most of the points above it (minimal stress) and only about a quarter of the points below it (larger stress). Using a value of vegetation ratio = 0.93

keeps the stress that occurs minimal and shouldn't affect the grain yield. It would be more accurate to create a trigger for each vegetation ratio, but with limited data the irrigation trigger is being generalized for all three vegetation ratios. This may not be as accurate, but is more accurate than creating a trigger with only six points.

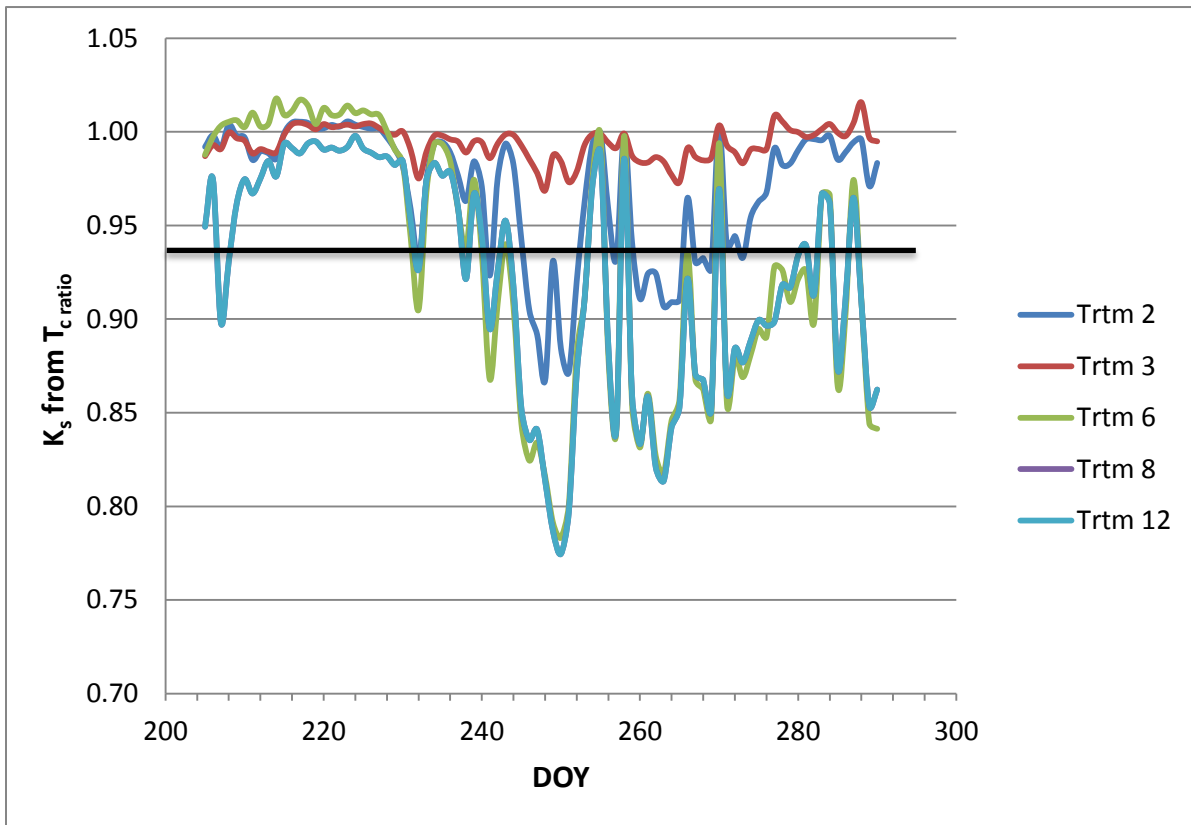


Figure 3.28.  $K_s$  from  $T_c$  ratio calculated using the second method values for the second half of the growing season, the thick black line being the proposed irrigation trigger point. The  $K_s$  values are used as a representation of the index ratios because of the lack of enough data for determining an irrigation trigger using just index ratio values.

From the irrigation events in the water balance most of the irrigations for the treatments where large deficits did not occur the ARS-WMU irrigated for the most part when  $K_s$  started to fall below 0.93. Depending on the treatment the ARS-WMU let  $K_s$  drop further past 0.93.

### 3.6.1 Irrigation Amount Determination

After a farmer uses the proposed method to decide whether or not irrigation is needed, he/she would then need to determine the amount of irrigation that would be required. Most farmers would determine this using a soil water balance. In order to determine the net amount of irrigation VWC at FC would need to be determined. VWC at FC can be determined by taking gravimetric samples from the field and taking them to a soils lab to determine the VWC at field capacity. Then the net amount to irrigate can be determined by using either a water balance or soil moisture sensors to estimate/measure VWC for a particular day ( $VWC_i$ ), then subtracting  $VWC_i$  from VWC at FC. Thus, the difference between VWC at FC and  $VWC_i$  is the required irrigation amount. The VWC at the irrigation trigger will be much lower than the VWC at FC, since the VWC at FC describes how much water within the root zone can be stored. For this project FC was taken into account in the beginning of the  $D_i$  calculations, and therefore  $D_i$  were calculated in terms of FC. Thus it was found for LIRF, that has a sandy loam soil, when a  $K_s$  of 0.93 occurred then the corresponding  $D_i$  (or the associated amount of water to be replenished each irrigation) in the root zone was 60 mm. Therefore a farmer that has a similar soil type as LIRF (sandy loam) could then use this value and know that the corn requires 60 mm of water depth to irrigate. This value of course would change depending on the different soil types, and would need to be determined for the farmer's soil type. For large fields this can also be inaccurate as soil properties could easily vary quite a bit throughout the whole field.

### 3.7 Calculation of Index Ratio with Minimal Data

Out of the final three vegetation indices, all three performed about the same based on visual observation and  $R^2$  values. While  $N_{ratio}$  (based on NDVI) had the largest  $R^2$  value of 0.53,  $G_{ratio}$

and  $O_{ratio}$  had  $R^2$  values not that much lower and visually looked as good as  $N_{ratio}$ . Even though  $G_{ratio}$  had the lowest  $R^2$  value (0.46) it had the best RMSE (0.062) and MBE (0.024) values. Therefore any of the three could be used. But in order to use the index ratios, a farmer would need to know the NDVI, GNDVI, or OSAVI value for non-stressed corn, and the NDVI, GNDVI, or OSAVI value for their corn. Most farmers will just have a field of corn that receives the same amount of water; therefore to be able to use the index ratios the farmer would need to obtain a non-stressed value for NDVI, GNDVI or OSAVI from some other source. NDVI, GNDVI and OSAVI indices can be calculated using the equations found in Figures 3.5 and 3.7 respectively, but VF would need to be known. Using VF data collected using the Canon camera by the ARS-WMU over 2009 to 2011 field seasons for corn a table could be constructed of when VF values occur with different corn growth stages, for Treatment 1 (non-stressed). These values allow farmers to estimate NDVI, GNDVI, or OSAVI for a non-stressed treatment based on corn growth stages. This value can then be used to calculate the index ratio of their choice to see if they need to irrigate or if their crop is stressed. Growth staging corn requires no special equipment, just prior knowledge of corn growth stages. Information on corn growth stages can be easily obtained online or from other sources, and taking growth stages in the field takes very little time. Therefore using corn growth stages allows the farmers to easily obtain vegetation indices for a non-stressed field of corn. Table 3.4 shows the VF, NDVI, GNDVI, and OSAVI values that correspond to corn growth stages. From Table 3.4 the VF value and the vegetation indices for corn can be estimated. NDVI, GNDVI, and OSAVI values in Table 3.4 were calculated using Equations 3.5, 3.6, and 3.7. Equations 3.5 to 3.7 came from Figures 3.5 to 3.7 respectively. The farmer can then use the value of NDVI, GNDVI, or OSAVI for their field, and the NDVI, GNDVI, or OSAVI value obtained from Table 3.4 and calculate one of the vegetation

ratios depending on which index they choose to use. Therefore they can calculate the vegetation ratio and determine if they need to irrigate or if their crop is experiencing stress.

If spectral reflectance data is not available it could be possible to use VF instead of the indices to calculate needed ratio. This would be VF of a stressed field divided by VF of a non-stressed field. Table 3.4 could still be used to obtain VF of a non-stressed field. Since the indices have almost a 1 to 1 relationship with VF the irrigation trigger most likely could be used but more research would be needed to verify that. The main drawback of using VF instead of the indices to calculate the ratio is that in order to get accurate VF data a higher end camera would be required, along with software to calculate the VF. This software is not as readily available as many institutions create a program themselves, and do not make them publically available. For this reason it is best to use the vegetation indices if spectral reflectance data is available since no special software is required.

Table 3. 4. VF, NDVI, GNDVI, and OSAVI values for fully irrigated corn corresponding to corn major growth stages using data collected in 2009 to 2011 by the ARS-WMU.

Growth Stage	VF	NDVI	GNDVI	OSAVI
Emergence	0.01	-0.03	0.02	-0.07
V1	0.02	-0.02	0.02	-0.06
V3	0.03	-0.01	0.03	-0.05
V5	0.10	0.07	0.09	0.04
V7	0.28	0.25	0.25	0.26
V9	0.65	0.64	0.57	0.73
V11	0.75	0.75	0.66	0.85
V14	0.88	0.89	0.77	1.01
V16	0.89	0.90	0.78	1.03
V18 (VT)	0.90	0.91	0.80	1.05
R1	0.86	0.87	0.76	1.00
R2	0.82	0.83	0.73	0.94
R3	0.77	0.77	0.68	0.88
R4	0.75	0.75	0.66	0.86
R5	0.68	0.67	0.60	0.76
R6	0.09	0.06	0.09	0.03

$$NDVI = 1.0568 \cdot VF - 0.039 \quad (3.5)$$

$$GNDVI = 0.8778 \cdot VF + 0.0066 \quad (3.6)$$

$$OSAVI = 1.2535 \cdot VF - 0.0829 \quad (3.7)$$

### 3.8 Validation of Method to Obtain Vegetation Ratios

In order to make sure that the proposed method would work to obtain the  $N_{ratio}$ ,  $G_{ratio}$ , or  $O_{ratio}$ , and see if the field needs to be irrigated multispectral data from one of the ARS-WMU past studies were used to obtain multispectral data. Multispectral data were obtained using multispectral radiometers as described in Bausch et al. (2011). For this validation  $N_{ratio}$  will be calculated and used as NDVI data were obtained from ARS-WMU. Data from DOY 207 in the

growing season of 2010 for corn were used. NDVI value for DOY 207 for Treatment 5 was 0.78. The growth stage of the Corn for this day was V18 as recorded by the ARS-WMU. According to Table 3.4 at a growth stage of V18 the VF was equal to 0.90. Plugging this VF value into Equation 3.4 gave an NDVI for a fully irrigated treatment of 0.91. Plugging in 0.78 as the stressed NDVI value and 0.91 as the non-stressed NDVI value into Equation 3.1 resulted in an  $N_{ratio}$  value of 0.86, therefore the crop was stressed and irrigation was needed to occur in order to prevent decreases in yield. Since the ARS-WMU was purposely stressing (Treatment 5) the crop it was expected to get a value less than 0.93. A V18 growth stage indicates that the crop is starting/about to go into reproduction therefore the ARS-WMU should be applying significant irrigations about this time to keep the crop from going into stress during reproduction. After checking the ARS-WMU water balance for this year, it was verified that the plot received a full irrigation two days after DOY 207 in order to keep it from stressing as it went into reproductive stages. Therefore, the occurrence of this full irrigation event corroborates the results of this study that the corn indeed was in stress and did need the irrigation event. As shown above this method of using the measured NDVI from the field and growth stages to obtain VF and therefore obtain NDVI of a non-stressed field, seems to work. It requires minimal data and may not be as accurate as applying a water balance, but for farmers with limited resources this method maybe an applicable method to making irrigation decisions.

### 3.9 Use of the index ratio as $K_s$

As discussed in section 3.5.2 the vegetation ratios correlate with  $K_s$  calculated from  $T_{c\ ratio}$  well. Therefore it is proposed that any of the vegetation ratios could be related to  $K_s$  in the calculation of ET actual. Bausch et al. (2011) proposed method cannot be used until full cover has been

reached because of stationary IRT's wide field of view and soil background affects therefore its applicability is limited to late season. Using a vegetation ratio as  $K_s$  will allow for  $K_s$  to be calculated throughout the whole season, not just when full cover is achieved. The main drawback to using a vegetation ratio as a  $K_s$  value is daily or frequent multispectral data may not always be available if using satellite imagery. Therefore it might be best to use the index ratio in the beginning of the season and then switch to Bausch et al. (2011) when full cover is achieved.

### 3.10 Validation Using SWIIM Field Data

To validate the results found from the data from LIRF, data collected from SWIIM field (South of LIRF) were used. Two water balances were created using SWIIM field data just like for LIRF; one using  $K_s$  from FAO-56, and one using  $K_s$  from  $T_{c \text{ ratio}}$ . The potential ET was also calculated following FAO-56 procedures assuming  $K_s = 1$  in the calculation of ET. As mentioned in the methodology SWIIM field has three treatments one fully irrigated (Treatment 1), a low frequency deficit irrigated (Treatment 2), and a high frequency deficit irrigated (Treatment 3). Daily ET for the Treatment 1, 2, and 3 is shown in Figures 3.29, 3.30, and 3.31 respectively.

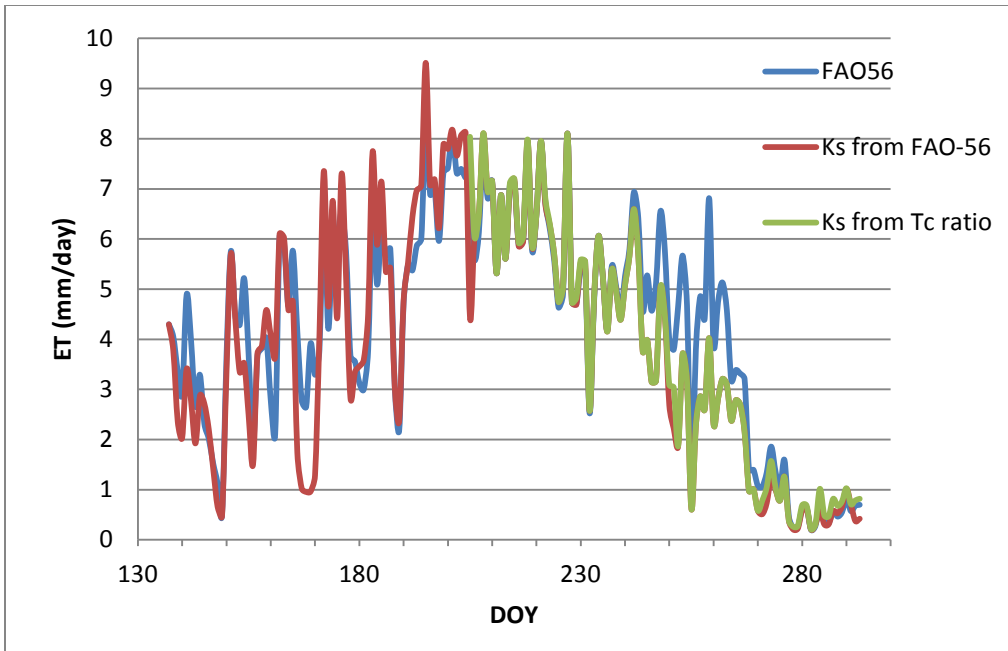


Figure 3.29. Daily ET (mm/day) for Treatment1 (FI) in SWIIM field

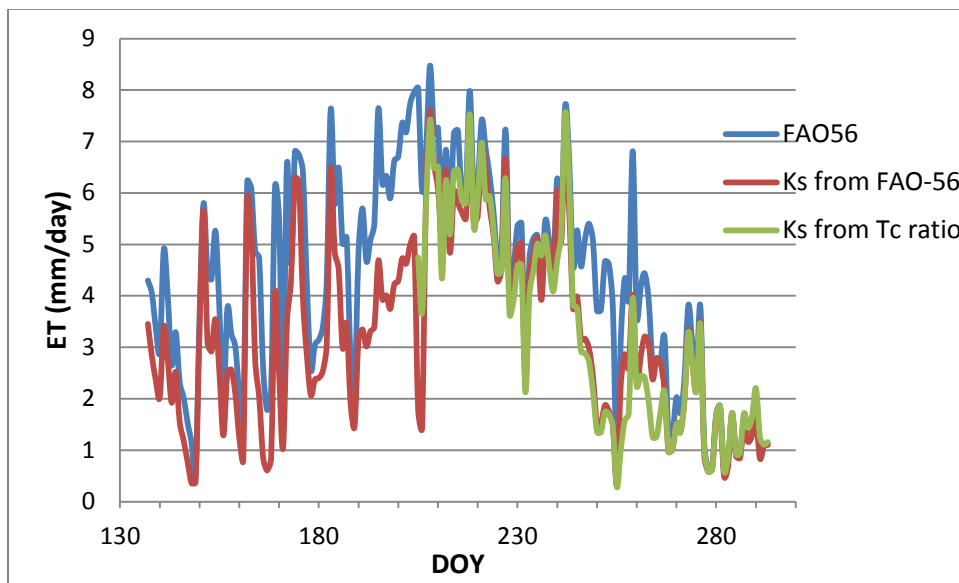


Figure 3. 30. Daily ET (mm/day) for Treatment 2 (LFDI) in SWIIM field

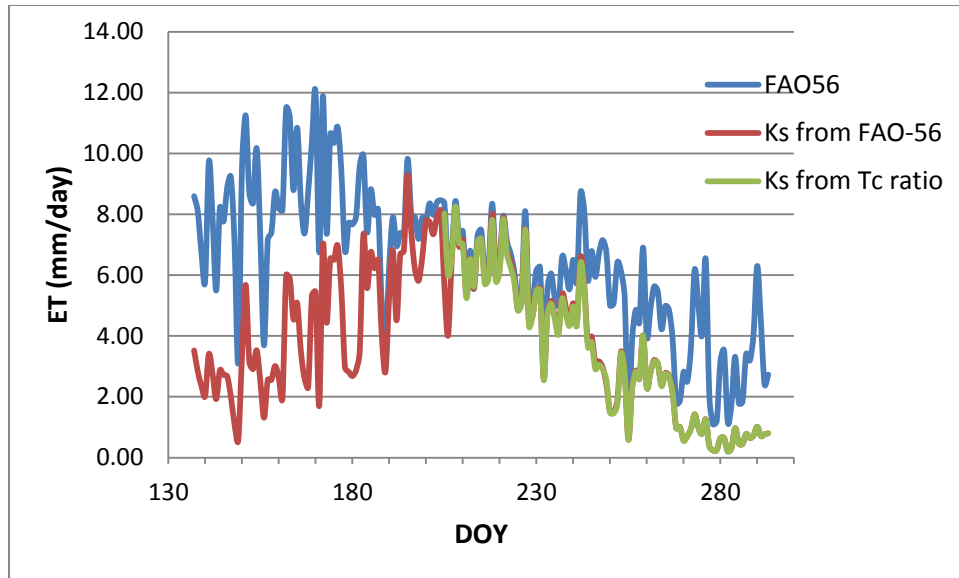


Figure 3. 31. Daily ET (mm/day) for Treatment 3 (HFDD) in SWIIM field

Unlike what occurred in LIRF, the potential corn ET calculated following FAO-56 methods does behave as its suppose to and acts at the upper limit for the ET in all three figures 3.29 to 3.31. The potential ET calculated from FAO-56 does not account for water stress unlike the other two methods. Therefore it is easy to see that including  $K_s$  in the calculation of ET made a large impact, especially in Treatment 3 (Figure 3.31). The actual ET was much lower than the potential ET from FAO-56, except in the middle of the season (around DOY 210). Another reason ET from FAO-56 is much larger is that the  $K_{cb}$  tabular values were consistently larger than the  $K_{cb}$  calculated from Equation 2.9. Treatment 1 shown in Figure 3.29, for all three methods of calculating ET gave very similar results, because the  $K_{cb}$  for all three methods was very similar, and not much stress was experienced.  $K_{cb}$  calculated for Treatment 2 and 3 are shown in Figure 3.32. Note that it was assumed all three treatments progressed at the same rate, so  $K_{cb}$  calculated from FAO-56 was the same for all three treatments.

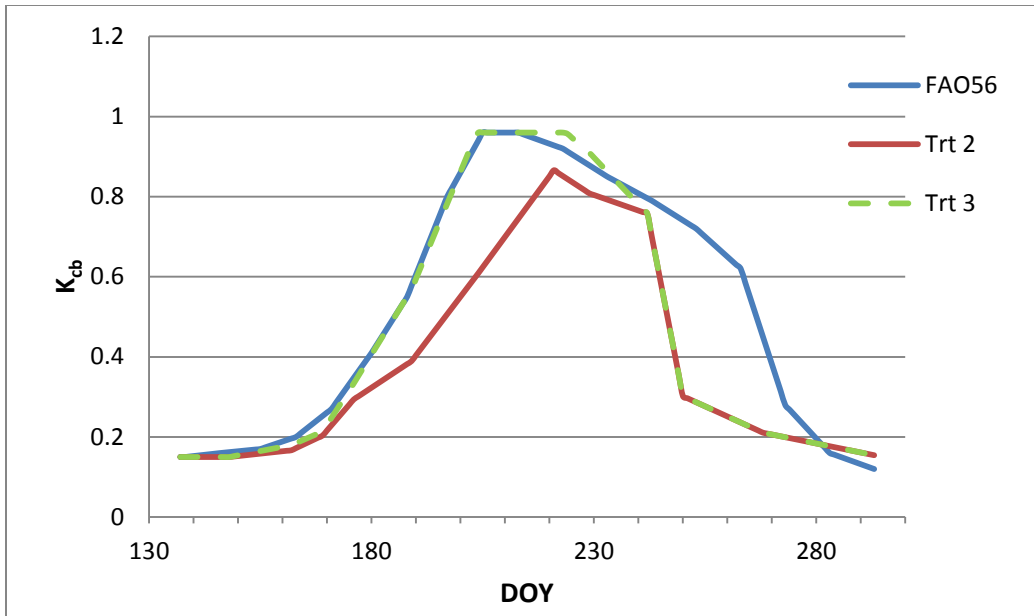


Figure 3.32. Daily  $K_{cb}$  values for FAO-56, and calculated from Trout and Johnson (2007) for Treatment 2 and 3.

$K_{cb}$  is calculated the same for both main methods of calculating ET using Equation 2.9. In Figure 3.32 the  $K_{cb}$  is just shown for FAO-56 and then Treatments 2 and 3. In Figure 3.32, the difference between the treatments can be seen very well. Treatment 2 (LFDI) had a  $K_{cb}$  that was consistently lower than  $K_{cb}$  calculated from FAO-56. Treatment 3 followed  $K_{cb}$  from FAO-56 for the first part of the season, and then followed Treatment 2's  $K_{cb}$  line for the second half of the season.  $K_s$  for both methods showed very different results, which was also seen with the data from LIRF. Daily  $K_s$  values for Treatment 2 for both methods are shown in Figure 3.33.

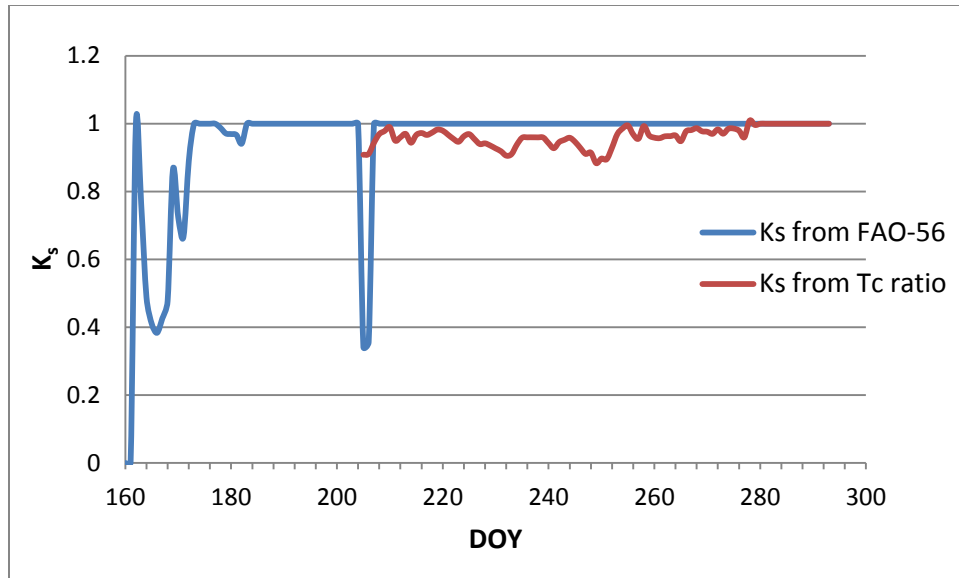


Figure 3.33. Daily  $K_s$  values for Treatment 2

Like the results from LIRF, at the SWIIM field, the  $K_s$  from the two different methods behave very differently.  $K_s$  from FAO-56 yielded large water stress events ( $K_s < 0.9$ ).  $K_s$  from  $T_c$  ratio identified smaller along with larger water stress events and therefore seems to be more sensitive to detecting crop water stress. This is most likely because  $K_s$  from  $T_c$  ratio is based on canopy temperatures which is more responsive to water stress compared to  $K_s$  calculated from FAO-56 which relies on soil water deficit which isn't always very sensitive and accurate measurements are not always available. The daily  $D_i$  over the season along with RAW for Treatment 2 for both methods are shown in Figures 3.34 and 3.35 respectively.

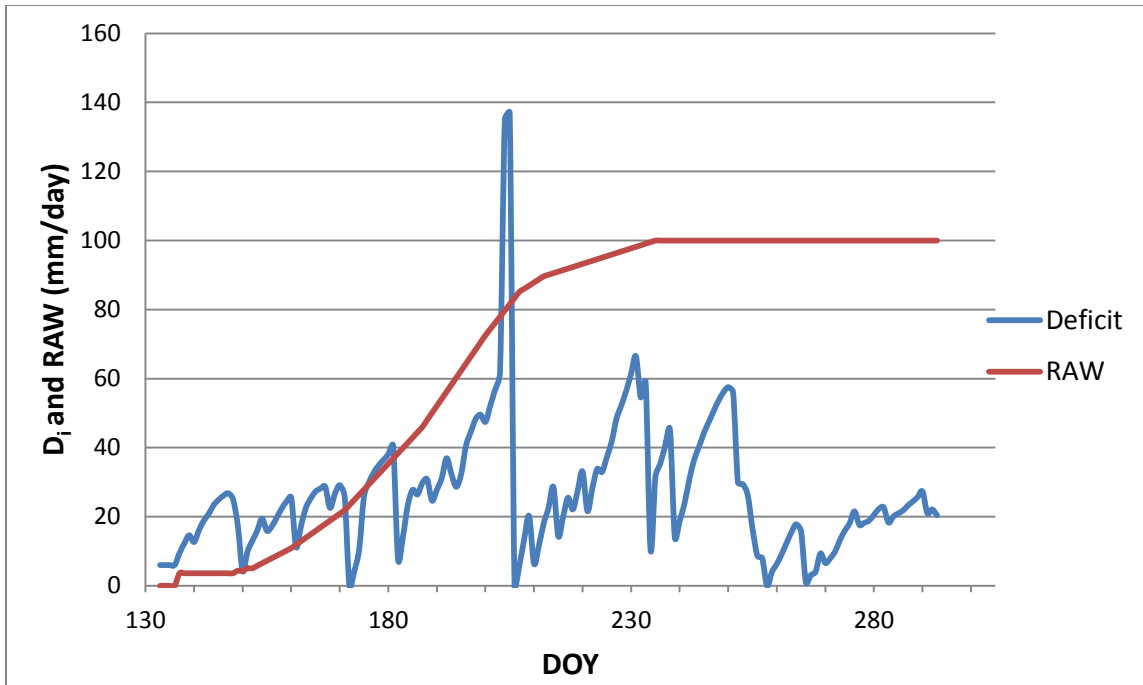


Figure 3.34. Time-series of daily  $D_i$  and RAW for Treatment 2, calculated using  $K_s$  from FAO-56

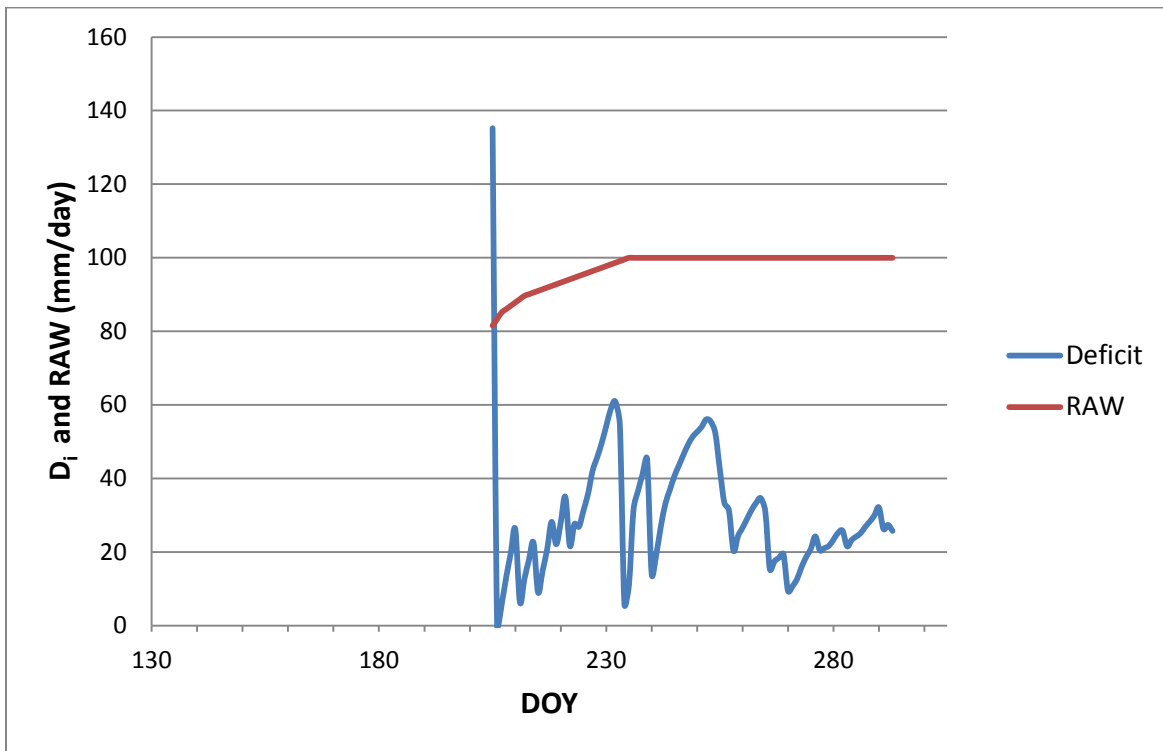


Figure 3.35. Time-series of daily  $D_i$  and RAW for Treatment 2, calculated using  $K_s$  from  $T_c$  ratio

Figure 3.34 shows that most of the major water stress events (when  $D_i > \text{RAW}$ ) occurred at the beginning of the season, and one major one around DOY 204 and 205. Figure 3.35 shows only the second half of the season after full cover was achieved. The deficit calculated in the second half of the season for both methods (Figure 3.34 and 3.35) was very similar even though they were calculated with different  $K_s$  values.

The vegetation indices (NDVI, GNDVI, and OSAVI) were calculated using the multispectral light (reflectance) data collected using an MSR5 as explained in Chapter 3. There were seven days of data through July and August. For all seven of these days the vegetation ratios were calculated and compared to  $K_s$  calculated from  $T_{c \text{ ratio}}$  for those days. Figure 3.36, 3.37, and 3.38 shows  $K_s$  versus  $N_{\text{ratio}}$ ,  $G_{\text{ratio}}$ , and  $O_{\text{ratio}}$ , respectively.

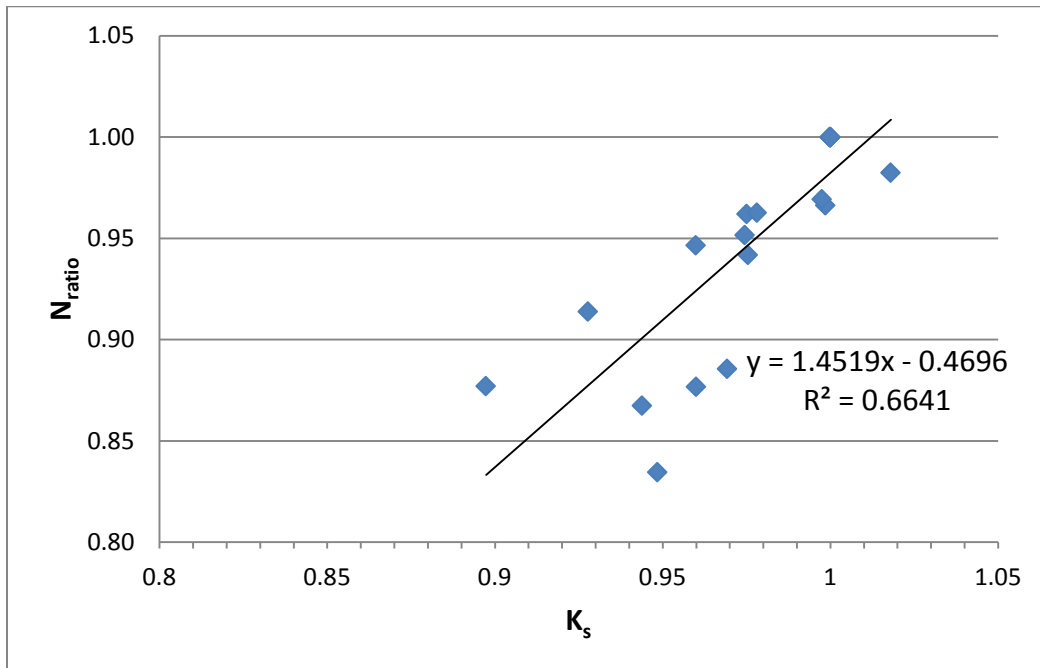


Figure 3.36.  $K_s$  from  $T_{c \text{ ratio}}$  versus  $N_{\text{ratio}}$  for Treatment 1, 2, and 3

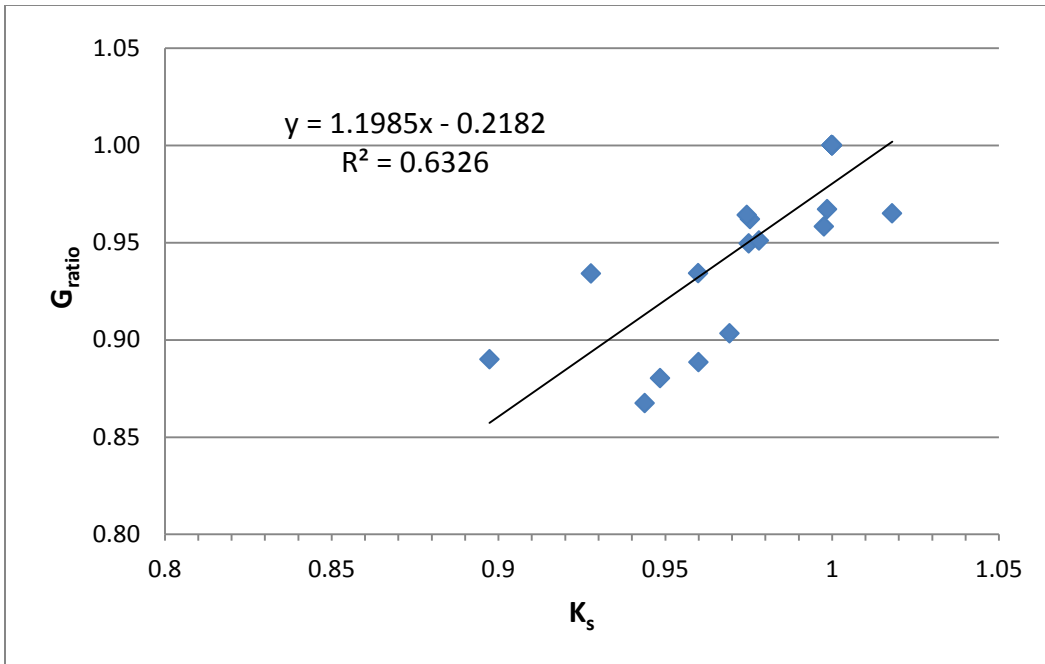


Figure 3.37.  $K_s$  from  $T_c$  ratio versus  $G_{ratio}$  for Treatment 1, 2, and 3

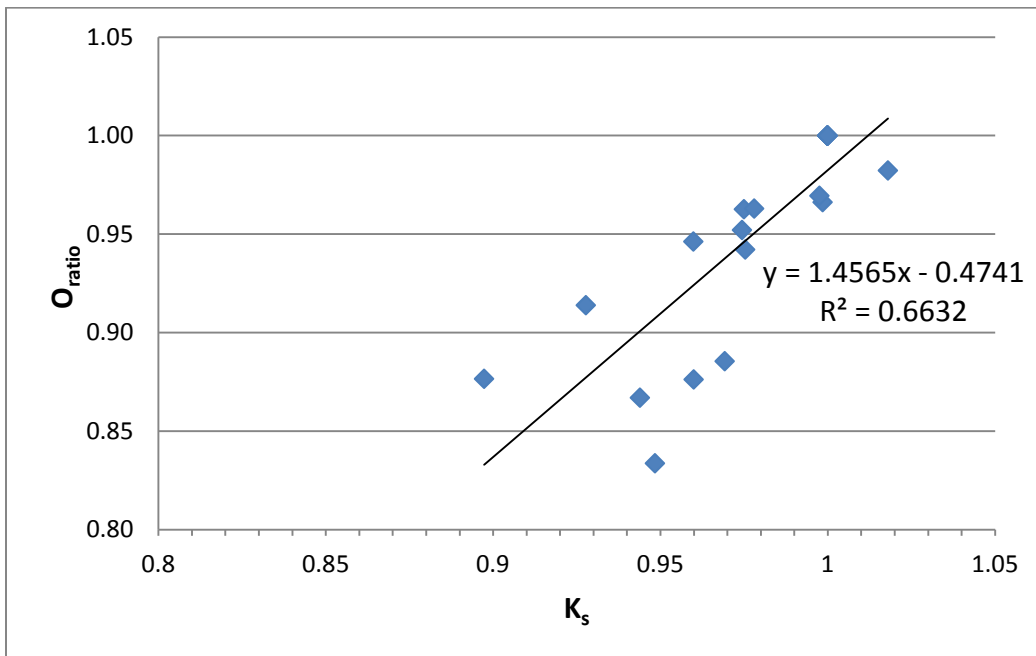


Figure 3.38.  $K_s$  from  $T_c$  ratio versus  $O_{ratio}$  for Treatment 1, 2, and 3

Table 3.5. RMSE and MBE values for the vegetation ratios obtained from SWIIM field

	RMSE	MBE
N <sub>ratio</sub>	0.043	-0.028
G <sub>ratio</sub>	0.036	0.004
O <sub>ratio</sub>	0.043	-0.004

As it can be seen in Figure 3.36, 3.37, and 3.38 all of the vegetation ratios showed a good relationships with  $K_s$ . N<sub>ratio</sub> and O<sub>ratio</sub> achieved the highest  $R^2$  value of 0.66. From Table 3.5 G<sub>ratio</sub> had the lowest RMSE value (0.036), but both O<sub>ratio</sub> and G<sub>ratio</sub> had the lowest MBE value ( $\pm 0.004$ ). This result is deemed good. As seen in Figures 3.36 to 3.38 there are four outliers causing the lower  $R^2$  values, and higher RMSE and MBE values than what would occur without these outliers. These values occurred throughout the season and were not during one particular part of the growing season. They were most likely caused by days where soil background affects were larger than normal (i.e. VF had decreased due to stress), or the data was maybe taken on a partly cloudy days where clouds effected incoming solar radiation. Thus, not enough is known about the four points in order to justify removing them. The results at SWIIM field seem to validate the results obtained from LIRF, that there may be evidence that vegetation indices could be used to monitor corn water stress. The vegetation ratios had better results for SWIIM field compared to LIRF based on  $R^2$ , RMSE, and MBE values. This may have been caused by the SKYE light sensors never being used before the 2013 field season; therefore there was probably some first time user error in the data obtained from LIRF. Compared to the SKYE light sensors the MSR5 multispectral scanner sensor had been around much longer and had been used, in the same SWIIM field since 2010 in other studies (Taghvaeian et al., 2013) and is known to be accurate and consistent, while not as much is known on the SKYE sensors. Since the highboy tractor could only be run on days when irrigation was not taking place this limited the amount of

data that could be taken with clear sky conditions. The MSR5 is handheld and the user could be more selective about what days of the week data was taken on. Therefore, it is not surprising that the SWIIM field actually had better results, which seem to validate and corroborates results obtained from LIRF.

Since these results, that vegetation indices seem to be a viable way to monitor corn water stress, seem to be valid then the irrigation trigger point now needs to be validated. From the data at LIRF an irrigation trigger point of 0.93 was chosen. In a way that when the vegetation ratios values result below 0.93 the corn is assumed water stressed and therefore it needs to be irrigated before considerable yield loss is experienced. It can be seen that for SWIIM the largest SWD also occurs when  $K_s$  and the vegetation ratios were equal or less than 0.93. Since Treatment 3 was high frequency deficit it received more irrigation events so the  $K_s$  value in the second half of the season never resulted below 0.93; while Treatment 2 received less irrigation events and had a couple of days with the vegetation ratios below 0.93. The greater  $D_i$  events occurred when the vegetation ratios were less than 0.93, this  $D_i$  could then cause a decrease in grain yield.  $D_i$  that occurs when  $K_s$  is greater than 0.93 are smaller and most likely wouldn't have a large effect on the grain yield. Although, more research needs to be done to verify this observation. Unlike in LIRF, no  $D_i$  greater than RAW occurred during the second half of the season (Figure 3.34, and 3.35), thus not many water stress events occurred that could have caused a vegetation ratio to be below 0.93, as shown in Figure 3.39. Looking at data obtained from the ARS-WMU irrigation events when  $K_s$  (from  $T_{c \text{ ratio}}$ ) dropped close to 0.93 the corn  $D_i$  was rarely greater than RAW; therefore, evidence that corn water stress was mild. From this analysis, it is inferred that the corn could have been allowed to be further stressed, especially for the deficit irrigation treatments. To

be able to better appreciate whether the 0.93 irrigation trigger value could be applied to surface irrigation it would be best to obtain more data from a higher degree of deficit irrigated corn.

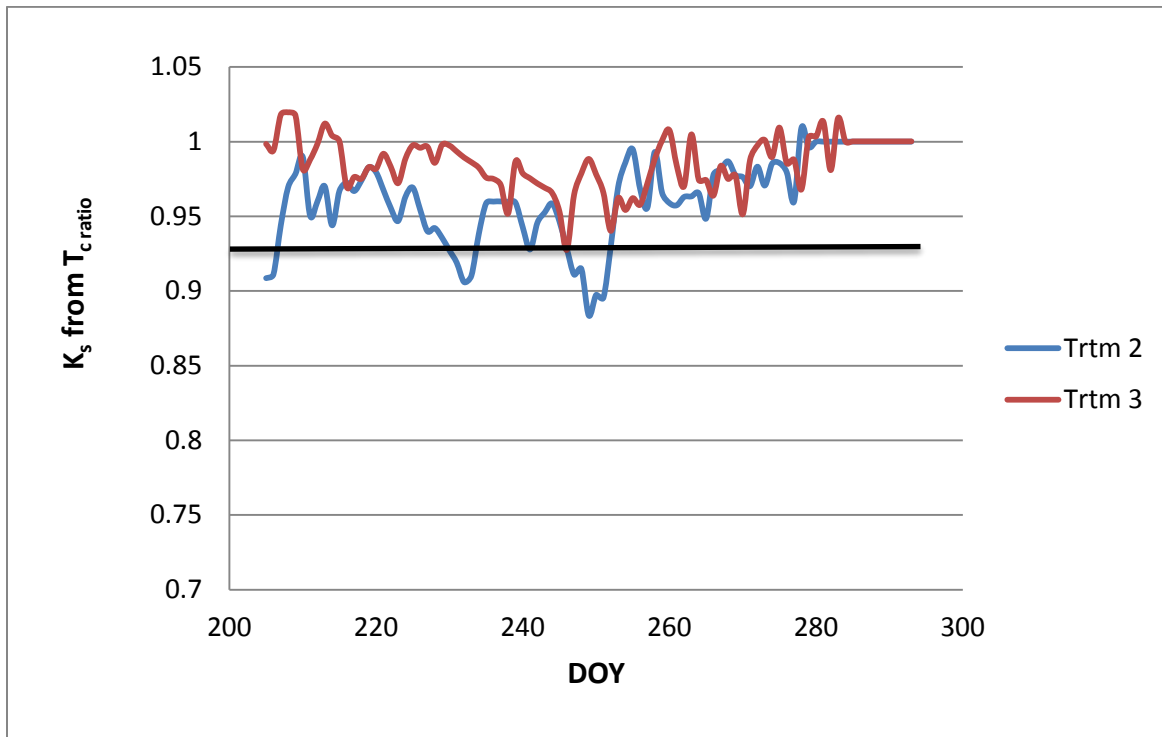


Figure 3.39. Time-series of  $K_s$  from  $T_c$  ratio with irrigation trigger point highlighted by black line. Like with LIRF this line is an estimate for the irrigation trigger point for the vegetation ratios since not enough data was available to use the vegetation ratios to determine it.

## CHAPTER 4: CONCLUSION

Research was conducted to assess whether corn spectral reflectance is sensitive to induced water stress. In order to study this ground based remote sensing method, corn spectral reflectance data were collected throughout the 2013 growing season. Irrigation, precipitation, ET, and deep percolation were monitored to determine soil water deficit through the soil water balance method. Two different water balances were made, one with  $K_s$  calculated from FAO-56 and the other with  $K_s$  calculated from  $T_{c\ ratio}$ . After comparing the two different  $K_s$  values with each other and the water balances it was concluded that calculating  $K_s$  from  $T_{c\ ratio}$  seems to be a viable option because it gave better results than  $K_s$  from FAO-56 for prediction of  $D_i$  compared to measured  $D_i$ .  $K_s$  from  $T_{c\ ratio}$  had lower RMSE (15.45), MBE (-3.59), and MAE (12.41) values than  $K_s$  from FAO-56 (RMSE=19.69, MBE, -13.03, MAE=16.86). Four different vegetation ratios were calculated from the crop spectral reflectance data: NDVI, GNDVI, OSAVI, and WDRVI. After comparing WDRVI to VF it was found that WDRVI could not be calculated correctly using the SKYE sensor data, therefore was not able to be tested for sensitivity to water stress. Two different types of imagery were used to obtain measured VF (1) RGB from a Canon 50d camera and (2) multispectral from a multispectral FLUX camera. It was decided that calculating VF from the RGB imagery was more accurate because the multispectral imagery became over saturated by soil background effects during periods of water stress in the growing season and could not accurately measure VF. Plotting NDVI, GNDVI, and OSAVI versus measured VF (from RGB imagery) it was found that all three were linearly correlated with VF and had almost a 1 to 1 relationship with VF. This relationship and that RGB imagery works best to measure VF was verified by many other sources (Jiménez-Muñoz et al. [2009], Carlson and

Ripley [1997], Barati et al. [2011] ), . In order to be able to compare the vegetation indices to  $K_s$ , vegetation ratios were developed for NDVI, GNDVI, and OSAVI. These ratios were based on the vegetation index value of a stressed field divided by the vegetation index value of a non-stressed field. These vegetation ratios were compared to  $K_s$  from  $T_{c \text{ ratio}}$  to see how they responded to water stress. Comparing the vegetation ratios to  $K_s$  from  $T_{c \text{ ratio}}$  gave good  $R^2$  values ( $N_{\text{ratio}} = 0.53$ ,  $G_{\text{ratio}}=0.46$ ,  $O_{\text{ratio}}=0.49$ ) and low RMSE values ( $N_{\text{ratio}} = 0.076$ ,  $G_{\text{ratio}}=0.062$ ,  $O_{\text{ratio}}=0.076$ ). It was found that the vegetation ratios were correlated with  $K_s$  and therefore these findings seem to verify that corn spectral reflectance is sensitive to corn water stress. The vegetation ratios were calculated for an adjacent furrow irrigated field (SWIIM field) in order to validate the results obtained in LIRF. Results at SWIIM field were found to be better than results obtained at LIRF, with  $R^2$  values closer to 1 ( $N_{\text{ratio}} = 0.66$ ,  $G_{\text{ratio}} = 0.63$ ,  $O_{\text{ratio}} = 0.66$ ), and lower RMSE values ( $N_{\text{ratio}} = 0.043$ ,  $G_{\text{ratio}} = 0.036$ ,  $O_{\text{ratio}} = 0.043$ ). There are many reasons this could have occurred, the main one being that the SKYE light sensors used in LIRF were being used for the first time. User error along with not having any previous record of how SKYE sensors perform in heat could have caused some of the error. The MSR5 sensor used in SWIIM had been used many times before and is more widely used in research. Therefore, it is not surprising that the results from SWIIM field using the MSR5 data, were better than in LIRF.

An irrigation trigger would allow a farmer to know when to irrigate based on the vegetation ratios. Since there seems to be evidence that spectral reflectance of corn is sensitive to water stress then a method was developed to trigger irrigation events. A trigger point of  $K_s = 0.93$  was found to be recommended after observing that  $K_s$  less than 0.93 indicates a more significant stress event and could potentially cause decrease in yields. Therefore for a farmer using vegetation ratios to monitor his crops when the vegetation ratio hits 0.93 the farmer should

irrigate. This trigger point was also found to work for the SWIIM field. The trigger could vary from field to field, but in order to make the method simpler the value of 0.93 was tested on SWIIM and was found it worked there as well.

To be able to use the vegetation ratios a farmer would need two vegetation index values, one for fully irrigated corn, and one for water stressed corn. Unlike at research farms most farmers would not have multiple treatments of deficit irrigated corn; they would manage to obtain maximum economic potential, and often with heterogeneous fully irrigated fields. Therefore, for this project a VF table (for fully irrigated corn) based on growth stages was developed, in which the farmer would only need to know the growth stage of the corn and from the table the VF of fully irrigated corn can be obtained. This VF could then be inserted into one of the developed equations to determine the vegetation index for fully irrigated corn. This is important, i.e. to make this method of using vegetation ratios to monitor corn water stress a viable option for farmers outside of research.

This method of using vegetation ratios and growth stages instead of building a water balance requires much less time and data processing, therefore making it an option for smaller scale farmers who do not have the resources to build an accurate water balance. It would help farmers still make smart irrigation decisions, instead of just applying a certain amount of water every week.

While this project has shown positive results there are still limitations to the results.  $K_s$  from  $T_{c \text{ ratio}}$  was shown to capture small and large stress events, it is easily affected by soil background effects and can go outside of its theoretical limits of 0 to 1. This occurs when the canopy temperature from a stressed treatment is cooler than the canopy temperature from a non-stressed

treatment. When using IRT's that have a wide view angle,  $K_s$  from  $T_{c \text{ ratio}}$  cannot be used until full cover has been achieved. One way to get around this limitation is to use hand held IRT's with a narrow field of view to obtain canopy temperature before full cover has been achieved. By using a narrow field of view, it can be made sure that the canopy temperature reading is of the corn, not of the soil background. The proposed method depends on frequent and accurate samples of multispectral data, which are not always available or can be costly to obtain. Other limitations for this study are that the proposed method can only be used for corn, as other types of crops develop differently, and therefore Table 3.4 cannot be used for other crops. Another limitation is that the vegetation indices needed to calculate the vegetation ratios can only be measured on clear days, around solar noon. If the measurements are made other than solar noon this can affect the amount of stress seen and therefore the vegetation ratio value. Even with these limitations, of the proposed method, the vegetation ratios seem to have the potential to allow for irrigation management with limited data not requiring monitoring volumetric water content.

#### 4.1 Recommendations for Future Study

While this study obtained some good results, there is still a lot of room for future research in the spectral response of corn to water stress. More research is needed on the use of SKYE sensors in agriculture to be able to feel more confident about the results SKYE sensors give, since this is one of the first times SKYE sensors have been used in this setting. Further study needs to include the changes in magnitude of spectral reflectance in the different wavelengths considered when certain levels of water stress are applied. Another area would be to apply this study to different crops, as this study was corn specific and additional work would be necessary to apply the same methods to other crops, and see how the results differ. Another study could look into applying

the proposed method at three different levels of remote sensing (ground based, aerial [manned and un-manned platforms], and satellite imagery and comparing the results. This is especially important because the easiest way to apply the results of this project would be to use satellite imagery. Since using satellite imagery was outside scope of this project it would be interesting to see what results were obtained, compared to the ground based measurements used in this study.

## REFERENCES

- Alganci, U., M. Ozdogan, E. Sertel, and C. Ormeci. 2014. Estimating maize and cotton yield in southeastern Turkey with integrated use of satellite images, meteorological data and digital photographs. *Field Crops Research* 157: 8-19.
- Allen, R.G., J.L. Wright, W.O. Pruitt, L.S. Pereira, and M.E. Jensen. Chapter 8: Water Requirements. *Design and Operation of Farm Irrigation Systems*. 2<sup>nd</sup> ed. American Society of Agricultural and Biological Engineers, 209-288.
- Allen, R.G., L.S. Pereira, and M. Smith. 1998. Crop evapotranspiration: Guidelines for computing crop water requirements. *United Nations Food and Agriculture Organization, Irrigation and Drainage Paper 56*, Rome, Italy, 300.
- ASCE-EWRI. 2005. The ASCE Standardized Reference Evapotranspiration Equation. Report 0-7844-0805-X, *ASCE Task Committee on Standardization of Reference Evapotranspiration*. Reston, Va.: American Society of Civil Engineers.
- Arnell, N. 1999. Climate Change and Global Water Resources. *Global Environmental Change* 9: 31-49.
- Aydinsakir, K. 2013. The influence of regular deficit irrigation applications on water use, yield, and quality components of two corn (*Zea mays* L.) genotypes. *Agricultural Water Management* 128: 65-71.
- Barati, S., B. Rayegani, M. Saati, A. Sharifi, and M. Nasri. 2011. Comparison the accuracies of different spectral indices for estimation of vegetation cover fraction in sparse vegetated areas. *The Egyptian Journal of Remote Sensing and Space Science*. 14: 49-56.
- Baret, F., G. Guyot, and D. Major. 1989. TSAVI: a vegetation index which minimizes soil brightness effects on LAI and APAR estimation. *Canadian Synopsis. On Remote Sensing and IGARSS'90*. 4.
- Baret, F., and G. Guyot. 1991. Potentials and Limits of Vegetation Indices for LAI and APAR Assessment. *Remote Sensing of Environment* 35: 161-171.
- Bausch, W., T. Trout, and G. Buchleiter. 2011. Evapotranspiration adjustments for deficit-irrigated corn using canopy temperature: a concept. *Irrigation and Drainage* 60: 682-693.
- Çakir, R. 2004. Effect of water stress at different development stages on vegetative and reproductive growth of corn. *Field Crops Research* 89: 1-16.

- Carlson, T.N., and D.A. Ripley. 1997. On the Relation between NDVI, Fractional Vegetation Cover and Leaf Area Index. *Remote Sensing of the Environment* 62: 241-252.
- Cristiano, P.M., G. Posse, C.M. Di Bella, and F.R. Jaimes. 2010. Uncertainties in fPAR estimation of grass canopies under different stress situations and differences in architecture. *International Journal of Remote Sensing* 31(15): 4095-4109.
- Doorenbos, J., and A.K. Kassam. 1979. Yield response to water. *Irrigation and Drainage Paper 3*, FAO, United Nations, Rome, 176.
- Doorenbos, J., and W.O. Pruitt. 1977. Crop water requirements. *Irrigation and Drainage Paper 24*, FAO, Rome, Italy.
- Dore, M. H.I. 2005. Climate Change and changes in global precipitation patterns: What do we know? *Environment International* 31(8): 1167-1181.
- Ertek, A., and B. Kara. 2013. Yield and quality of sweet corn under deficit irrigation. *Agricultural Water Management* 129: 138-144.
- Farré, I., and J.M. Faci. 2009. Deficit Irrigation in maize for reducing agricultural water use in a Mediterranean environment. *Agricultural Water Management* 96: 383-394.
- Fischer, G., F. Tubiello, H. Vanvelthuisen, and D. Wiberg. 2007. Climate Change Impacts on Irrigation Water Requirements: Effects of Mitigation, 1990–2080. *Technological Forecasting and Social Change*, 74.7: 1083-107.
- Genc, L., M. Inalpulat, U. Kizil, M. Mirik, S. Smith, and M. Mendes. 2013. Determination of water stress with spectral reflectance on sweet corn (*Zea mays* L.) using classification tree (CT) analysis. *Žemdirbystė*, 100(1): 81-90.
- Geerts, S. and D. Raes. 2009. Deficit irrigation as on-farm strategy to maximize crop water productivity in dry areas. *Agricultural Water Management* 96: 1275-1284.
- Geerts, S., D. Raes, M. Garcia, J. Vacher, R. Mamani, J. Mendoza, R. Huanca, B. Morales, R. Miranda, J. Cusicanqui, and C. Taboada. 2008. Introducing deficit irrigation to stabilize yields of quinoa. *European Journal of Agronomy* 28(3): 427-436.
- Gitelson, A.A., Y.J. Kaufman, and M.N. Merzlyak. 1996. Use of a Green Channel in Remote Sensing of Global Vegetation from EOS-MODIS. *Remote Sensing of Environment*, 58: 289-298.
- Gitelson, A.A., Y.J. Kaufman, R. Stark, and D. Rundquist. 2002. Novel algorithms for remote estimation of vegetation fraction. *Remote Sensing of Environment* 80: 76-87.

- Gitelson, A.A. 2004. Wide Dynamic Range Vegetation Index for Remote Quantification of Biophysical Characteristics of Vegetation. *Journal of Plant Physiology* 161: 165-173.
- Gitelson, A. 2013. Remote estimation of crop fractional vegetation cover: the use of noise equivalent as an indicator of performance of vegetation indices. *International Journal of Remote Sensing* 34(17): 6054-6066.
- Hatfield, J. L., A. A. Gitelson, J. S. Schepers, and C. L. Walthall. 2008. Application of Spectral Remote Sensing for Agronomic Decisions. *Agronomy Journal* 100. Supplement 3: S-117-131.
- Hoffman, G. J., and R.G. Evans. 2007a. Chapter 1: Introduction. *Design and Operation of Farm Irrigation Systems*. 2<sup>nd</sup> ed. American Society of Agricultural and Biological Engineers, 12-13.
- Hoffman, G. J., R. G. Evans, M. E. Jensen, D. L. Martin, and R. L. Elliott. 2007b. *Design and Operation of Farm Irrigation Systems*. 2nd ed. American Society of Agricultural and Biological Engineers. (2007b): 211-215.
- Huete, A. R. 1988. A Soil-Adjusted Vegetation Index (SAVI). *Remote Sensing of Environment* 25: 295-309.
- Huete, A. R., R.D. Jackson, and D.F. Post. 1985. Spectral response of a plant canopy with different soil backgrounds. *Remote Sensing of Environment* 17: 37-53.
- IPCC. 2013. Climate Change 2013: The Physical Science Basis. Retrieved from <<http://www.buildingclimatesolutions.org/view/article/524b2c2f0cf264abcd86106a>>.
- Jackson, R.D. and C.E. Ezra. 1985. Spectral response of cotton to suddenly induced water stress. *International Journal of Remote Sensing* 6: 177-185.
- Jackson, R.D., P.J. Pinter, Jr., R.J. Reginato, and S.B. Idso. 1986. Detection and Evaluation of Plant Stresses for Crop Management Decisions. *IEEE Transactions on Geoscience and Remote Sensing* 24: 99-106.
- Jackson, R.D., P.N. Slater, and P.J. Pinter, Jr. 1983. Discrimination of Growth and Water Stress in Wheat by Various Vegetation Indices Through Clear and Turbid Atmospheres. *Remote Sensing of Environment* 13: 187-208.
- Jiang, Z., A.R. Huete, J. Chen, Y. Chen, J. Li, G. Yan, and X. Zhang. 2006. Analysis of NDVI and scaled difference vegetation index retrievals of vegetation fraction. *Remote Sensing of Environment* 101: 366-378.
- Jiménez-Muñoz, J.C., J.A. Sobrino, A. Plaza, L. Guanter, J. Moreno, and P. Martínez. 2009. Comparison Between Fractional Vegetation Cover Retrievals from Vegetation Indices

- and Spectral Mixture Analysis: Case Study of PROBA/CHRIS Data over an Agricultural Area. *Sensors*. 9: 768-793.
- Kang, S., W. Shi, and J. Zhang. 2000. An improved water-use efficiency of maize grown under regulated deficit irrigation. *Field Crops Research* 67: 207-214.
- Katerji, N., J.W. Hoorn, A. Hamdy, and M. Mastrorilli. 2004. Comparison of corn yield response to plant water stress caused by salinity and by drought. *Agricultural Water Management* 65: 95-101.
- Köksal, E.S., Y. Güngör, and Y.E. Yildirm. 2011. Spectral reflectance characteristics of sugar beet under different levels of irrigation water and relationships between growth parameters and spectral indexes. *Irrigation and Drainage* 60: 187-195.
- Liu, H.Q., and A. Huete. 1995. A Feedback Based Modification of the NDVI to Minimize Canopy Background and Atmospheric Noise. *IEEE Transactions on Geoscience and Remote Sensing*. 33: 457- 465.
- Major, D.J., F. Baret, and G. Guyot. 1990. A ratio vegetation index adjusted for soil brightness. *International Journal of Remote Sensing* 11: 727-740.
- Mancino, G., A. Nolè, F. Ripullone, and A. Ferrara. 2014. Landsat TM imagery and NDVI differencing to detect vegetation change: assessing natural forest expansion in Basilicata, southern Italy. *Journal of Biogeosciences and Forestry* 7: 75-84.
- Meza Díaz, B. and G.A. Blackburn. 2003. Remote sensing of mangrove biophysical properties: evidence from a laboratory simulation of the possible effects of background variation on spectral vegetation indices. *International Journal of Remote Sensing* 24: 53-73.
- Pandy, R.K., J.W. Maranville, and A. Admou. 2000. Deficit irrigation and nitrogen effects on maize in a Sahelian environment I. Grain yield and yield components. *Agricultural Water Management* 46: 1-13.
- Peng, Y., A. Gitelson, and T. Sakamoto. 2013. Remote estimation of gross primary productivity in crops using MODIS 250 m data. *Remote Sensing of Environment* 128: 186-196.
- Pradhan, S., K.K. Bandyopadhyay, and D.K. Josh. 2012. Canopy reflectance spectra of wheat as related to crop yield, grain protein under different management practices. *Journal of Agrometeorology* 14: 21-25.
- Qi, J., A. Chehbouni, A.R. Huete, Y.H. Kerr, and S. Sorooshian. 1994. A Modified Soil Adjusted Vegetation Index." *Remote Sensing of Environment* 48: 119-126.
- Rondeaux, G., M. Steven, and F. Baret. 1996. Optimization of Soil-Adjusted Vegetation Indices. *Remote Sensing of Environment* 55: 95-107.

- Smith, M. O., S.L. Ustin, J.B. Adams, and A.R. Gillespie. 1990. Vegetation in Deserts: I.A Regional Measure of Abundance from Multispectral Images. *Remote Sensing of Environment*. 31: 1-26.
- Strachan I.B., E. Pattey, and J.B. Boisvert. 2002. Impact of nitrogen and environmental conditions on corn as detected by hyperspectral reflectance. *Remote Sensing of Environment* 80: 213-224.
- Trout, T.J, and L.F. Johnson. 2007. Estimating crop water use from remotely sensed NDVI, crop models, and reference ET. *The Role of Irrigation and Drainage in a Sustainable Future: Proceedings of the USCID Fourth International Conference on Irrigation and Drainage, Sacramento, CA, 3-6 October 2007*. Ed A.J. Clemmens, and S.S. Anderson. 275-285.
- Taghvaeian, S., J.L. Chávez, W.C. Bausch, K.C. DeJonge, and T.J. Trout. 2013. Minimizing instrumentation requirement for estimating crop water stress index and transpiration of maize. *Irrigation Science*.
- United Nations. 2012. The 2012 Revision of the World Population Prospects. United Nations, New York.
- Vescovo, L., G. Wohlfahrt, M. Balzarolo, S. Pilloni, M. Sottocornola, M. Rodeghiro, and D. Gianelle. 2012. New Spectral vegetation indices based on the near infrared shoulder wavelengths for remote detection of grassland phytomass. *International Journal of Remote Sensing* 33: 2178-2195.
- Viña, A., A.A. Gitelson, A.L. Nguy-Robertson, and Y. Peng. 2011. Comparison of different vegetation indices for the remote assessment of green leaf area index of crops. *Remote Sensing of Environment* 115(12): 3468-3478.
- Viña, A. 2012. Evaluating vegetation indices for assessing productivity along a tropical rain forest chronosequence in Western Amazonia. *Israel Journal of Plant Sciences* 60: 123-133.
- Wang, S., X. Chen, Q. Wang, P. Li, and X. Cao. 2012. Identification of the best spectral indices to remotely trace the diurnal course of water use efficiency of *Tamarix ramosissima* in the Gurbantungut Desert, China. *Environmental Earth Science* 65: 11-20.
- Xiao, J., and A. Moody. 2005. A comparison of methods for estimating fractional green vegetation cover within a desert-to-upland transition zone in central New Mexico, USA. *Remote Sensing of Environment* 98: 237-250.
- Zhang, H., and T. Oweis. 1999. Water-yield relations and optimal irrigation scheduling of wheat in the Mediterranean region. *Agricultural Water Management* 28: 195-211.

## APPENDIX A: COMPARISON OF DAILY $K_s$ VALUES

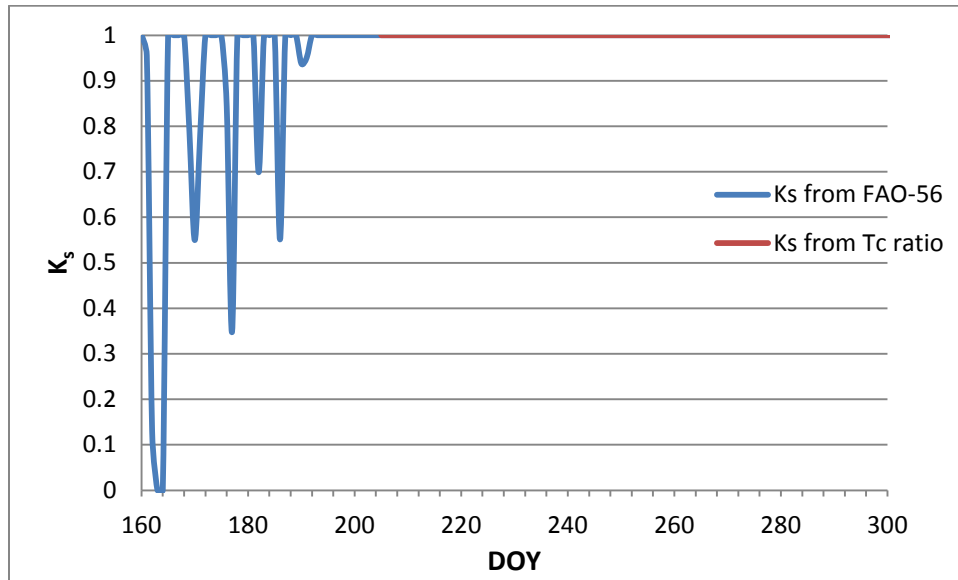


Figure A.1.  $K_s$  Daily values from Treatment 1 for the two different methods

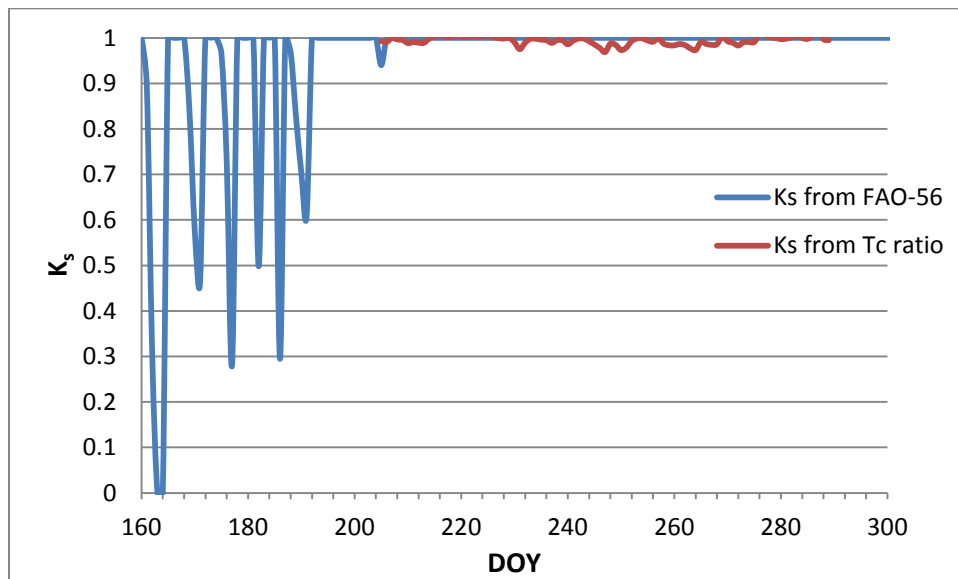


Figure A.2.  $K_s$  Daily values from Treatment 3 for the two different methods

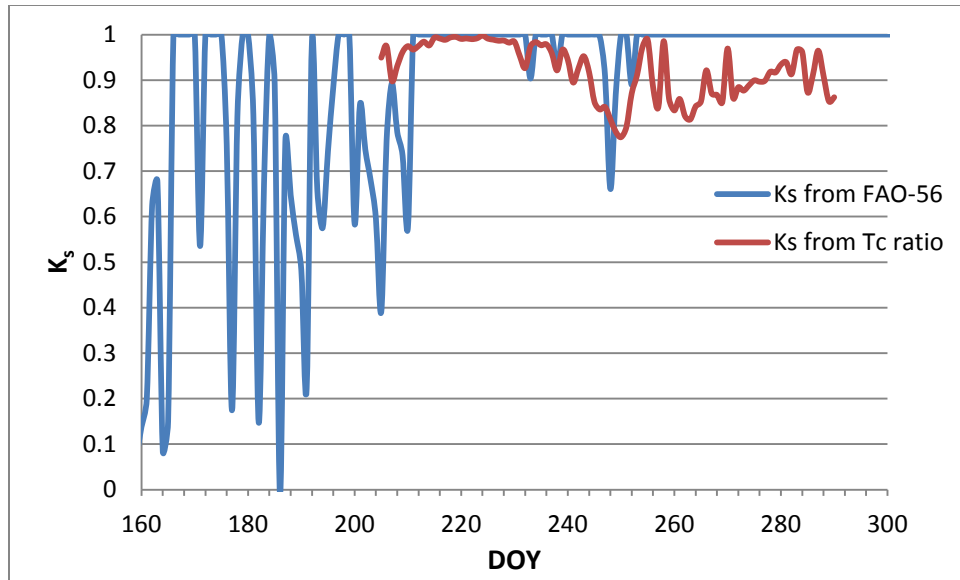


Figure A.3.  $K_s$  Daily values from Treatment 8 for the two different methods

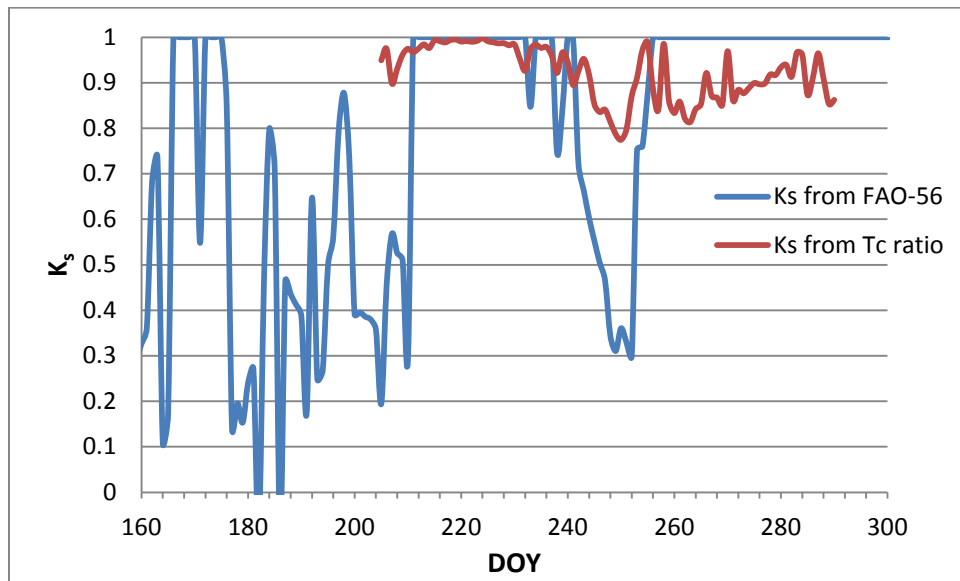


Figure A.4.  $K_s$  Daily values from Treatment 12 for the two different methods

APPENDIX B: DAILY  $D_i$  AND RAW GRAPHS FOR  $K_s$  FROM  $T_{c \text{ ratio}}$

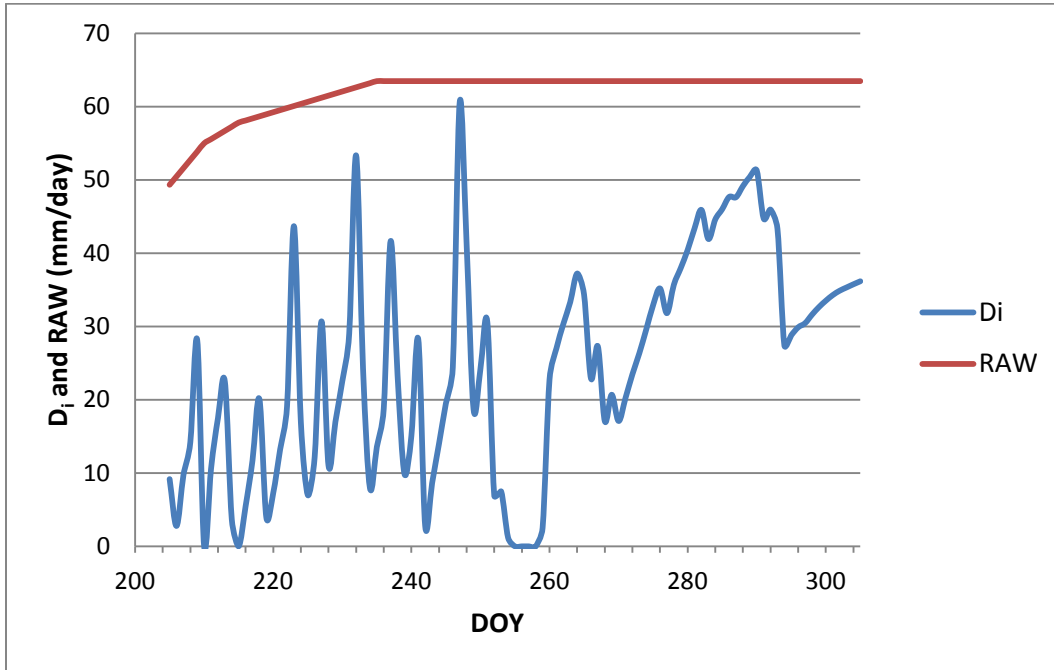


Figure B.1.  $D_i$  and RAW for Treatment 1 calculated with  $K_s$  from  $T_{c \text{ ratio}}$

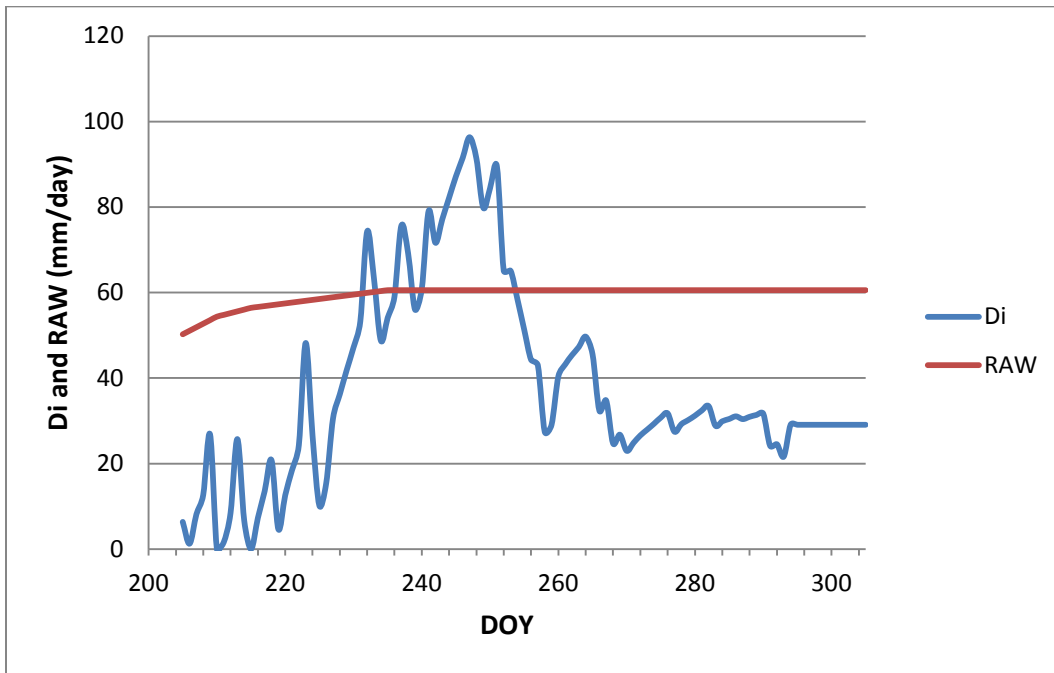


Figure B.2.  $D_i$  and RAW for Treatment 2 calculated with  $K_s$  from  $T_{c \text{ ratio}}$

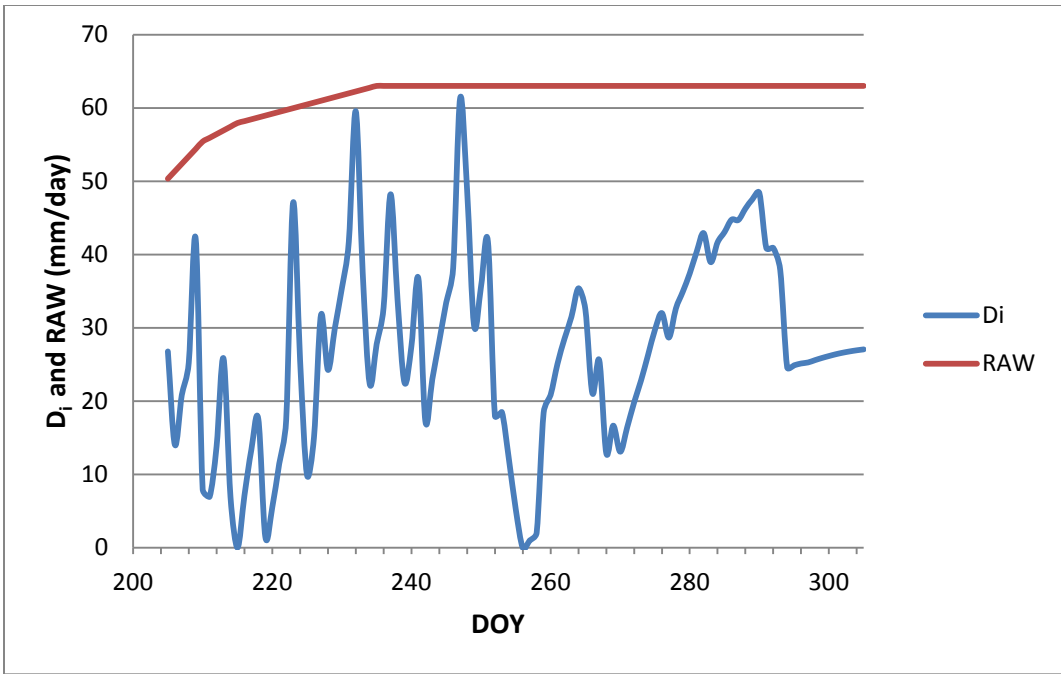


Figure B.3.  $D_i$  and RAW for Treatment 3 calculated with  $K_s$  from  $T_c$  ratio

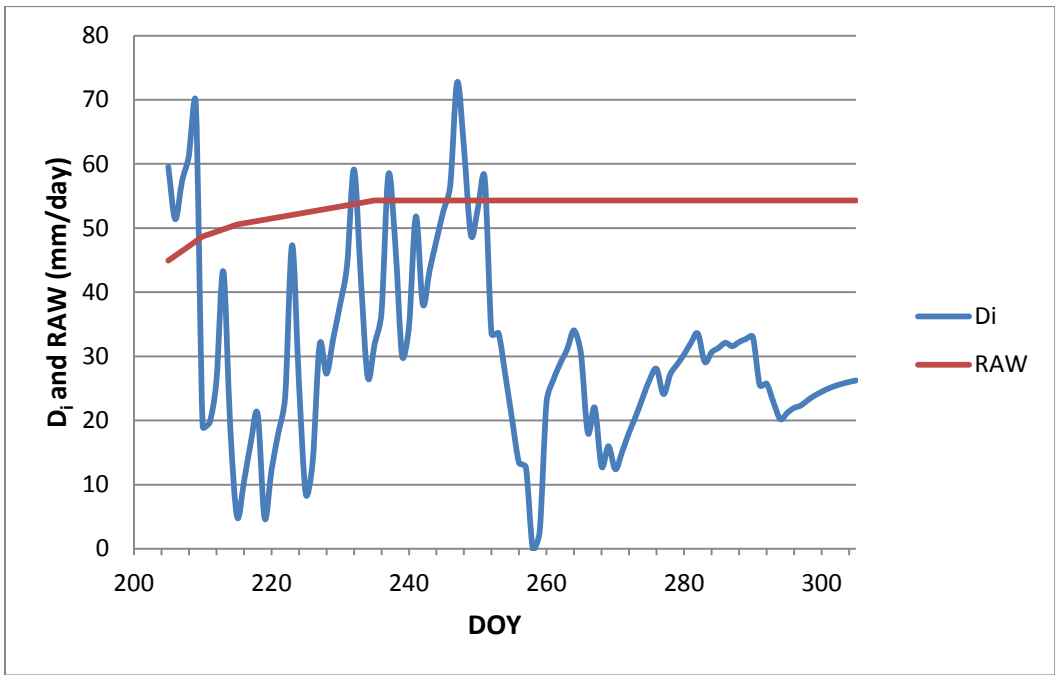


Figure B. 4.  $D_i$  and RAW for Treatment 8 calculated with  $K_s$  from  $T_c$  ratio

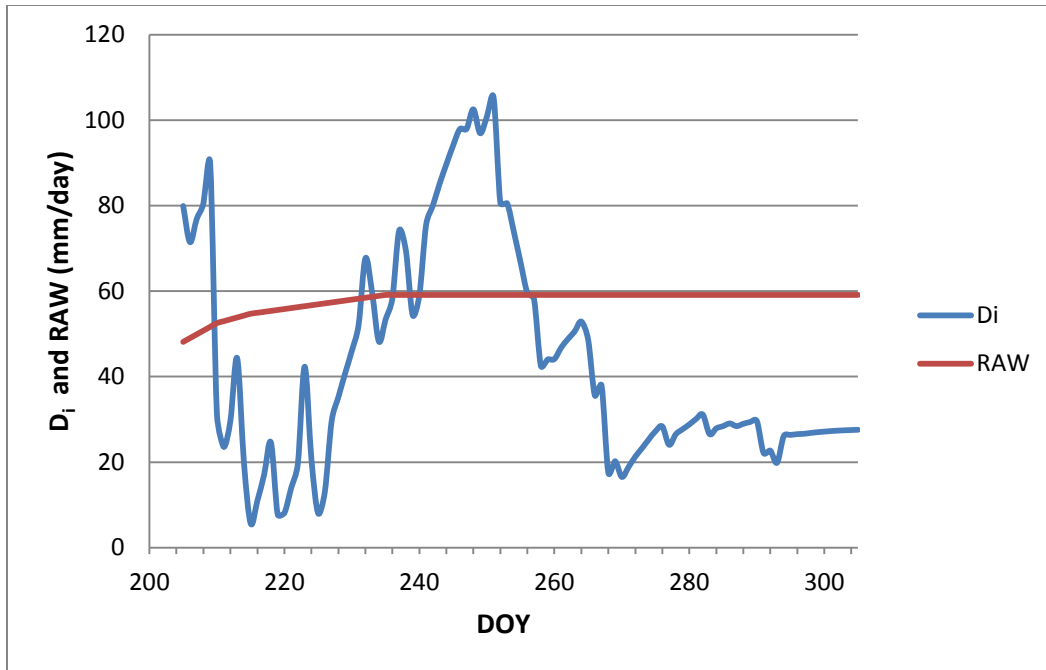


Figure B.5.  $D_i$  and RAW for Treatment 12 calculated with  $K_s$  from  $T_{c \text{ ratio}}$

APPENDIX C: DAILY  $D_i$  AND RAW GRAPHS FOR  $K_s$  FROM FAO-56

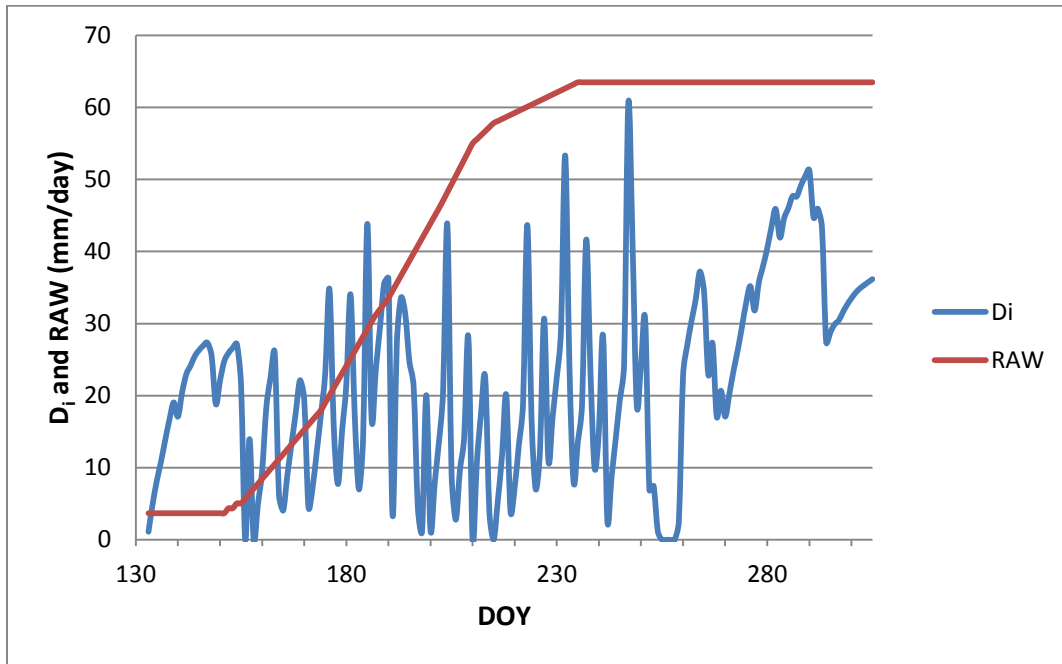


Figure C.1.  $D_i$  and RAW for Treatment 1 with  $K_s$  from FAO-56

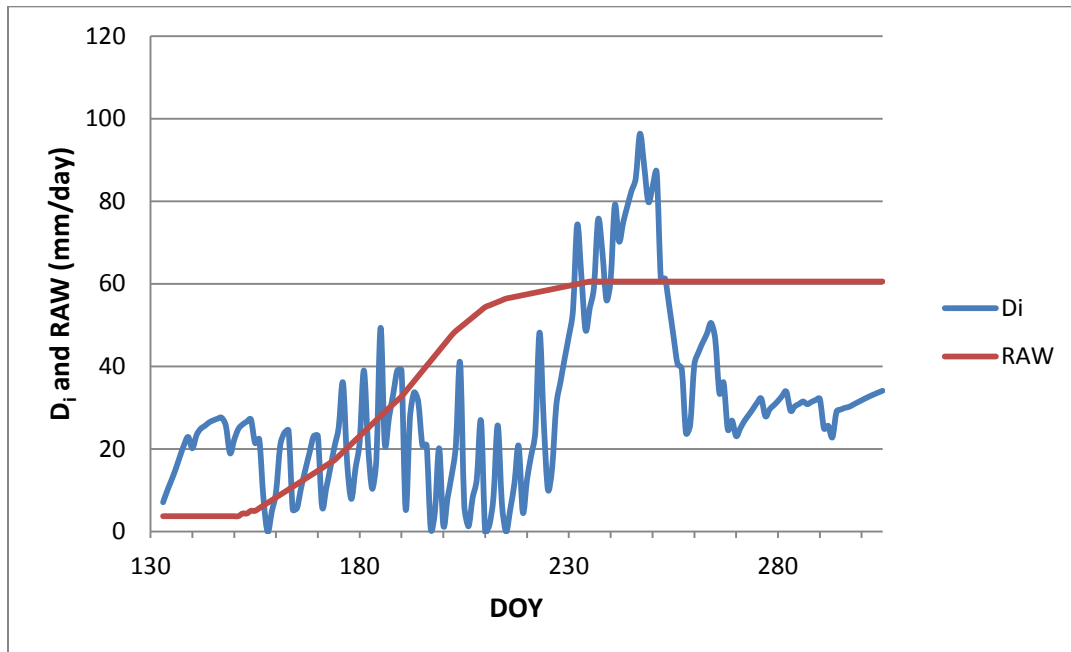


Figure C.2.  $D_i$  and RAW for Treatment 2 with  $K_s$  from FAO-56

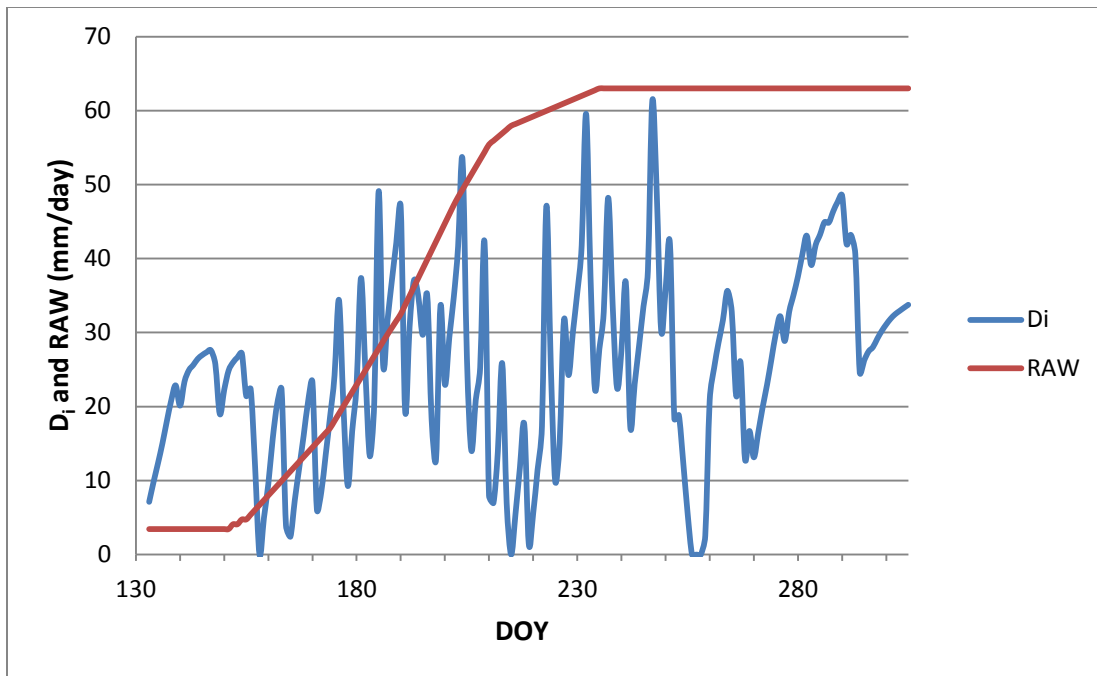


Figure C.3.  $D_i$  and RAW for Treatment 3 with  $K_s$  from FAO-56

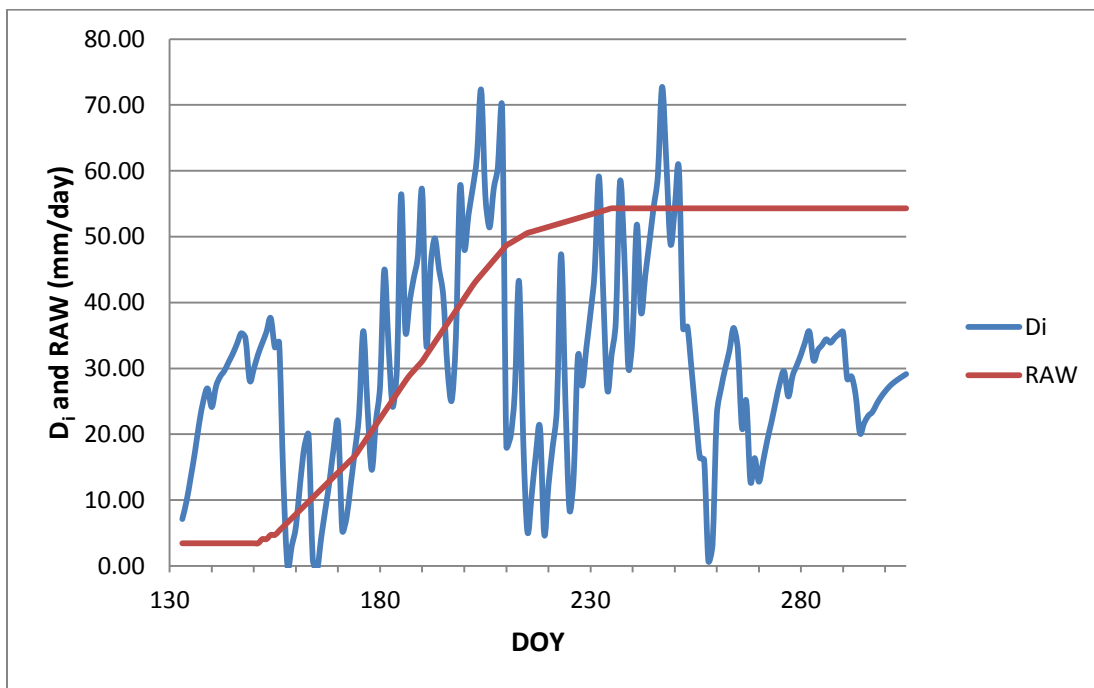


Figure C.4.  $D_i$  and RAW for Treatment 8 with  $K_s$  from FAO-56

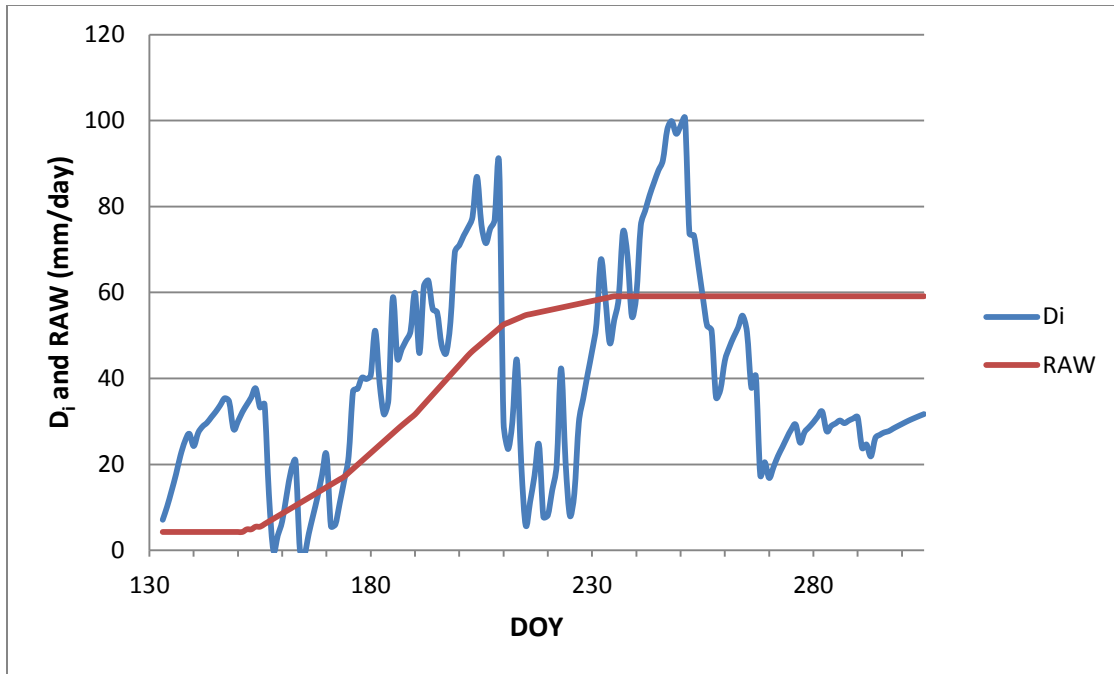


Figure C.5.  $D_i$  and RAW for Treatment 8 with  $K_s$  from FAO-56